Mineralogy and Chemistry of Rare Earth Elements in Alkaline Ultramafic Rocks and Fluorite in the Western Kentucky Fluorspar District

Warren H. Anderson

Report of Investigations 8 doi.org/10.13023/kgs.ri08.13 Series XIII, 2019

Cover Photo:

Various alkaline ultramafic rocks showing porphyritic, brecciated, and aphanitic textures, in contact with host limestone and altered dike texture. From left to right:

- Davidson North dike, Davidson core, YH-04, 800 ft depth. Lamprophyre with calcite veins, containing abundant rutile.
- Coefield area, Billiton Minner core BMN 3. Intrusive breccia with lamprophyric (alnöite) matrix.
- Maple Lake area, core ML-1, 416 ft depth. Lamprophyre intrusive.
- Maple Lake area, core ML-2, 513 ft depth. Lamprophyre (bottom) in contact with host limestone (top).

Kentucky Geological Survey
University of Kentucky, Lexington

Mineralogy and Chemistry of Rare Earth Elements in Alkaline Ultramafic Rocks and Fluorite in the Western Kentucky Fluorspar District

Warren H. Anderson

Report of Investigations 8 doi.org/10.13023/kgs.ri08.13 Series XIII, 2019

Our Mission

The Kentucky Geological Survey is a state-supported research center and public resource within the University of Kentucky. Our mission is to support sustainable prosperity of the commonwealth, the vitality of its flagship university, and the welfare of its people. We do this by conducting research and providing unbiased information about geologic resources, environmental issues, and natural hazards affecting Kentucky.

Earth Resources—Our Common Wealth

www.uky.edu/kgs

For further information contact:
Technology Transfer Officer
Kentucky Geological Survey
228 Mining and Mineral Resources Building
University of Kentucky
Lexington, KY 40506-0107

Technical Level

General **Intermediate** **Technical**

Statement of Benefit to Kentucky

Rare earth elements are used in many applications in modern society, from cellphones to smart weapons systems. The igneous rocks of the Western Kentucky Fluorspar District are slightly enriched in these elements, and although the limited dataset of this study did not reveal economic deposits, there could still be economic quantities in western Kentucky, as well as occurrences of titanium, niobium, iridium, cobalt, molybdenum, zirconium, and lithium.

ISSN 0075-5591

Contents

Figures

Figures (continued)

Plate

Table

Mineralogy and Chemistry of Rare Earth Elements in Alkaline Ultramafic Rocks and Fluorite in the Western Kentucky Fluorspar District

Warren H. Anderson

Abstract

Rare earth elements, or REE, are used in modern society in televisions, computers, cellphones, military equipment, and smart weapons systems. These metals are also used by the medical industry in magnetic resonance imaging and in medical products.

The igneous rocks in the Western Kentucky Fluorspar District of the New Madrid Rift System are considered alkaline ultramafic rocks that are slightly enriched in REE. These rocks are rare and only occur in several hundred locations in the world. They have a complex history of emplacement, fractionation, metasomatism, and alteration, and are overprinted with Mississippi Valley-type mineralization. They are classified as lamprophyres and peridotites, and the rare mineralogy of the district suggests that there may be other facies of these rocks, such as carbonatite, kimberlite, and lamproite. The rare minerals wüstite and moissanite also suggest a deep lithospheric and asthenospheric mantle contribution to these igneous rocks and raise the level of interest in the igneous complex, which occurs in a Midcontinent rift system.

The petrogenesis of these rocks allows them to fractionate and concentrate REE by natural means, and although this study's limited dataset did not reveal any economic deposits, there could still be economic quantities in western Kentucky. If higher concentrations of REE are found in the igneous dikes in the area, the economics and mining of the dikes might be feasible. Millions of tons of fluorite and thousands of tons of sphalerite, galena, and barite have been mined in the district, and small amounts of REE have been detected in the fluorite. Other elements of interest are titanium, niobium, iridium, cobalt, molybdenum, zirconium, and lithium, which suggest other elemental phases of mineralization. Many of these rare minerals and elements have never been described in the Western Kentucky Fluorspar District, and future research is warranted to further classify them.

Introduction

Rare earth elements, or REE, are a group of chemical elements, called lanthanides, that are of strategic importance to the security of the United States. REE, together with other trace metals, are critical materials in the modern world, and are used in the aerospace and military industries in precision military weapons systems, night vision goggles, communications, magnets, lasers, batteries, and nuclear propulsion. Other uses for REE are in cellphones, computers, electronics, magnetic resonance imaging, green energy applications, and wind turbines. Titanium, an associated element, is a high-strength, lightweight, corrosion-resistant metal used in aviation and jet aircraft. The U.S. Congress has enacted legislation to promote research on strategic and critical minerals, and sever-

al National Strategic and Critical Mineral Production Acts were enacted in 2013 and 2015 to facilitate the research and development of domestic REE deposits in the United States. The 2017 House Bill was submitted but has not yet been enacted. For many years, the only operating REE mine in the U.S. was the Mountain Pass Mine in California (Castor, 2008), which was shut down in 2015, but reopened under MP Materials' new ownership in 2018 (www.mpmaterials.com). With the decrease in Chinese exports of raw REE materials beginning in 2010, the United States' supply of REE has become unstable and prices have increased dramatically. In addition, limited reserves from other sources make these elements a national security issue. Today, academic, government, and industry personnel are conducting research and exploration in the U.S. to search for new REE deposits and reduce our reliance on foreign suppliers.

The primary purpose of this study is to evaluate the mineralogy and elemental chemistry of a group of REE-bearing alkaline igneous rocks and the associated mineral fluorite (CaF_2) in the Western Kentucky Fluorspar District and the Southern Illinois Mineral District (Fig. 1). Combined, the two districts form the Illinois-Kentucky Fluorspar District, which was once the largest producer of fluorite and base metals in the United States. These igneous rocks are dikes and sills that intrude Paleozoic rocks and contain REE. The analytical information in this study will help characterize rocks of the Illinois-Kentucky Fluorspar District for REE to determine if there is an undiscovered resource in the Western Kentucky Fluorspar District. More than 50 distinct alkaline ultramafic igneous dikes, sills, diatremes, and other intrusions have been identified and mapped in western Kentucky (Fig. 1, Plate 1).

Analytical data were normalized and compiled into diagrams and bivariant plots that suggest complex metallogenesis for REE in alkaline ultramafic rocks from the Western Kentucky Fluorspar District. Various lithofacies of these alkaline ultramafic lamprophyre rocks originated in the subcontinental lithospheric mantle and have undergone fractionation and metasomatism. The most favorable rock types for hosting REE are niobium-bearing carbonatites (Verplanck and others, 2014).

Geologic History and REE-Related Mineralization

The western Kentucky portion of the Illinois-Kentucky Fluorspar District (Fig. 1, Plate 1) occurs in the northern New Madrid Rift Zone in the central United States, and is part of a failed late Precambrian continental extensional rift (Braile and others, 1986). The New Madrid Rift Zone extends from the Ouachita Fold Belt in Arkansas northeastward into western Kentucky, where it turns abruptly east to form what is locally known as the Rough Creek Graben, and continues directly east farther into Kentucky (Nelson, 2010). The Rough Creek Graben is bounded on both sides by large listric normal faults that cut deep into the Precambrian basement (Potter and others, 1995). The rift zone has a complex tectonic history: northeast-trending normal faults periodically reactivated throughout the Paleozoic, which induced structural compression, faulting, arching, and an extensional phase during the Alleghenian Orogeny (Kolata and Nelson, 2010; Nelson, 2010). These magmatic and structural events prepared the late Paleozoic rocks to receive both deep-seated igneous intrusive and basinal brine mineralizing fluids during the Permian Period. Snee and Hayes (1992) dated actual emplacement of the northwest-trending igneous dikes and Mississippi Valley-type mineralization (Ohle, 1959) in the district using argon geochronology on biotite at the Grants Intrusive in Illinois and the Hutson dike in Kentucky and suggested an age of 271–272 Ma; Chesley and others (1994) determined the age, based on samarium and neodymium yields in fluorite, to be 272 Ma; and Denny (2010) and Denny and others (2017) suggested a broader range of ages between 258 and 281 Ma. Paragenetic studies of the mineralization by Hayes and Anderson (1992) suggest early, middle, and late stages of mineralization, which can be used to correlate intrusion, alteration, and mineralizing fluid events. There is an association between some altered dikes and sphalerite mineralization. Pollitz and Mooney (2014) used mantle viscosity profiles and mantle flow in the Midcontinent to describe a weakened mantle in the study area. These important processes in the New Madrid Rift Zone influenced mantle dynamics, melting, fractionation, and carbonatite metasomatism.

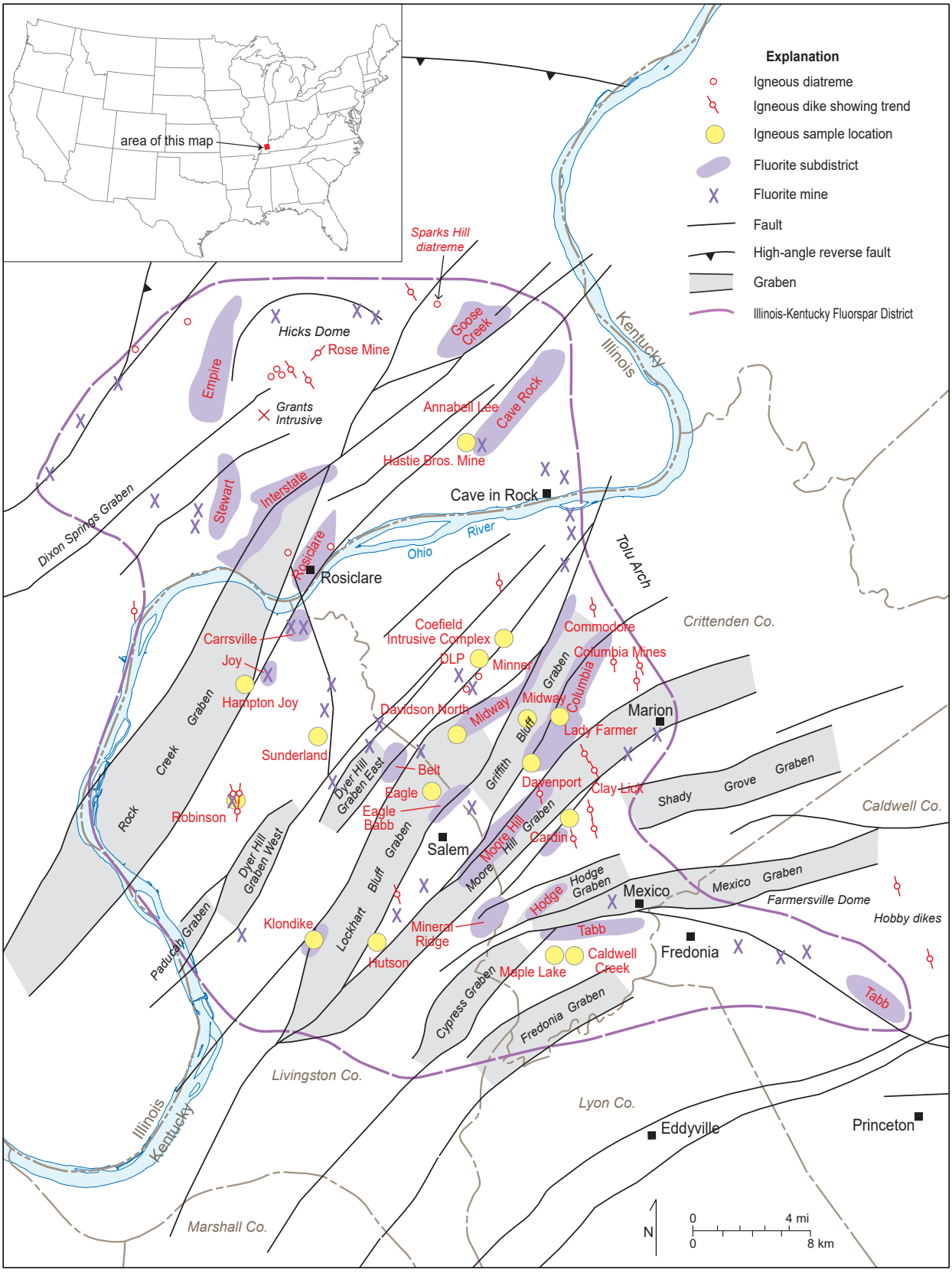

Figure 1. Location of the Western Kentucky Fluorspar District, showing faults, dikes, grabens, mineral districts, and sample locations.

KENTUCKY GEOLOGICAL SURVEY
William C. Haneberg, State Geologist and Director
UNIVERSITY OF KENTUCKY, LEXINGTON

Plate 1: Mines, Minerals, and Magnetics of the Western Kentucky Fluorspar District

Warren H. Anderson

Modified from Hanley and Vorhees (1984), Gaylord and others (1998), and Anderson and Sparks (2012).

SCALE 1:50,000

Lambert conformal projection, 1983 North American datum
Kentucky Single Zone Coordinate System

Cartography by Terry Hounshell

7.5-minute quadrangle index

Introduction

This map is modified from Anderson and Sparks (2012). It contains a layer of magnetic data compiled from various sources to enhance the understanding of the district. Point data were also added to highlight which dikes were analyzed during this study.

Purpose

The map shows all the known and identified mines, mineral prospects, and igneous intrusions (dikes or sills) in the Western Kentucky Fluorspar District, compiled from thousands of maps and files, creating an up-to-date, comprehensive catalog for the district. The district has been extensively mined for more than 120 years and was once the largest producer of fluorspar (fluorite) in the United States.

Millions of tons of vein ore minerals (fluorite, zinc, lead, and barite) have been produced from these mines, and substantial reserves still remain. New mining and exploration activity has renewed interest in the district, and the industry will benefit from the use of this new map. Historic iron ore mines are also included because of their immediate proximity to this mapped area.

Procedure

The map was compiled from numerous sources, including those resulting from the U.S. Geological Survey–Kentucky Geological Survey Geologic Mapping Program (1960–78), Strategic and Critical Minerals Program (1983), Conterminous United States Mineral Assessment Program (1987–92), KGS Digital Geologic Mapping Program (1996–2005), and numerous KGS mineral investigations (1838–present). Some data were from KGS research, and others were collected and donated by mining geologists, field mappers, mining companies, federal and state geologists, and exploration consultants. Many of the data are in the form of surface and underground mine maps, property maps, field notes, drill logs, cross sections, summary reports, and reserve studies.

Database

This map is an introduction to the Kentucky Minerals Database (www.uky.edu/KGS/minerals/im_database.php). This new GIS database provides immediate online access to detailed information about the mines on this map. For some of the larger mines, abundant data are available, but for others, only limited information or just a reference to a publication or report is available. Also included in the database is information about the igneous dikes in the district, which are important for the exploration of ore deposits and other geologic studies. There are some identical mine names for different properties on the map and in the database, along with various spellings of mine names on the same property, and multiple mine names for the same property. The database will ultimately be the most up-to-date, geospatially accurate catalog for western Kentucky mineral deposits.

Magnetics

The magnetic data on this map were compiled from several different sources. During the 1980s, Billiton Metals and Ores USA Inc. flew an aeromagnetic survey of the district, and their residual magnetic data were acquired by KGS after Billiton ceased exploration activities. During the 1990s, Savage Zinc Inc. drilled around the Columbia Mine area and compiled additional total intensity aeromagnetic data. From 2006 to 2008, Dynamex Resources Corp. flew another aeromagnetic survey and produced a total intensity magnetic map of the Coefield portion of the district. To create Plate 1, data from the above sources were overlaid on Anderson and Sparks's (2012) "Mines and Minerals Map of the Western Kentucky Fluorspar District." The magnetic data used on Plate 1 are total intensity data and may be somewhat imprecise because of the various generations and scales of data, the quality of which is unknown; only generalized magnetic intensity data (highs greater than 2 gammas and lows less than 2 gammas) are shown because of magnetic data conflicts noticed during compilation of this plate. The differences are related to petrologic differences, magnetic susceptibility, and alteration events (which affect magnetics) in certain parts of the district. The Billiton residual data are available via the KGS Minerals Database (www.uky.edu/KGS/minerals/im_database.php).

Mineral Deposit Classification

The locations of three classes of mineral deposits are shown on this map, the first of which is Mississippi Valley–type hydrothermal mineral deposits (vein deposits, bedded deposits, and igneous intrusives). The second class is vein deposits, which are narrow mineral deposits that extend vertically and horizontally for hundreds of feet and consist of fluorite, sphalerite, calcite, barite, and galena. Stratabound, or bedded, deposits, also classified as MVT and containing fluorite, occur mainly in the Joy and Carrsville areas; bedded sphalerite may occur in other areas. The third class is igneous intrusives, similar to Hicks Dome, a carbonatite complex located in Hardin County, Ill. More than 50 documented igneous intrusions, including dikes, sills, and diatremes, are found in the district. These igneous rocks can host rare earth elements, titanium, and fluorite minerals.

Mining History

The earliest mining in the district was for lead at the Columbia Mine, Crittenden County, Ky., in 1835 (Ulrich and Smith, 1905, p. 115). From 1835 to the early 1870s, little fluorspar was mined. Only small amounts were produced from the early 1870s to about 1890, when an expanded market was created by the development of the basic open-hearth steel furnace, in which fluorspar was used for flux. Production since 1890 has been erratic, but in general has risen. During World Wars I and II and the Korean conflict, production rose sharply, but because of rising imports from 1955 to 1958, production in the district decreased. It rose in 1970, but declined rapidly, and all production ceased in Kentucky by 1985. Sporadic milling of recycled government stockpiles continued into the 1990s. Exploration is intermittent in the district, and currently there is one operating mine, near the Klondike Mine complex.

Since mining began, the Western Kentucky Fluorspar District has produced about 3.5 million tons of fluorspar, 70,000 tons of zinc, 12,500 tons of lead, and 45,000 tons of barite concentrate (Anderson and others, 1982). Some trace elements, such as silver, copper, cadmium, and gallium, have also been recovered. Thirty percent of the fluorspar came from the Tabb Fault System, a major curvilinear fault in southern Crittenden and western Caldwell Counties (Trace and Amos, 1984).

Zinc has been produced since 1940, some as a byproduct of mining fluorite. The Hutson Mine was a primary zinc producer in the district. Substantial quantities of barite have also been produced. Lead has been a minor byproduct in recent years, as have silver, cadmium, and germanium.

Acknowledgments

Thanks are extended to Walter Gaylord, Bill Frazer, and T. Ballard, Savage Zinc Inc.; Ed Hanley, Billiton Metals and Ores USA Inc.; and Boyce Moodie III, Moodie Minerals Inc., Dynamex Resources Corp., and North American Exploration Inc. Additional thanks go to Terry Hounshell and Thomas Sparks, Kentucky Geological Survey, for cartographic services.

Special thanks for the development of this map and database are extended to William R. Frazer, Marion, Ky., who allowed KGS to scan his company's mining data and make them publicly available in the new Kentucky Minerals Database; and Robert D. Trace, USGS and KGS, who worked in the district between 1942 and 1985 and provided numerous rock samples, maps, notes, sections, and logs of mine data. Trace's numerous maps, publications, and interpretations are important components of this new database, as is the igneous sample set he archived and donated to KGS.

Early mine geologists, including Harry J. Klepser, G.C. Hardin Jr., Stuart Weller, X.B. Starnes, Dewey H. Amos, and William R. Thurston, contributed vital information and documentation on the early mining activity in the district. Many of them wrote publications and contributed to earlier War Minerals and U.S. Bureau of Mines reports. John Tibbs and many other persons contributed to the understanding of the Western Kentucky Fluorspar District and therefore have contributed much to the Kentucky Minerals Database.

Disclaimer

Although this map was compiled from digital data that were successfully processed on a computer system at the Kentucky Geological Survey, no warranty, expressed or implied, is made by KGS regarding the utility of the data on any other system, nor shall the act of distribution constitute any such warranty. KGS does not guarantee this map or digital data to be free of errors or inaccuracies. KGS disclaims any responsibility or liability for interpretations from this map or digital data, or decisions based thereon.

The views and conclusions contained in this document are those of the authors and should not be interpreted as necessarily representing the official policies, either expressed or implied, of the U.S. Government.

EXPLANATION

- Mine, surface cut; fluorspar, zinc, or barite
- Mine, surface cut; iron
- Mine shaft; underground
- Prospect activity
- Occurrence or outcrop
- Dike location at surface
- Dike or sill in corehole
- Drillhole; DDH, mineral, oil, etc.
- Igneous dike; lamprophyre, peridotite (vein)
- Mineral vein; fluorite, zinc, lead, barite
- Fluorspar mine; includes zinc, etc.
- Igneous dike intrusives (area)
- Iron ore mine
- Prospect area
- Magnetic high > 2 gammas
- Magnetic low < 2 gammas
- Fault
- Concealed fault
- Inferred fault
- Parkway
- U.S. highway
- State highway
- City boundary
- State boundary
- County boundary
- Populated place
- 7.5-minute quadrangle boundary
- Creek
- Pond

Map data current as of October 4, 2017

For information on obtaining copies of this map and other Kentucky Geological Survey maps and publications call:
Public Information Center
(859) 257-3896
Toll free: (877) 778-7627
View the KGS website at www.uky.edu/kgs

Kentucky Geological Survey

Much has been written about the structure, age, and mineral deposits of the fluorspar districts in western Kentucky and southern Illinois, including studies by Fohs (1907), Grogan and Bradbury (1968), Richardson and Pinckney (1984), Trace and Amos (1984), Goldhaber and Eidel (1992), Plumlee and others (1995), and Potter and others (1995). Previous studies that specifically discuss the REE content of the igneous dikes and fluorite in western Kentucky are by Bradbury (1962), Richardson and Pinckney (1984), Hall and Heyl (1968), Mitchell (1986), Burruss and others (1992a, b), Chesley and others (1994), Barnett (1995), Plumlee and others (1995), Heck and others (2006), Moorehead (2013), and Denny and others (2017). These studies all suggest the presence of REE in the igneous rocks of the Illinois-Kentucky Fluorspar District.

Hicks Dome is a major structural feature in the Illinois-Kentucky Fluorspar District and has also been called a cryptoexplosive that has a deep-seated igneous diatreme component to it. It has been considered the primary igneous and hydrothermal source of mineralizing fluids in the district, based on MVT mineralization, composition, and temperature studies (Hall and Heyl, 1968; Goldhaber and Eidel, 1992; Taylor and others, 1992; Plumlee and others, 1995). Hicks Dome is also the site of low-grade metamorphism in surface rocks, it has a magnetic signature, and was classified as a carbonatite by Pinckney (1976), Bradbury and Baxter (1992), Potter and others (1995), Denny (2010), and Denny and others (2017), but questions remain about this classification because the exposed surface rocks are not a classic carbonatite as seen in other parts of the world, implying that the carbonatite is at depth. Carbonatites generally contain large amounts of magmatic calcite and igneous textures in a central igneous plug, although lenticular or sheeted intrusive bodies also occur. In addition to Hicks Dome, the Kentucky portion of the Illinois-Kentucky Fluorspar District contains several structural features important to this study, including Tolu Arch and the Coefield Intrusive Complex, as well as several major faulted graben structures (Plate 1, Fig. 1). Tolu Arch in northern Crittenden County, Ky., is a major northeast-trending structure aligned with many northeast-trending dike systems in Kentucky, and several magnetic features related to these dikes are mapped on Plate 1.

Alkaline Ultramafic Rocks

The International Union of Geological Sciences' Subcommission on the Systematics of Igneous Rocks has long debated the classification scheme for alkaline ultramafic igneous rocks (Streckeisen, 1978; Mitchell, 1986, 1993, 1994; Rock, 1986, 1987, 1991; Rudnick and others, 1993; Woolley and others, 1996; Woolley and Kjarsgaard, 2008; Le Maitre, 2002; Wall and Zaitsev, 2004; Tappe and others, 2006; Zeng and others, 2010; Jones and others, 2013; Verplanck and others, 2014). REE-bearing alkaline ultramafic rocks are classified as lamprophyre (alnöite, aillikite, minette), peridotite, carbonatite (greater than 50 percent igneous carbonates), kimberlite (CO_2-rich peridotite), nepheline syenite, lamproite, and orangeite. These alkaline rocks are formed under conditions of ultra-high temperature and pressure; are rich in calcium, sodium, and potassium; and are undersaturated in silica. Fractional crystallization of a cooling parental magma is one of the primary causes of formation of carbonatites that contain silica phases (Bell and others, 1998). By definition, alnöites (Rock, 1986, 1987) and aillikites (Mitchell, 2008) can grade into carbonatites, which also have a CO_2-rich volatile phase (Plumlee and others, 1995). These carbonatites are of interest in the study area because they are a primary host for REE mineralization throughout the world and can form from partial melting of basement peridotite. Most of these rock types are hypabyssal and diatreme intrusions, uniquely forming at various depths and pressures within the mantle (Mitchell, 1986, 1993, 2005), and have undergone extensive melting, differentiation, metasomatism, and alteration (Figs. 2–3). Carbon dioxide degassing is a product of carbonatite formation both before and during the ascent of igneous intrusions, and is an important process for this investigation. Many igneous intrusions are composed of different geochemical and mineralogical lithofacies, which results in an overlapping intrusion complex rather than an isolated single intrusion. The carbonatite formation process covers a broad range of temperatures and is a direct result of magmatic differentiation (Lapin, 1982). Carbonatite metasomatism is usually a hybrid between carbonatite and silicate metasomatism, but more analytical data are needed to define the silicate component of the metaso-

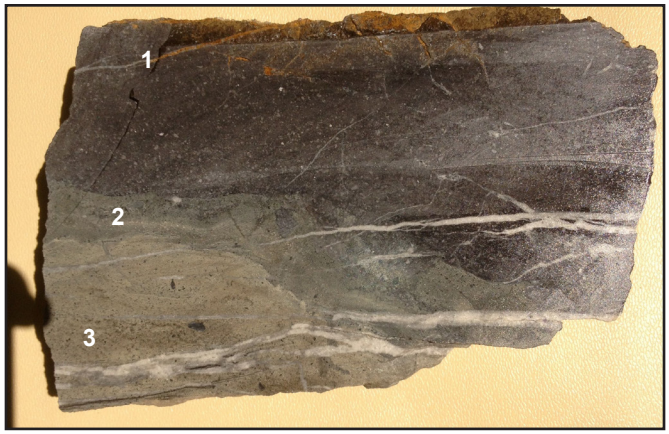

Figure 2. Rogers Quarry lamprophyre dike, Crittenden County, Ky. Dike, exposed on the surface in an active limestone quarry, shows variability in lithology and petrology. The primary facies present in the dike is subdivided into (1) slightly altered dike, magnetic, containing clinopyroxene and serpentine, progressing downward into (2) a more highly altered part of the dike containing serpentine, clinopyroxene, titanium oxides, and abundant calcite veins, changing to (3) a very altered, light green dike, nonmagnetic, composed of calcite, dolomite, and ankerite with quartz and calcite veins.

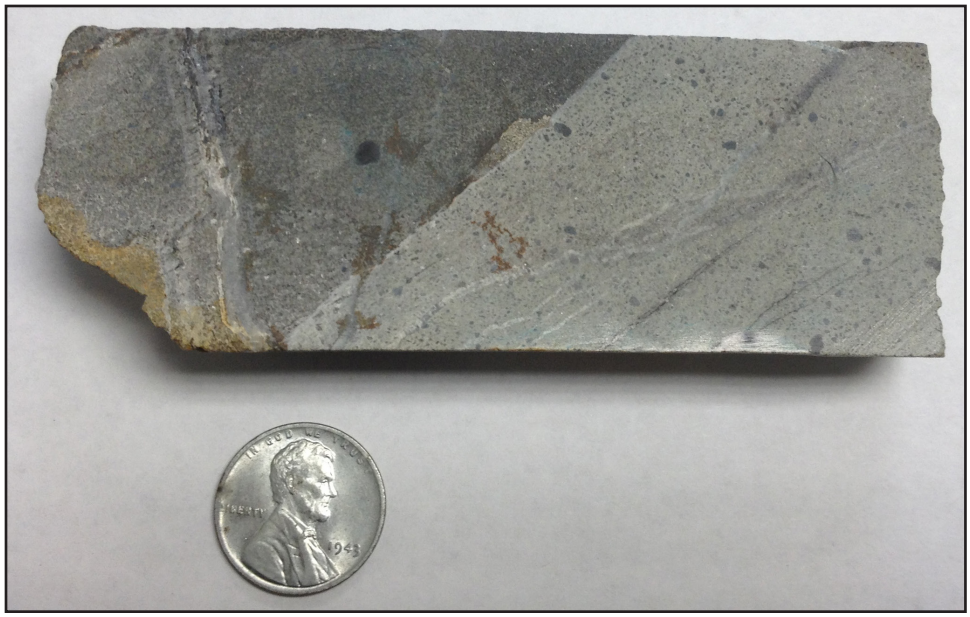

Figure 3. KGS dike 801, Frontier Spar core 6, located north of the Klondike Mines, Livingston County, Ky. This unique core shows both a dark green unaltered dike (left), which is slightly magnetic, and a light green altered dike (right), which is nonmagnetic. Pyrite occurs in both altered (less than 10 percent and finely disseminated) and unaltered rock (greater than 10 percent and coarsely disseminated) and is concentrated near their contact. Black clasts are clinopyroxene, and some veins of serpentine (dark colored) and carbonate (light colored) are also visible. Penny for scale.

matism; therefore, the focus of this study is on the formation of carbonatite.

The association of alkaline ultramafic intrusions and massive amounts of fluorite in the Illinois-Kentucky Fluorspar District is a direct indication of carbonatite formation (Modreski and others, 1995; Kogut and others, 1996; Lee and Wylie, 1998; Yang and others, 2003; Schwinn and Markl, 2005; Denny, 2010; Jones and others, 2013; Makin and others, 2014; Denny and others, 2017). Some of these carbonatites are associated with fluorite, which is mined in the United States, China, Russia, Sweden, Africa, and other parts of the world; many of these carbonatites are combined with a syenite facies (Xu and others, 2012). Fluorite and hydrothermal fluids are discussed in Möller and others (1998). Two carbonatites occur near the New Madrid Rift Zone: at Magnet Cove, Ark., where nepheline syenite and a diamond-bearing lamproite also occur (Scott Smith and Skinner, 1984; Rock, 1991), and at Avon, Mo.; both locations contain magmatic carbonates (Howard and Chandler, 2007; Shavers and others, 2016). Ultramafic rocks at Aillik Bay, Labrador (Tappe and others, 2006), and basalts at Shadong, China (Zeng and others, 2010), are also carbonated peridotites-carbonatites, and are similar to the western Kentucky dikes; they are mentioned here because of their similar petrogenesis. Since there is a paragenetic association of REE with these various rock types, the chemistry of both igneous dikes and fluorite were examined in this study.

Lewis and Mitchell (1987) classified igneous rocks in the Illinois-Kentucky Fluorspar District as an alnöite lamprophyre intrusive complex (Plate 1, Figs. 2–3); individual intrusions have been classified as minette by Moorehead (2013), aillikite by Maria and King (2012), and alnöite by Heck and others

(2006). An older report by Koenig (1956) identified serpentine, garnet, perovskite, ilmenite, phlogopite, and apatite in many Kentucky dikes and classified them as mica peridotites and lamprophyre. Robert Trace (U.S. Geological Survey, written communication, 1960; 1974) detected florencite, monazite, brookite, and xenotime in the dike rocks of the Illinois-Kentucky Fluorspar District and classified them as altered mafic dikes (Trace and Amos, 1984), meaning they essentially contain a mineralogy of an alkali ultramafic intrusive complex. The Coefield Magnetic Anomaly (Plate 1), a significant geologic and magnetic feature in the Western Kentucky Fluorspar District, was discovered in the 1980s, and several cores (Minner and DLP) from this feature were used in this study. The intrusion contains some unusual minerals, such as titanium garnets, and is now called the Coefield Intrusive Complex because of its varied mineralogy and petrology and the rare xenoliths and xenocrysts associated with mantle and basement rock petrology. Many of the dikes are north-trending and can extend for miles, and some of the dikes are thin, but several are tens to hundreds of feet wide. Many of the dikes in the Western Kentucky Fluorspar District are actually twin dikes (Hutson, Old Jim, Columbia, Midway, Caldwell Creek), consisting of one dike that is slightly altered and another dike that is more heavily altered. Some dikes are splintered or brecciated, and many contain the associated sphalerite mineralization.

Model for the District

A model of the geologic processes that formed the Illinois-Kentucky district is based on the results of this study and in part on previous work by Lapin (1982), Mitchell (1986), Lewis and Mitchell (1987), Hayes and Anderson (1992), Hildenbrand and Hendricks (1995), Plumlee and others (1995), Wall and Zaitsev (2004), Tappe and others (2005), and Nelson (2010).

During Precambrian rifting, a thinning lithosphere allowed subcontinental lithospheric mantle magmas to form and ascend toward the crust in response to a thinned lithosphere and reduced lithospheric stress, but full crustal intrusion stalled when the rift failed to fully develop. Some of these magmas were generated in the asthenospheric mantle at depths of the stability field of ultra-high temperature and pressure minerals; carbonatite metasomatism also took place. These upwelling magmas underwent fractionation and metasomatism during the late Precambrian and early Paleozoic, while the magmas were stalled. The fractionation process started to separate the REE, whereas metasomatism concentrated other incompatible elements in the melts. Extensional tectonics and structural reactivation of faults during the Alleghenian Orogeny caused the upwelling, fractionated, and metasomatized magma fluids to begin intruding into the Paleozoic rocks. About the same time, during the Permian Period, base-metal-rich Mississippi Valley-type hydrothermal fluids were migrating toward the Illinois-Kentucky Fluorspar District and began to deposit the mineral veins and to mix with CO_2-rich igneous alteration fluids and be emplaced in the Permian faulted structures. During these processes, REE and other trace elements were mobilized from magmas, and CO_2-rich volatile magma degassing events concentrated the REE into subeconomic quantities in the dikes, at the same time altering the igneous dikes and selected mineral deposits. Several processes, including the post-crystallization alteration of igneous dikes and mixing of base-metal-rich MVT mineralization with post-emplacement, CO_2-rich fluids caused some of the lithofacies to form. These important processes created a complex igneous intrusion overprint on the mineral paragenesis. Other igneous complexes in the New Madrid Rift Zone of interest for this study are adjacent to the craton and have been identified at Magnet Cove, Ark., and Avon, Mo.

Rare Earth Elements

Rare earth elements are a group of 15 chemical elements with atomic numbers from 57 to 71: lanthanum, cerium, praseodymium, neodymium, samarium, europium, gadolinium, terbium, dysprosium, holmium, erbium, thulium, ytterbium, lutetium, and promethium. Promethium does not occur naturally on Earth, but has been detected as a product in nuclear reactions and radioisotopes. Yttrium and scandium are also sometimes included in the REE category because of their 3+ ionization and geochemical behavior similar to REE. The lower REE atomic numbers (57–60) are referred to as light REE (LREE), the middle range (61–67)

as medium REE (MREE), and the higher atomic numbers (68–71) as heavy REE (HREE). Rare earth elements are not really rare, since they occur in many rock types and in many minerals. They are broadly distributed, including in primitive meteorites, which are used to normalize terrestrial values of REE. Because of their similar atomic structures, REE usually occur together in ore deposits, which makes extraction, separation, and beneficiation from host rocks and from each other difficult. Their "rare" designation is because they rarely occur in native form; usually, REE occur as trace elements in other minerals until the concentration becomes high enough for them to compound and form their own minerals, such as REE-carbonates, -oxides, -phosphates, and -fluorides. REE can be enriched in igneous rocks by fractionation and magmatic differentiation. Along with REE, other important elements are considered incompatible in igneous melts, but also demonstrate a propensity to help concentrate REE and thus help determine the petrogenetic history of magmas. These elements are zirconium, niobium, hafnium, thorium, uranium, cobalt, molybdenum, chromium, and tantalum; they have difficulty entering into a solid crystal structure, will fractionate, sometimes become immiscible, or mix with metasomatized mantle material to form mineral deposits.

REE Concentrations in Alkaline Ultramafic Rocks and Fluorite

REE concentrations in ultramafic rocks that have differentiated or have been hydrothermally enriched would be expected to be higher than primitive chondrite concentrations, which have not been affected by such Earth processes. Fluorite associated with such ultramafic rocks would also be enriched in REE. Sufficient enrichment could enable a deposit to become anomalously enriched or economically mineable. Most economic deposits, such as at Mountain Pass, Calif. (Long and others, 2010), or Bayan Obo, China (Yang and others, 2003), have whole-rock values greater than 10,000 ppm for some individual REE and whole-rock total REE greater than 100,000 ppm. Carbonatites host most of Earth's REE and normally have high REE concentrations (greater than 10,000–20,000 ppm) (Castor, 2008), whereas kimberlites and lamproites generally have lower LREE concentrations.

Carbonatite deposits typically have abundant fluorite and REE mineralization. The genetic origin of fluorite mineralization and REE in most carbonatite-type rocks for many mineral districts throughout the world is discussed in Mariano (1989), Möller and others (1998), Mitchell (2005), Makin and others (2014), and Simandl (2015). REE in carbonatite pegmatite, and hydrothermal and sedimentary fluorite, are discussed in Parekh and Möller (1977) and Möller and others (1998); these works interpret the genetic origin of REE in fluorites.

Hicks Dome contains significant REE in dark purple fluorite (A.V. Heyl, U.S. Geological Survey, written communication, 1963); the breccias have high concentrations of cerium, lanthanum, thorium, niobium, yttrium, and beryllium and are considered to be both a source and center of mineralization in the district (Hall and Heyl, 1968; Burruss and others, 1992a; Plumlee and others, 1995). The Hicks Dome fluorites from deep cores are clear to dark purple in color, suggesting early MVT-stage purple fluorites are more enriched in REE than later MVT-stage fluorite in general and exhibit REE zonation within the early fluorite (Burruss and others, 1992b). There may also be temperature zonation of REE, according to Möller and others (1998). Purple fluorites from the Rose Mine on Hicks Dome have much higher REE concentrations than other fluorites in the district (Burruss and others, 1992b). Fluorite from the Hamp core, drilled into Hicks Dome, contains less than 0.5 percent REE and more than 1.5 percent thorium and yttrium, but no uranium was detected (Robert Trace, U.S. Geological Survey, written communication, 1960; A.V. Heyl, U.S. Geological Survey, written communication, 1963). Hall and Heyl (1968) noted variation in fluorite color and REE content, and thorium content suggests that the dark purple fluorites have higher thorium and REE concentrations for the Hicks Dome mineralized fluorite breccia. This purple fluorite from the Rose Mine is also depleted in LREE and enriched in HREE, whereas the blue fluorite from the Rose Mine was depleted in both LREE and HREE, with a maximum value for europium (Burruss and others, 1992b).

Additional analyses of REE in Kentucky-Illinois fluorites by Richardson and Pinckney (1984), Trinkler and others (2005), and Denny and others

(2017) demonstrate a convex-downward pattern of enriched MREE. Burruss and others (1992b) noted examples of REE in colored fluorites in the Illinois-Kentucky Fluorspar District; they found the total REE from the Rose Mine was 10 to 20 times higher than in outlying mines, which suggests REE zonation and variable REE in fluorite composition. They suggest LREE and HREE depletion requires extensive fractionation of the original hydrothermal fluids prior to mineralization. Trinkler and others (2005) worked on yellow fluorite from hydrothermal veins and determined both MREE enrichment and that optical adsorption irregularities in the fluorite lattice contributed to the yellow coloration of fluorite from the Victory Mine in Illinois. Heyl (1983) reported that green fluorite from the Hicks Dome area contains yttrium. Blue fluorite from the Rose Mine is depleted in LREE and HREE, according to Burruss and others (1992b). Robert Trace (U.S. Geological Survey, written communication, 1960; 1974) detected a monazite-like mineral, later identified as brookite, and measured radioactive anomalies at Hicks Dome. Harry Rose of the U.S. Geological Survey used an electron microprobe to identify a thorium-, yttrium-, erbium-, dysprosium-bearing fluorine mineral intergrown with fluorite from the Hamp Hole at Hicks Dome and tentatively identified it as yttrioparisite, as reported by Hall and Heyl (1968).

Methods

Samples were collected and analyzed for mineralogical identification and major, minor, and rare earth elemental values. REE data were normalized with chondrite values. Geochemical data were compared to data from other locations in the world. The samples' geochemical compositions were evaluated in part from how they vary in relation to distance from Hicks Dome; other workers have used Hicks Dome as a temperature and mineralization center (Taylor and others, 1992) on many charts and diagrams.

Sample Set

Dike samples were collected from 50 locations (Table 1) in the Western Kentucky Fluorspar District (Plate 1); 30 samples were analyzed with X-ray diffraction and 12 samples were analyzed for major, minor, and trace elements. Samples were prepared depending on the type of analysis: thin sections or polished sample surfaces for X-ray diffraction and pulverized whole-rock samples for elemental analysis.

Mineralogy and Petrography

Optical petrography and photography were conducted in the KGS petrographic laboratory using a polarizing petrographic microscope and a binocular scope on petrographic slides prepared in house. Both transmitted and reflected-light photography were conducted. More than 100 photographs were used to record the mineralogy of various dikes, some of which are included in this report; additional photographs and data are in the KGS Minerals Database (www.uky.edu/KGS/minerals/im_database.php; accessed 04/22/2019).

An X-ray diffractometer in the KGS laboratory was used to identify minerals in 40 samples, but the resulting diffractograms are not included in this report. Confidence in the mineral phases obtained with X-ray diffraction is high because most samples were flat and polished, resulting in an accurate X-ray beam angle for acquiring two theta-angle measurements. These angles were correlated to a mineral identification and accompanying crystallographic system classification in the Bruker crystallographic database (www.bruker.com/products/x-ray-diffraction-and-elemental-analysis/x-ray-diffraction/xrd-software/eva/cod.html; accessed 04/22/2019). Standards were also used to calibrate the two theta angles for the X-ray diffraction scans.

Backscatter image analysis and mineral identification were conducted on a few samples using scanning electron microscopes at Northern Kentucky University and the University of Kentucky.

Elemental Analysis

Cores or rock-outcrop samples from ultramafic dikes were collected and crushed for whole-rock elemental analysis, and fluorites were carefully hand-selected for color content, crushed, and analyzed for REE. Whole-rock major, minor, and trace elements of dikes were analyzed using a sodium peroxide fused-pellet method with an inductively coupled plasma atomic emission spectrometer in 2015 by SGS Laboratories of Burnaby, British Columbia, Canada. Some outcrop samples were weathered, which could affect their REE composi-

Table 1. Inventory of igneous dikes in the Western Kentucky Fluorspar District. An online database (www.uky.edu/KGS/minerals/im_database.php) is searchable by site name. Dikes used in the study are highlighted in red. Site No. = compilation reference. Record No. = database reference. TS = thin section. X-ray = X-ray diffraction.

Site No.	*Record No.*	*Field Map/ Analysis ID*	*Site Name*	*Analysis Type*	*Trace Minerals*	*Lithology*
78	78	T-2-76	Hurricane lamprophyre dike	TS, X-ray	anatase	lamprophyre
79	79	597-V	Little Hurricane lamprophyre dike in core drillhole (Pennwalt)	TS, X-ray	anatase, ilmenite, garnet	lamprophyre
80	80	T-84?	lamprophyre dike in core drillhole			lamprophyre
81	81		Cyclone lamprophyre dike			lamprophyre
94	94		Hobby North lamprophyre dike			mica peridotite
1385	1061	T-9-76	Midway (Davidson) Eaton northwesternmost lamprophyre	TS, X-ray	anatase	lamprophyre
3017	3017	YH-004	Davidson North		REE-bearing fluorite, perovskite, rutile	lamprophyre
1385	1385	T-799	Eaton dike			lamprophyre
261	1401	T-800	Guilless dike northeastern lamprophyre	TS, X-ray		lamprophyre
261	1401	T-1-76	Guilless dike lamprophyre	TS, X-ray	fluorapatite, anatase magnetite	lamprophyre
262	262	TH	Dike South lamprophyre	TS, X-ray	anatase (Ce), rutile (Nb)	lamprophyre
262	262	T-4-76	Dike South lamprophyre	TS, X-ray	altered to calcite and dolomite	lamprophyre
262	262	CH 49-165	Dike South lamprophyre	TS, X-ray		lamprophyre
262	262	CH 48-198	Dike South lamprophyre			lamprophyre
279	279	565	Glendale dike			mica peridotite
280	280	T-214	Moore Hill lamprophyre dike			lamprophyre
281	281	T-804 (RDT_10)	Fowler lamprophyre dike	TS, X-ray	andradite, schorlomite	lamprophyre
282	282	T-798b	Claylick East lamprophyre dike			mica peridotite
282	1273	T-1136	Claylick East lamprophyre dike			mica peridotite
283	283	T-1448	Cardin lamprophyre dike			lamprophyre
283	283	T-404-2	Cardin dike		yttriofluorite, anatase	lamprophyre
284	284	T-595?	Childress Bluff lamprophyre dike			lamprophyre
285	285	T-227-105	View (Lowery) lamprophyre dike	TS, X-ray	garnet	lamprophyre
286	286		Shell core (Adams) lamprophyre dike	TS, X-ray	schorlomite garnet	alnoite
302	302	T-8-76	Howard Stout lamprophyre dike	TS, X-ray	andradite	lamprophyre
1064	1064	T-798a	Claylick West lamprophyre dike	TS, X-ray		lamprophyre
1064	1064	T-798b	Claylick West lamprophyre dike	TS		lamprophyre
1366	1366	T-7-76	Robinson lamprophyre dike	chemical analysis	zinc with dike	lamprophyre
1367	1367	T-5-76	Sunderland lamprophyre dike		anatase	lamprophyre

Table 1. Inventory of igneous dikes in the Western Kentucky Fluorspar District. An online database (www.uky.edu/KGS/minerals/im_database.php) is searchable by site name. Dikes used in the study are highlighted in red. Site No. = compilation reference. Record No. = database reference. TS = thin section. X-ray = X-ray diffraction.

Site No.	*Record No.*	*Field Map/ Analysis ID*	*Site Name*	*Analysis Type*	*Trace Minerals*	*Lithology*
1368	1368		Mann lamprophyre dike			lamprophyre
1369	1369		Butler lamprophyre dike			lamprophyre
1370	1370	BMN-1	Minner lamprophyre dike	TS, X-ray	breccia, REE perovskite	alnoite
1370	1370	BMN-3	Minner lamprophyre dike	TS, X-ray	breccia, REE perovskite	alnoite
1370	1370	BMN-4	Minner lamprophyre dike	TS, X-ray	anatase, ilmenite	alnoite
1370	1370a	BMN-7-a	Minner lamprophyre dike	TS, X-ray	anatase, andradite/schorlomite, perovskite	alnoite
1370	b	BMN7-227-b	Minner lamprophyre dike	TS, X-ray	andradite (Ti), double perovskite, spinel, magnetite	alnoite
1370	c	BMN7-227-c	Minner lamprophyre dike	TS, X-ray	andradite, schorlomite (Ti), perovskite (La, Pr, Ta, Eu, Y)	alnoite
1370	d	BMN7-227d	Minner lamprophyre dike	TS, X-ray	schorlomite (Ti), perovskite (Y, Ta), spinel	alnoite
1370	1370	DLP-2	DLP-2 Kennecott core sample	TS, X-ray	iridium, fluoro-tetraferriphlogopite	lamprophyre
		DLP-3	DLP-3 Kennecott core sample	TS, X-ray	astrophyllite, moissanite, zinc in dike, rare garnet, marimotoite	lamprophyre
1371	1371		Gray lamprophyre dike			lamprophyre
1373	1373	T-565	Commodore lamprophyre dike	TS, X-ray		lamprophyre
1284	1284	1971	1971 Hickory Cane roadcut, Commodore lamprophyre dike	TS		lamprophyre
1377	1377		Holly lamprophyre dike			lamprophyre
1378	1378	TK	Crystal (Flannery) lamprophyre dike	TS, X-ray	anatase, ankerite	lamprophyre
1378	1378	TL-78	Crystal lamprophyre dike	TS		lamprophyre
1379a	1379a		Mary Belle Columbia South lamprophyre dike		anatase	mica peridotite
1380	1380	KGS-1380	Columbia South lamprophyre dike			mica peridotite
1402	1402	RD	Columbia North lamprophyre dike	TS, X-ray	fluocerite	mica peridotite
1381	1381		Mary Belle Southwest lamprophyre peridotite			mica peridotite
1383	1383	BLF-4	Lady Farmer lamprophyre dike	341.5 ft depth	fluorite, anatase	mica peridotite
1383	1383	BLF	Lady Farmer lamprophyre dike			mica peridotite
1384	1384	D-1	Old Jim lamprophyre dike	TS, X-ray	zinc in dike, molybdenite	mica peridotite
1267	1267	105	Freedom South lamprophyre dike			mica peridotite
1389	1389	T-681	Barnes lamprophyre dike	TS, X-ray		lamprophyre
1390	1390	T-796	Watson lamprophyre dike			lamprophyre

Table 1. Inventory of igneous dikes in the Western Kentucky Fluorspar District. An online database (www.uky.edu/KGS/minerals/im_database.php) is searchable by site name. Dikes used in the study are highlighted in red. Site No. = compilation reference. Record No. = database reference. TS = thin section. X-ray = X-ray diffraction.

Site No.	*Record No.*	*Field Map/ Analysis ID*	*Site Name*	*Analysis Type*	*Trace Minerals*	*Lithology*
			Hutson core BH-7		astrophyllite, zinc in dike	mica peridotite
2	619	T-10-76	Hutson Mine shaft dike (underground)	TS, X-ray		mica peridotite
1406	1406	BHN-1	Hutson North	TS	REE	mica peridotite
1406	1406	BHN-4	Hutson North			mica peridotite
1391	1391	T-3-76	Hutson core 228, depth 329 ft	TS, X-ray	fluorapatite, anatase, pyrite	mica peridotite
1392	1392		Holly South lamprophyre dike 8			mica peridotite
1407	1407	ML-1_420	Maple Lake dike core 1	TS, X-ray	rutile	lamprophyre
1407	1407	ML-1_424	Maple Lake dike core 1	TS, X-ray	rutile, fluorite	lamprophyre
1408	1408	ML-2_509	Maple Lake dike core 2	TS, X-ray	rutile	lamprophyre
1408	1408	ML-2_510	Maple Lake dike core 2	TS, X-ray	rutile	lamprophyre
1408	1408	ML-2_513	Maple Lake dike core 2	TS, X-ray	rutile	lamprophyre
1409	1409	HJ-13_277	Hampton Joy dike	TS, X-ray	massive sulfide	mica peridotite
		KGS 1390			anatase, diopside, antigorite	
1405	1405	T-801	Frontier (Little property)		andradite	mica peridotite
		BCN-3	BCN-3		grossular	alnoite
		BCS-2B	Billiton Crittenden Springs core, 247 ft depth		anatase, rhodochrosite	lamprophyre
		BCS-2B	Crittenden Springs		rhodochrosite, anatase, carbonate	
		HD	Eagle Mine	TS		
1265	1265	LD	Lucille Mine	TS		lamprophyre
		OL	Orrs Landing, Illinois	TS		
		MD	Mix dike, Illinois	TS		
1385	1385	E	Eaton dike	TS		
1370	1370	DLP-2-152	Minner dike			mica peridotite
1370	1370	DLP-2-824	Minner dike		altered to calcite and dolomite	mica peridotite
1385	1385	T-6-76	Eaton vein			lamprophyre
		HJ-5	Hampton Joy area, core		rutile	mica peridotite
		T-183-	near Sisco Chapel, Salem quadrangle			
		Maxus well	well in Crittenden County	USGS analysis	beryllium, titanium copper detected	

tion. Some of the analyzed samples were collected by previous researchers, but precise location information was available for all samples.

Normalization of REE Data

The full suite of REE were analyzed for numerous dike and fluorite samples, and raw concentrations were normalized using Taylor and McLennan's (1985) values for chondrites. REE concentrations are thus reported as chondrite-normalized, in order to establish a standard for comparison and to remove elemental odd-even oscillations inherent in REE raw data. Chondrites are considered "primitive" in that they have not been influenced by Earth processes, such as differentiation or hydrothermal mineral enrichment, and so REE values of the reference chondrites (Taylor and McLennan, 1985) are considered free of Earth's concentration influences. Primitive mantle material should have similar values to chondrites.

Standards and Analysis of REE Data

Apart from determining overall REE abundances and patterns, REE data from igneous rocks are frequently evaluated by using normalized ratios of light to heavy REE and by comparing compatible and incompatible elemental data. Ratios of the REE end-members are one way to measure degrees of fractionation, metasomatism, enrichment, and depletion in an igneous body. The ratios La/Yb, Tb/Yb, Sm/Yb, Nb/Ta, Y/Yb, U/Th, Zr/H, and Zr/Y are commonly used, and others are also used to evaluate the effect of mantle dynamics and metasomatism in rift systems. Niobium is also commonly used to evaluate the potential for carbonatite formation. Because of their ionic structure, other elemental ratios of importance are Zr/Hf and Zr/Y; they measure fractional crystallization and metasomatism.

Results

Petrology and Major Element Analysis

Whole-rock major-element analyses of the igneous dikes sampled across the Western Kentucky Fluorspar District (Fig. 1, Plate 1) vary substantially in calcium, magnesium, iron, potassium, titanium, chromium, and aluminum concentrations. Whole-rock, major-element compositional data are used to determine petrologic classification, and as shown in Figures 4 and 5, the variation in petrology is complex. Based on the Al_2O_3, FeO, and MgO ternary diagram shown in Figure 5a, most of the dikes would fit into the alnöite or aillikite lamprophyre category, with some trending toward kimberlite or carbonatite. Based on the CaO, FeO, and MgO ternary diagram shown in Figure 5b, some dikes would fit into a carbonatite category or have been influenced by carbonatite fluids; others, near the Coefield Intrusive Complex, fit into a lamprophyre-kimberlite and a calcio-ferro-magnesio carbonatite category. The high CaO content (Fig. 5b) in some dikes suggests an influence of carbonatite-type rocks or that these dikes have been influenced by crustal contamination; isotopic work is needed for confirmation. All Coefield Intrusive Complex dikes (including Minner, Davidson, and Lady Farmer) are rich in iron and magnesium.

The range of Ca/Al ratios (0.29–46) allows different magma types to be distinguished, and large variations in strontium (186–960 ppm) suggest crustal contamination of mantle material. Low calcium concentrations in four calcium-depleted mantle dikes (Stout, Davidson Midway, Sunderland, and Caldwell Creek), where Ca/Al ratios are less than 1, can be distinguished from a second set that have Ca/Al ratios greater than 1 (Hampton Joy, Davidson North, Cardin, Minner 4, Minner 7, and Lady Farmer). Two dikes are extremely enriched in calcium (Maple Lake and Hutson 7); Ca/Al ratios are greater than 15. These differences may represent influences from carbonatite and silicate metasomatic fluids or contamination from crustal materials such as limestone; this study is focused on carbonatite metasomatism, however, since the silicate component is considered poorly defined. Because no true carbonatite has been found in surface rocks, the Coefield Intrusive Complex appears to be an altered group of ultramafic rocks and may be the closest to a carbonatite lithofacies in the district.

Some of the lamprophyre subclassifications are based on aluminum content; the aillikite facies generally contain less aluminum than the alnöites, according to Rock (1991), and by definition can trend toward carbonatite. The titanium and aluminum concentrations place most of the dikes into the broad ultramafic lamprophyre alnöite and aillikite categories, but the high titanium content would place some of the dikes into a carbonatite,

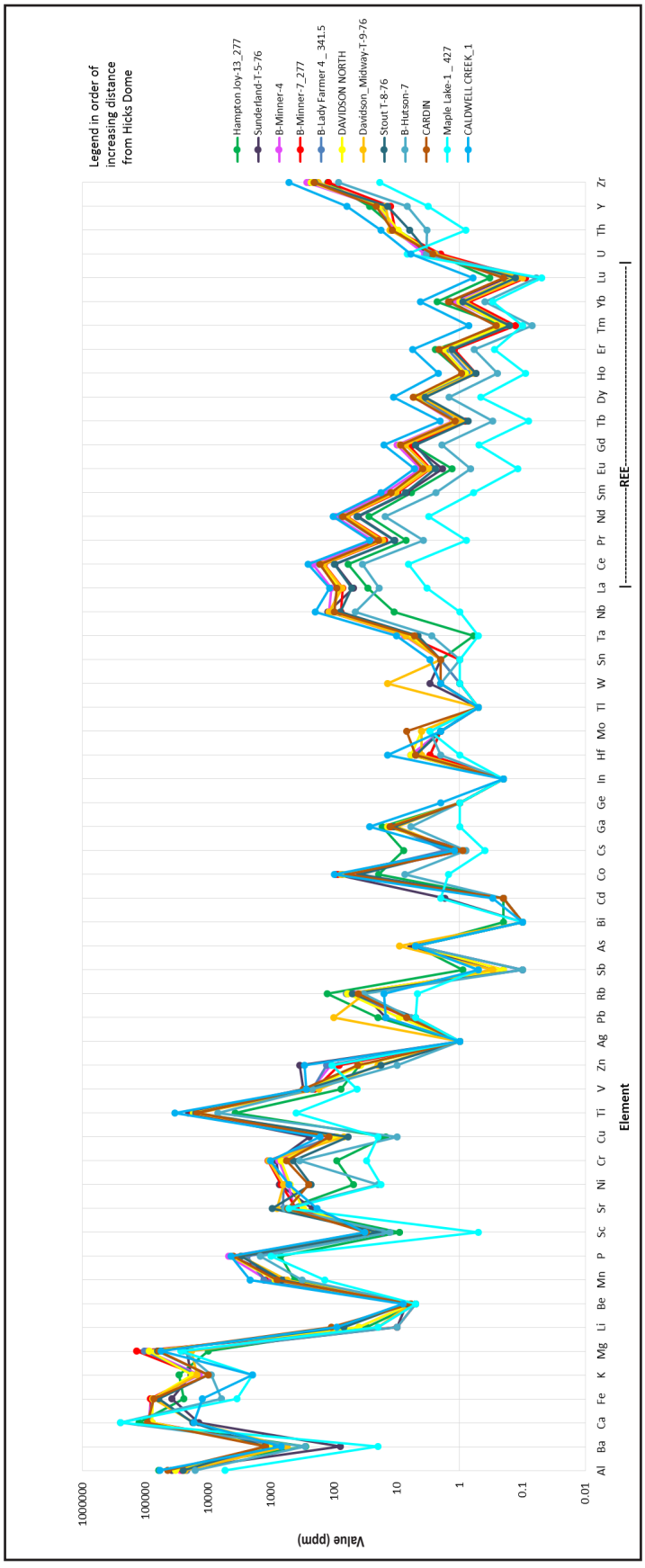

Figure 4. Raw-data analysis by inductively coupled plasma atomic emission spectrometry of various dikes with increasing distance from Hicks Dome, showing REE enrichment. The REE elemental oscillations and gentle negative slope of decreasing values of REE reflect decreasing cosmic abundance of REE. Note high elemental values for Ti (0.04–3.4 percent), Nb (1–199 ppm), P (0.07–0.47 percent), Mg (1.01–13.7 percent), Fe (0.35–12 percent), and Zr (18–521 ppm). There is also variability in other metals—Cr, Ni, Zn, Ga, Pb, and Co—and in U and Th, particularly Th daughter products.,

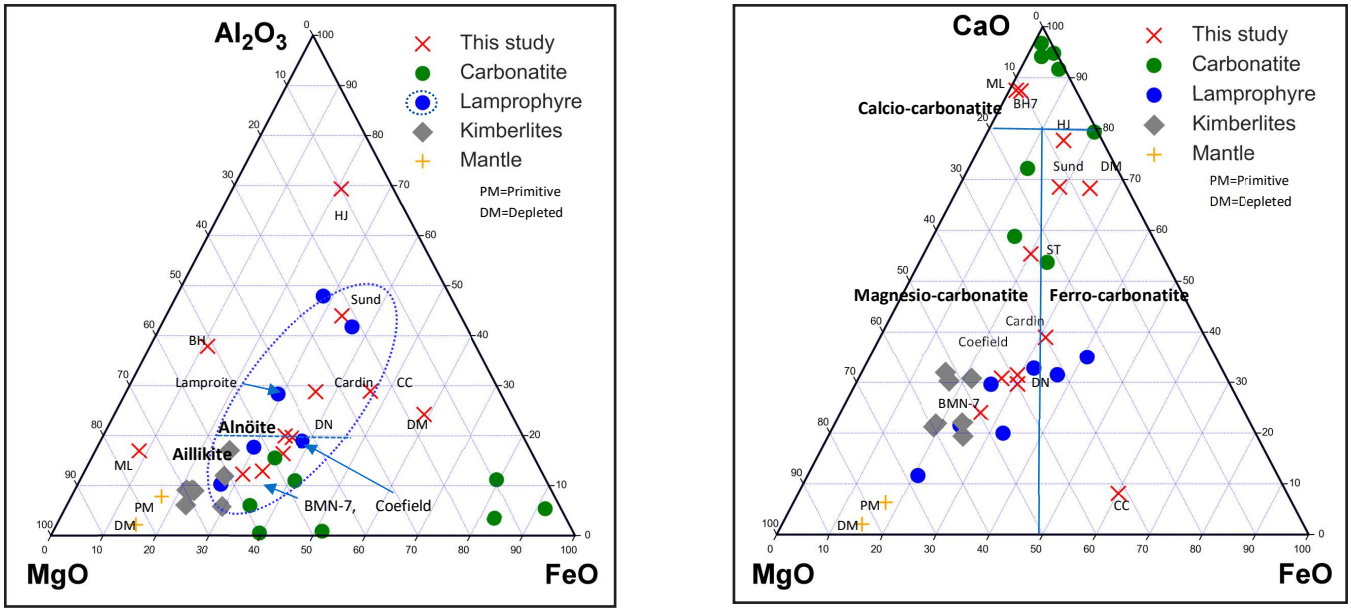

Figure 5. Ternary composition diagrams showing Al_2O_3, CaO, FeO (total), and MgO concentrations of intrusive rocks of the Western Kentucky Fluorspar District. The heterogeneous nature of the Kentucky ultramafics fits with the overlapping compositional variations of lamprophyre, kimberlite, and carbonatite. Lamprophyres (including lamproite facies) have low aluminum oxide values, placing them in the alnöite and aillikite categories. Alnöite generally has high aluminum concentrations, according to Rock (1991). Kimberlite and, in some cases, carbonatite have similar compositions, but their mineralogy excludes some dikes from the kimberlite classification. High-titanium garnets in dike BMN-7 place this dike into an overlapping kimberlite, carbonatite, and aillikite classification, whereas high iron in the Caldwell Creek dike suggests a ferro-carbonatite. Primitive and depleted mantle categories are shown for comparison. Although composition of the rocks overlaps several classifications, a deep mantle origin is the primary common factor in the analyzed rocks; aqueous and hydrothermal alteration influenced the composition. Worldwide background data for carbonatites from Jones and others (2013), for lamprophyres from Rock (1991), and for kimberlites from Mitchell (1986). Mantle values from McDonough and Sun (1995) and Condie (1997).

kimberlite, or lamproite category (Fig. 5). The presence of titanium and calcium garnets (schorlomite and andradite) is important during melting and fractionation and is diagnostic for certain aillikite lamprophyre classifications, which determine carbonatite and ultramafic mantle melt and mixing scenarios (Tappe and others, 2005; Rogers, 2006).

The Mg/(Mg + Fe) ratios of the analyzed dikes range from 0.20 to 0.90, and, according to Mitchell (1986), the Mg/(Mg + Fe) ratios of kimberlitic magma containing crustal material are less than 0.85. Higher Mg/(Mg + Fe) ratios (between 0.9 and 0.95) in biotite in the Billiton Minner lamprophyre core were determined to be the result of interaction with late-stage high-magnesium alteration fluids (Heck and others, 2006). Many of the dikes in the Coefield Intrusive Complex are high in magnesium and fit into a magnesium-carbonatite category (Figs. 4–5); when these values are plotted, the high-magnesium values form a semi-concentric zonation in the complex. The high iron content (greater than 7 percent) in seven of the dikes examined in this study also suggests that a few dikes may trend toward an iron-rich ferro-carbonatite, as at Caldwell Creek, or assimilations of high iron-dolomite crustal material. Only two dikes, Hutson and Maple Lake, had less than 1 weight-percent iron.

Primary processes are magma melting, mixing, fractionation, and metasomatism, and secondary processes are post-crystallization alteration, MVT mineralization, and post-MVT alteration. The later-stage CO_2 volatile event mixed with MVT fluids to create a series of altered dikes and mineral veins in the district. This suggests that the variable whole-rock chemistry is an indicator of complex source-rock mixing, fractionation, metasomatism, and alteration. The lithologic, petrologic, and mineralogic similarities of the igneous intrusions and fluorite deposits of the Illinois-Kentucky Fluorspar District to economic REE deposits elsewhere in the world (Rock, 1991) raise the level of interest in the

Illinois-Kentucky Fluorspar District for more advanced research and exploration for REE deposits.

Mineralogy of Alkaline Ultramafic Dikes

The mineralogy of the varied lithofacies in these dikes was studied by whole-rock X-ray diffraction (Figs. 6–11). Although the dikes may appear to be homogeneous, many have subtle changes in mineralogy and all of them have been fractionated, altered, or brecciated. The original alkaline ultramafic olivine mineralogy has undergone post-crystalline alteration to form clinopyroxene, serpentine, and carbonate minerals (calcite and dolomite), including the alteration of the titanium mineral ilmeno-magnetite to rutile and leucoxene, as at the Clay Lick dikes. X-ray diffraction studies have noted only one occurrence of olivine, in the Guilless dike, whereas many of the original olivine has been serpentinized, and altered to clinopyroxene, serpentine, and carbonate minerals, some of which are pseudomorphs of the original olivine orthorhombic morphology. Post-MVT-mineralization alteration of sphalerite to smithsonite, and phlogopite to sericite, occurred during the middle paragenetic stage (Hayes and Anderson, 1992), during the Permian Period; where the sphalerite became more reddish orange and accompanied the CO_2-rich alteration of the dike material. The high carbonate and oxide mineral contents suggest an influence by carbonatite-type fluids; the presence of abundant ferro-magnesium silicate minerals such as clinopyroxene and garnets is evidence of a silica fraction in this alkaline melt. No unaltered dikes have been observed in the Western Kentucky Fluorspar District, except at Maple Lake.

Alteration of the dikes and the effects of metasomatism create some areas of mineral enrichment in the Western Kentucky Fluorspar District, particularly near the Coefield Intrusive Complex. Dikes in numerous cores, including from the Minner, Midway-Davidson, and Davidson North dikes and the Coefield Intrusive Complex, contain abundant titanium oxides and REE-bearing perovskites. Although perovskite is common in ultramafic rocks, REE-bearing perovskites are not as common. Rare minerals found in the district include perovskite and niobium rutile (Fig. 6), astrophyllite (Fig. 7), moissanite (Fig. 8), villiaumite, fluoro-tetraferriphlogopite, almandine garnet (Fig. 9), natrite, fluocerite, and wüstite. Sphalerite occurrence (Fig. 10) is also notable, since it provides evidence of mixing of MVT fluids and late-stage igneous alteration fluids. Monazite containing iridium also occurs (Fig. 11).

The following mineral identifications and descriptions are important petrologic indicators of alkaline ultramafic rocks that trend toward carbonatite and REE enrichment. Minerals are listed in order of importance and rarity, and some of them are alteration minerals from post-crystallization stage, MVT stage, and some are ultra-high temperature and pressure xenocryst minerals, probably unaltered. The origin of these rare xenoliths and xenocrysts are deep seated and deserve further research.

1. **Rutile,** $NbTiO_2$, tetragonal, a niobium and titanium oxide, and its polymorph, **anatase** (TiO_2, tetragonal) (Fig. 6); **ilmenite** ($(NiMg)TiO_3$) and **magnetite** (Fe_3O_4) were noted in several cores from the Davidson North and Minner dikes.

   Rutile and anatase have been found in numerous dikes, including the Frontier Spar (core 801), Dike South, Davidson North, Maple Lake, Crittenden Springs, Lady Farmer, Columbia South, Minner, Sunderland, Clay Lick, Robinson, and Cardin dikes. In four dikes, some of these rutiles and anatases are high in niobium. Cerium-bearing anatase ($(TiO_2Ce)O_2$, tetragonal) is present in the Dike South and Sunderland dikes. Some of the more altered dikes have a varied ilmeno-magnetite mineralogy ($(TiFeO_4)(NiMg)TiO_2$, rhombohedron) and various alteration titanium minerals such as leucoxene. The titanium, niobium, and REE were introduced into the magma melt by volatile metasomatizing fluids (Haggerty and Baker, 1967; Haggerty, 1976). Titanium is mobile in alkaline fluids and is altered to titanium oxide (rutile). Niobium rutile is essential in one style of metasomatism related to upper-mantle alkaline rocks and kimberlites (Haggerty and Baker, 1967; Haggerty, 1976) and is stable in high-CO_2 magmas (Barnett, 1995), but becomes de-

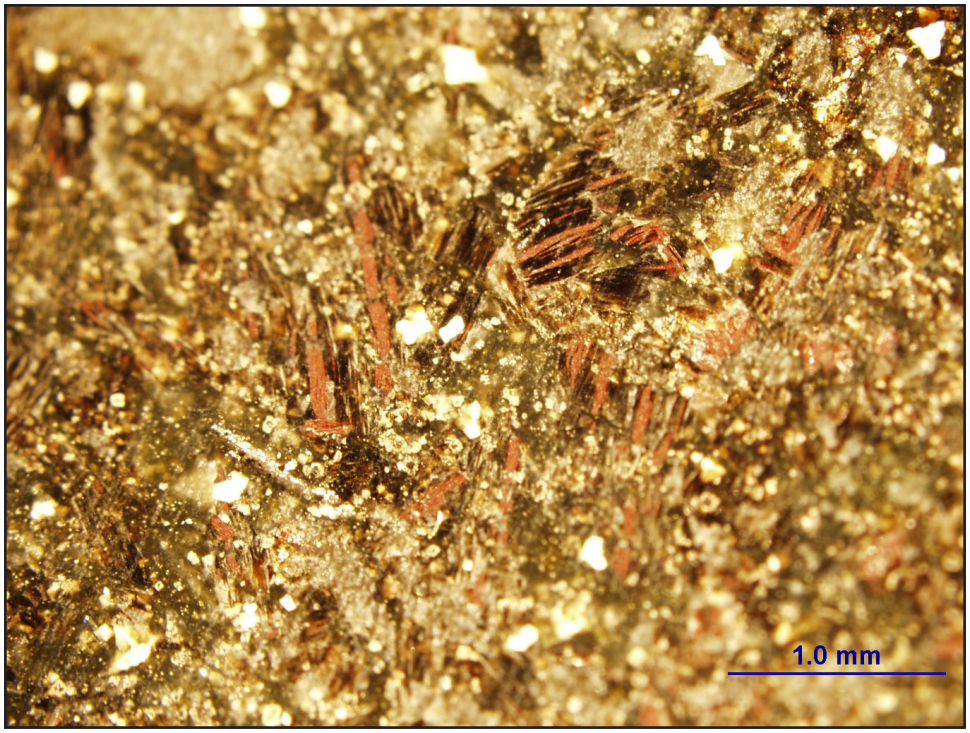

A.

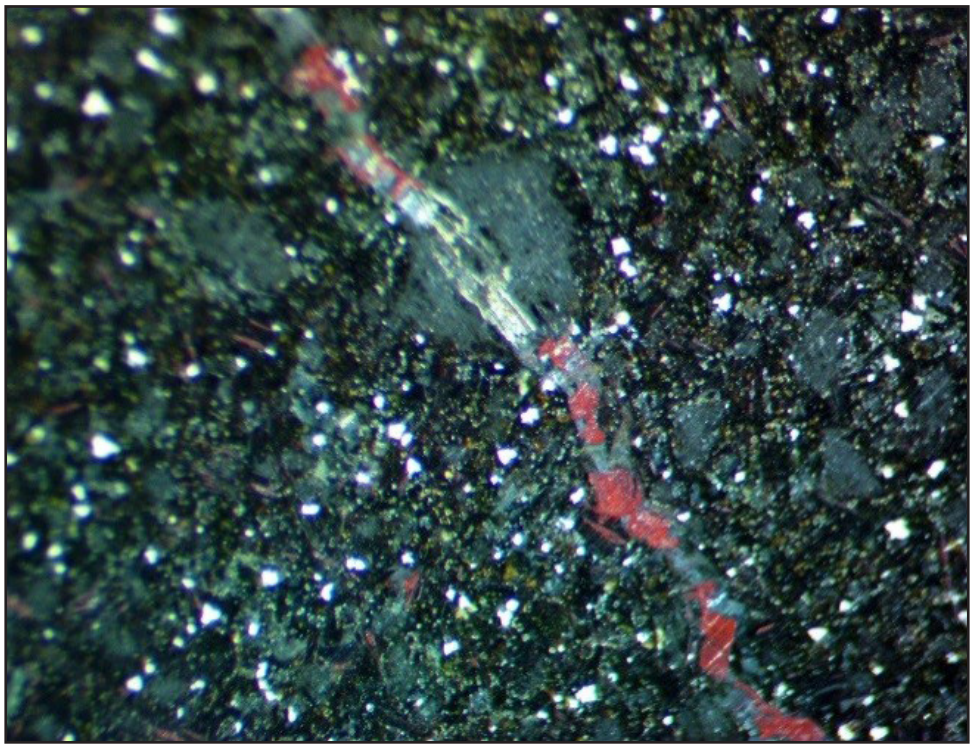

B.

Figure 6. A. Reflected-light photomicrograph of the Davidson North dike (analysis ID YH04_800), Crittenden County, Ky., near the northeastern Babb area and north of the Midway area. This lamprophyre shows post-crystallization alteration of ilmenite to red rutile, as well as white titanium oxide minerals such as leucoxene. Both rutile and leucoxene occur along cleavage planes in biotite and phlogopite. B. Davidson North dike, showing lamprophyre containing abundant clinopyroxene phenocrysts with the white titanium mineral leucoxene, and an alteration vein cutting the dike. The alteration vein has abundant red rutile that has crystallized in the titanium-rich groundmass of the dike, and abundant pyrite crystallized when the vein cut a large iron-rich clinopyroxene silicate crystal. This is an example of the post-crystallization alteration phase.

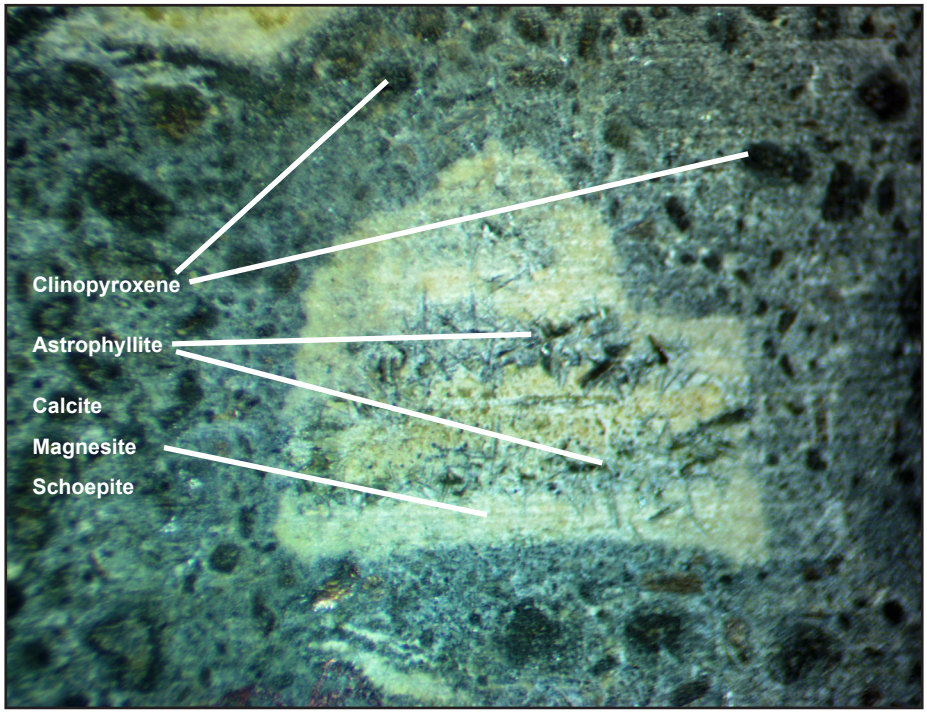

Figure 7. Xenolith in the Minner core (DLP 3, depth 329–330 ft): lamprophyre breccia, located in the Minner area, Crittenden County, Ky. Intrusive magnetic breccia contains mantle xenolith of yellow calcite with black acicular xenocryst crystals of astrophyllite, a potassium, sodium, iron, titanium silicate that contains niobium. Also detected in this xenolith was the yellow mineral metaschoepite, a uranium oxide, as well as magnesite, a magnesium carbonate. Xenolith is 1 in. wide; reflected-light photomicrograph, 2X.

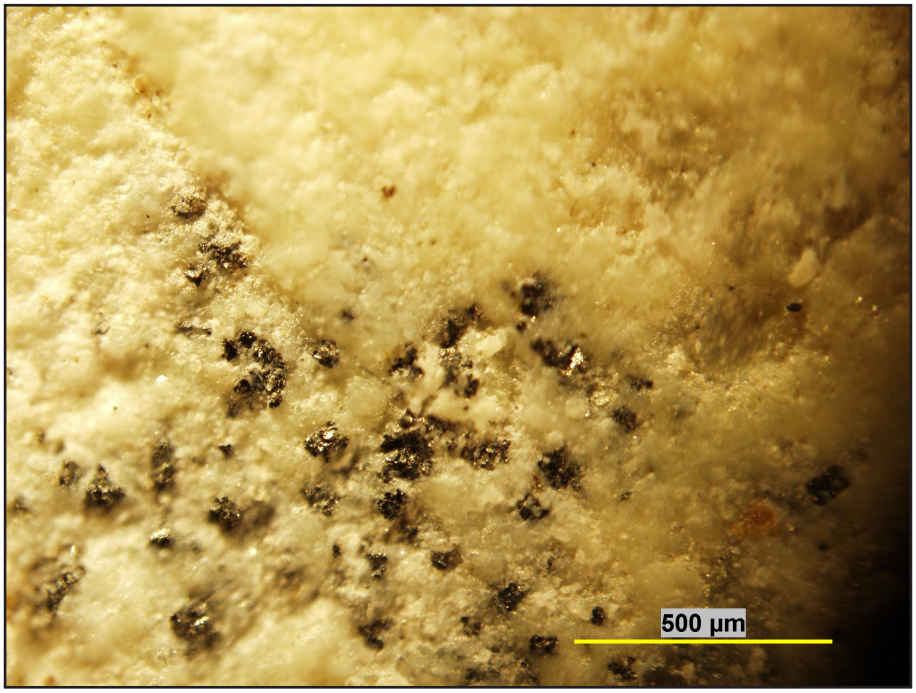

Figure 8. Moissanite (SiC) identified by X-ray diffraction in xenolith in core DLP-3 at 329 ft; Crittenden County, Ky. Moissanite is a very rare mineral that occurs in extremely reduced rocks in the deep mantle; it is sometimes associated with diamonds.

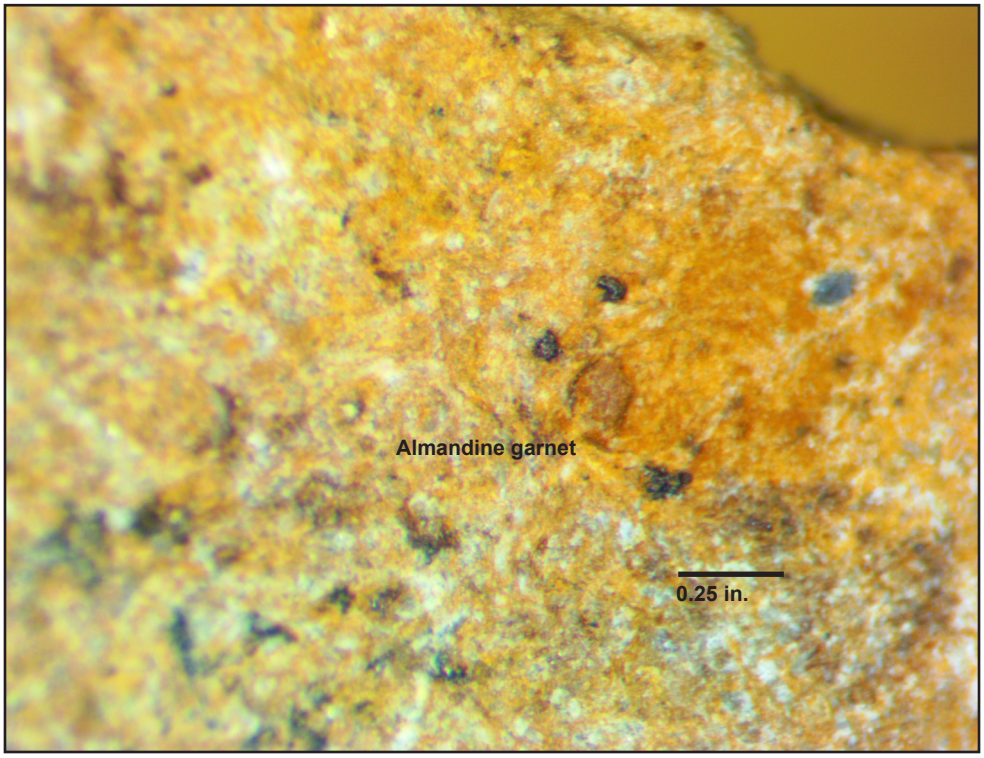

Figure 9. Almandine garnet in an altered dike matrix of calcite, anatase, muscovite, illite, lizardite, and the iron sulfate rozenite. Reflected-light microphotograph of the Hurricane dike, Crittenden County, Ky.

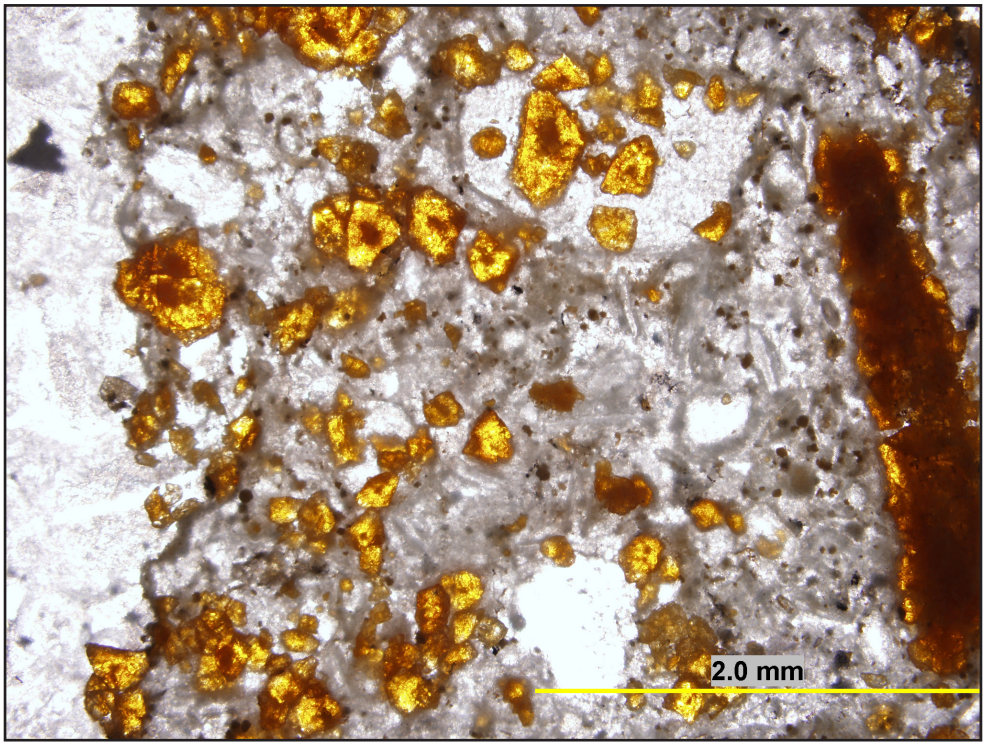

Figure 10. Transmitted-light photomicrograph of core DLP-2, showing the MVT sulfide sphalerite (yellow minerals), at a depth of 824 ft. These sphalerite crystals were emplaced when late-stage igneous alteration fluids mixed with middle-stage, MVT, sphalerite-rich fluids when the sphalerite was emplaced in the igneous dike. This is an example of MVT mineralization, although it occurs during a middle-stage mineralization event, and illustrates sphalerite association with light green, altered dikes.

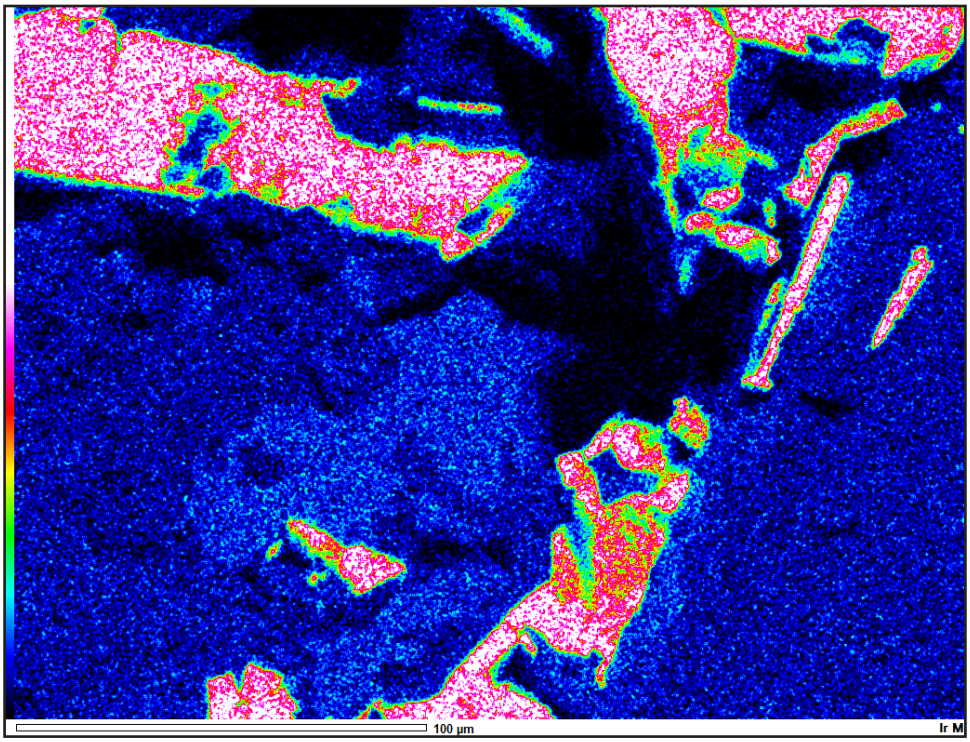

Figure 11. Scanning electron microscope photograph of core DLP-2 at a depth of 112 ft, showing the calcium phosphate monazite with iridium enrichment (red). Blue indicates oxygen and green indicates phosphorus.

stabilized in evolving magmas (Mitchell, 1986), suggesting that the niobium content of rutile and perovskite is important because its occurrence can indicate carbonatite formation. Rutile (Figs. 6a, b) occurs in numerous dikes along biotite cleavage planes and is of special interest since it occurs at the Magnet Cove igneous suite in Arkansas.

2. **Astrophyllite,** K_2Ba (NaCa)(Fe_3Mn,Mg_2 Na)(Ti,Nb)Si_8O_{14}, monoclinic, an ultra-high temperature and pressure, high-magnesium, -potassium, -niobium, -titanium, and -sodium silicate (Fig. 7).

   Astrophyllite was found in several spherical yellow xenoliths in core DLP-3 from the Minner area of Crittenden County. The astrophyllite occurs as black, acicular crystals in a yellow carbonate-syenite xenocryst contained in a matrix of calcium carbonate. Astrophyllite crystals were also detected in the pebble breccia in core BH-7 from the Hutson Mine of Livingston County in the southern part of the Western Kentucky Fluorspar District. Since astrophyllite can be high in niobium and has the niobium-rich end-member niobophyllite ($(K,Na)_3(Fe,Mn)_6(Nb,Ti)_2(Si_8(O(OH)F)_{31}$, triclinic), more work needs to be done to determine the implications for REE content. Astrophyllite occurs in opposite ends of the district and is significant in determination of a differentiated magma material; it also indicates an alkaline-carbonatite petrology beneath the fluorspar district and suggests mantle metasomatism. Astrophyllite also occurs at Magnet Cove, Ark. (Erickson and Blade, 1963), and its type locality is Laven Island near the Kola Peninsula REE complex in Norway and Russia.

3. **Schoepite** and **metaschoepite,** $(UO_2)_4O(OH)_6(H_2O)$, orthorhombic, yellow-green uranium oxides.

   Schoepite and metaschoepite were detected in xenocrysts in core DLP-3 at a depth of 329 ft. These minerals normally occur in hydrothermal mineral and uranium

deposits, and so the schoepite occurrence suggests uraniferious mantle xenocrysts, whereas the metaschoepite suggests hydration of schoepite. **Uraninite** (UO_2) was also detected in core DLP-3.

4. **Moissanite,** SiC, hexagonal (Fig. 8), a metallic ultra-high temperature and pressure silicon carbide.

   Moissanite was detected as crystals in xenoliths in core DLP-3 at 308, 314, 318, and 328–329 ft. It is a naturally occurring silica carbide metal (Fig. 8) and is very rare, occurring naturally only in the deep mantle material, usually in kimberlites and sometimes as inclusions in diamonds (Nixon, 1987). Moissanite is very hard (H=9.5) and only occurs in reducing alkaline ultramafic facies in sublithospheric upper-mantle rocks, kimberlites, and in some meteorites. The type locality is the Canyon Diablo meteorite from Arizona. The origin of moissanite has been suggested to be either from a primordial early mantle near the core-mantle boundary (Mathez and others, 1995) or from a highly fractionated, organic-carbon-rich, extremely reducing ultramafic environment with little to no iron components (Schmidt and others, 2014). Its presence in a xenolith in core DLP-3 from 300–329 ft is significant in that it indicates deep mantle rocks were thrust to near-surface exposure in western Kentucky. Further research should be conducted on wüstite and moissanite in western Kentucky.

5. **Wüstite,** FeO, cubic, iron oxide.

   Wüstite is also an ultra-high temperature and pressure mineral, and was detected by X-ray diffraction in a xenolith in the igneous breccia of core DLP-3, box 2, at 308 and 328–329 ft. Wüstite is very rare and only occurs in reduced, oxide-poor rocks in the lower mantle near the iron/wüstite boundary, where many peridotites, kimberlites, carbonatites, and other ultramafic alkaline rocks originate (Arculus and Delano, 1987). Wüsite is found in kimberlites (Nixon, 1987) and as inclusions in diamonds and meteorites; the type location is in Germany. A potassium richterite, $K(Na,Ca)Mg_5)Si_8O_{22}F_2$, monoclinic, was also tentatively identified in the xenolith from this core.

6. **Spodumene,** $LiAlSi_2O_6$, monoclinic.

   Spodumene, a lithium aluminum silicate of the sodium pyroxene group, was detected in the Hutson core BH-7 at 74 ft and in several xenoliths in core DLP-3. Spodumene is common in peralkaline granitic intrusive pegmatites and has been mined in the Black Hills of South Dakota. Its occurrence in core BH-7 is rare, and the lithium in fluoro-tetraferriphlogopite indicates a possible lithium phase in the fluids.

7. **Fluorides.**

   Numerous fluorides, CaF_2, isometric, cubic, were found in the ultramafic dikes. These unusual fluorides were detected within the altered or brecciated dikes, and their relation to the main ore-stage fluorite indicates there were various cations in the fluids to replace calcium in the fluoride crystal structure. Also notable are visible and microscopic inclusions within the fluorites examined; some barite inclusions were visible to the naked eye, so these inclusions may influence elemental analysis of fluorites.

   a. **Fluocerite,** $(La,Ce,Nd)F_3$, hexagonal, a rare REE neodymium fluoride, was identified at the Columbia Mine in a breccia clast of dike rock. The fluocerite was identified via red fluorescence under ultraviolet light, and its presence was confirmed with whole-rock X-ray diffraction analysis. The fluocerite occurs in a calcite crystal, suggesting an intergrown fluorite and calcite mineralogy that dates from a late-stage dike alteration and brecciation involving CO_2-rich fluids.

   b. **Villiaumite,** NaF_3, isometric, a rare sodium fluoride, was found in a pebble breccia in core BH-7.

c. **Yttrium-bearing fluoride,** $(CaY)F_2$, and **cadmium-bearing fluoride,** CdF_2, were also detected in this sample. An unnamed sodium- and REE-bearing fluoride, $(Ca_9Na,Eu,Lu(PO_4(SiO_2))F$, isometric, was detected in the Davidson North dike, and **yttrium fluorite,** YF_3, orthorhombic, was detected in the Cardin dike.

Fluorides bearing rare earth elements (neodymium, europium, and yttrium) occur in some of the altered dikes, and their relationship to the massive fluorite mineralization needs more research to determine the proper paragenetic sequence and any specific REE-bearing fluoride paragenesis. Fluorescent mineralization was observed in calcite-fluorite crystals at the Columbia Mine, and X-ray diffraction analysis showed fluocerite, a REE fluoride. The abundance of fluorides in the dikes, consisting of calcium fluorides, cadmium fluorides, sodium fluorides, REE-bearing fluorides (fluocerite), and yttrium-bearing fluorides, indicates abundant REE in the melt system that allowed them to replace the calcium in the fluorine crystal structure. The dike fluorite may be an initial phase or prolonged phase of the hydrothermal-metasomatic fluorite mixing with MVT fluids. Sodium-rich fluorite, such as villiaumite, may have been a component of the silica and carbonate fluids formed by liquid immiscibility during metasomatism.

8. **Mica.**

a. **Fluoro-tetraferriphlogopite,** $K(Mg_3LiNa)(Si_3,FeO_{10})F_2$, monoclinic.

Fluoro-tetraferriphlogopite is a rare fluoro-mica and was identified in the Davidson North dike, Robinson dike, and in core DLP-2 at 112 ft by X-ray diffraction. The type locality for this mineral is the Bayon Obo Complex in China (Miyawaki and others, 2011) and it has also been described in the Lovozero ultramafic complex in the Kola Peninsula, Russia (Mitchell and Chakhmouradian, 1996). These rare micas are usually bladed in appearance, and more detailed work on the micromineralogy is needed to determine evolving trends toward carbonatite or lamproite facies. This is a rare bladed mica whose petrogenesis is complex, but it forms during late-stage fractionation, and usually indicates an evolving reduced magma in which phlogopite evolves to **tetraferriphlogopite** containing iron and titanium and incorporating fluorine and barium in the crystal structure while displacing aluminum. Tetraferriphlogopite is known to occur in olivine lamproites (Mitchell, 1993). **Annite,** a potassium iron-rich member of the mica group, was noted in core DLP-3. The presence of fluorine suggests an abundant fluorine source, as does the occurrence of lithium and sodium, and further suggests a depleted aluminum source is available for these micas to form.

b. **Vermiculite,** $Mg_3(Si,Al)_4O_{10}(OH)_24H_2O$, monoclinic.

Vermiculite, an aluminum clay mineral, is an altered form of biotite mica commonly found in carbonatite deposits. It was found in the Guilless Mine, Minner Mine, Caldwell Creek area, and DLP core xenoliths. **Garnierite,** $(Ni,Mg_3)Si_2O_5(OH_4)$, a green nickel magnesium layered silicate, was detected in core MLK-1 at a depth of 424 ft, and barium mica was noted in core BMN-7**.**

9. **Garnets.**

a. **Schorlomite,** $Ca_3(Ti,Fe)_2((SiTi)O_4)_3$, isometric, a titanium garnet; **andradite,** $Ca_2(Fe,Ti,Al,V,Mn,Na)_2(SiO_4)_3$, isometric.

Both schorlomite and andradite are high-titanium garnet and sometimes synonymous with each other in alkaline ultramafic rocks. Schorlomite occurs in cores BMN-7 and DLP-3, and

Koenig (1956) identified titanium garnet in the Shell No. 1 Adams core from the Minner area in the Coefield Intrusive Complex. The high-titanium garnet is generally associated with REE in carbonatite, including at the type locality in Magnet Cove, Ark. An iron andradite was found in the Stout dike.

b. **Grossular** and **hibschite garnet,** $Ca_3Al_2Si_3O_{12}$, isometric.

These garnets have been found in the BMN-7 and DLP cores; aluminum andradite has been found in the Frontier Spar core north of the Hutson Mine dike.

c. **Almandine garnet,** $Al_2Fe^{+2}(SiO_4)_3$, isometric.

Almandine has been found in the Hurricane (Fig. 9), Fowler, and View dikes, and in the Shell No. 1 Adams and Hampton Joy 13 (at 277 ft) dike cores.

d. **Morimotoite,** $(Ca_2MgNa)(Ti,Fe,Al,Zr,Mg,Mn)Si_3O_{12}$.

Morimotoite, an iron titanium sodium garnet, type locality in Japan, has been found at Magnet Cove, Ark., and was detected in core DLP-3 at 318 ft. This high-iron garnet contains less titanium than schorlomite and is derived from a low-oxygen fugacity magma (Henmi and others, 1995).

e. **Uvarovite,** $Ca_3Cr_2(TiSi_3O_{12})$.

Titanium chromium uvarovite garnet was detected in core DLP-3 at 339 ft.

The high-titanium garnets schorlomite and andradite; a high-calcium garnet, grossular; and a high-iron garnet, almandine, might suggest the original melt was a peridotite-nepheline syenite material that underwent some element partitioning or that could be an overlapping alnöite-aillikite-kimberlite-carbonatite type of body (Fig. 5). A manganese garnet, **henritermierite,** was also detected. The lack of pyrope garnet is not encouraging for the potential discovery of diamonds in any kimberlite fraction; however, the carbon-rich nature of the magma and metasomatic events could influence diamond formation. There were also several garnets in core DLP-3 at depths of 332 and 338–339 ft that were not properly characterized or named.

10. **Sphalerite,** $Zn(Fe)S_2$, isometric.

Sphalerite has been found in or associated with numerous dikes in the Western Kentucky Fluorspar District, including five altered dikes: Old Jim, Hutson, Robinson, Minner, and Sunderland. Sphalerite was also detected in core DLP-2 at 824 ft (Fig. 10). These dikes contain visible sphalerite, sometimes abundant, both brown and reddish orange, and the presence of sphalerite in the altered dikes indicates a mixing of MVT fluids and CO_2 igneous fluids, causing dike alteration. A carbon dioxide alteration of the dike at the Old Jim Mine suggests alteration of both the dike rock and the accompanying sphalerite (zinc sulfide) mineralization, which altered to **smithsonite,** a zinc carbonate. Smithsonite occurs in several dikes.

a. The Old Jim dike has been mined for smithsonite ($ZnCO_3$, trigonal) and sphalerite. **Arsenopyrite,** $FeAsS_2$, monoclinic; **pyrite,** FeS_2, isometric; and **molybdenite,** MoS_2, hexagonal, were also detected in the Old Jim dike by scanning electron microscope backscatter analysis. **Pyrite** and abundant coarse- and fine-crystalline calcium carbonate were readily observed in thin section.

b. The Hutson Zinc Mine and dike were mined for sphalerite. Core examination and X-ray diffraction analysis of the dike confirmed sphalerite, and unusual REE-bearing fluorides and sodium and barium carbonates were also identified.

c. The Robinson dike is altered and contains large quantities of brown sphalerite, easily visible in hand samples of core, and the dike is high in niobium. X-ray diffraction confirmed fer-

roan sphalerite and several sodium zinc sulfates: **gordaite,** $NaZn_4(SO_4)(OH)_6Cl \cdot 6H_2O$, trigonal; and the iron sulfate **rosenite,** $FeSO_4(H_2O)_4$, monoclinic.

d. Core DLP-2 at a depth of 824 ft, located in the Minner area, contains yellowish orange sphalerite crystals in an altered dike (Fig. 10), and **langbeinite,** an iron sulfate, at a depth of 824 ft in the DLP-2 core. These sulfates indicate oxidation of sulfide mineral deposits and are interpreted to be a result of late-stage CO_2 alteration of the dikes.

Zinc concentrations in dikes (Figs. 4, 10) ranged from 10 to 350 ppm, and there are numerous associations of dikes and zinc deposits occurring as a mid-stage MVT deposit, in which both brown and reddish orange sphalerite occurred in altered dike intrusion material. Previous paragenetic studies (Hayes and Anderson, 1992) indicate that the MVT fluids introduced sphalerite into the dike alteration fluids during a middle paragenetic sequence of brown to reddish orange sphalerite mineralization.

11. **Carbonates.**

Some of the igneous xenoliths in cores DLP-2 and DLP-3 contain calcite, dolomite, and magnesite, which could be igneous carbonates; more isotopic work is needed on these minerals. Carbonates of interest are:

a. **Magnesite,** $MgCO_3$, hexagonal.

Magnesite was detected in the DLP cores.

b. **Natrite,** Na_2CO_3, monoclinic, sodium carbonate.

Natrite is found in core BH-7 and is a common mineral in peralkaline rocks in continental rift basins such as the New Madrid Rift. The type locality for natrite is the Lovozero ultramafic complex in Russia.

c. **Witherite,** $BaCO_3$, orthorhombic, a barium carbonate; smithsonite, $ZnCO_3$, hexagonal, zinc carbonate.

Witherite was detected at the Clay Lick dike and in the Hutson Mine core BH-7. Traces of **rhodochrosite** ($MnCO_3$, rhombohedral), a manganese carbonate, have been detected in a Billiton core (BCS-2B) from Crittenden Springs.

d. **Smithsonite,** $ZnCO_3$, hexagonal. The Old Jim dike is an oxidized igneous dike containing smithsonite, a large zinc deposit in a carbonate-rich vein deposit. This vein contains coarse-crystalline carbonate and very fine-crystalline replacement carbonate containing abundant smithsonite. Numerous dike/vein combinations contain smithsonite.

In addition to the ubiquitous calcium and magnesium carbonate in many altered dikes, the presence of **ankerite** ($MgFeCO_3$) and **rhodochrosite** ($MnCO_3$) and all carbonate minerals indicates a variable carbonate influence in the dike system.

12. **Perovskite,** $CaTiO_3$, orthorhombic.

A high-pressure mineral, perovskite is common in lamprophyres, but in several of the dikes of the Western Kentucky Fluorspar District, REE-bearing perovskite occurs, which is more unusual. The REE-enriched perovskites are similar to those at their type localities, which are in the Kola Peninsula, Russia (Mitchell and Chakhmouradian, 1996). For example, numerous forms of perovskite occur in core BMN-7: cubic ($Ba(InW)O_3$,Ba_2YTaO_6), monoclinic (Pr,Na,MnO_3), orthorhombic ($La(NiO_3)$), and orthorhombic (Eu_3InO) europium perovskite oxides—some of which are double perovskites ($Ba_2Na(ReO_6)$). Other variations occur that incorporate lanthanum, yttrium, tantalum, niobium, and nickel such

that they mimic the loparite perovskites ((Ce,Na,Ca)(TiNb)O_3, cubic) solid solution series. High-REE perovskites have been found in kimberlites and are common in carbonatites (Mitchell, 1986). These oxides form a layered structure, and many have been identified as double perovskites. Perovskites are important REE carriers during fractionation in magma melts (Beyer and others, 2013). The perovskites in the Western Kentucky Fluorspar District should be compared to those from the Lovozero deposit in Russia because of the high REE content in loparite, a member of the perovskite solid solution series. Some of the REE-rich perovskites in core BMN-7 are similar to loparite and suggestive of ultramafic lamprophyre and lamproite lithology.

13. **Phosphates.**

    Fluorapatite, $Ca_5(PO_4)_3F$, hexagonal, was identified in the Hutson, Davidson North, Guilless, and DLP-2 core dikes. A rare occurrence of **monazite,** (Ce,La,Y,Th)PO_4, a REE phosphate, was detected by X-ray diffraction in core DLP-2 at 112 ft; iridium was also detected and confirmed in this core by scanning electron microscope analysis (Fig. 11).

14. **Zircon,** $ZrSiO_4$, tetragonal.

    Zircon was detected in the xenoliths of cores DLP-2 and DLP-3, where this study found several occurrences of zircon. Although zirconium concentrations were high in many dikes, zircon crystals are rare in high-alkaline fluids.

15. **Other minerals.**

    Pure carbon, C, cubic, was detected in core DLP-3-332A, as well as a possible silicon carbide, but more work needs to be done on these rare minerals. **Spinel,** $(MgAl_2)O_4$, octahedral, was also detected in four separate dikes: Davidson-Midway, Minner 7, Clay Lick, and in the Pennwalt (597-V) core. A sodium tourmaline and abundant calcite, dolomite, and another sodium carbonate were also detected at the Old Jim Mine. **Topaz,** $Al_2SiO_4(OH)F$, was detected in the Stout dike, and **manganite,** $Mn_2O_3H_2O$, monoclinic, and a manganese oxide were detected in core BH-7-74 from the Hutson Mine. **Spodumene,** a lithium silicate, represents a lithium phase, and the phosphates are important carriers of REE. Other metallic minerals of interest, including **jamborite** (Ni,Co(OH)$(SO_4)H_2O$), **cooperite** (PtS), **carlinite** (Ti_2S), **wairauite** (CoFe), **zinc nickel ferrite** ((Zn,Fe)(Ni,Fe)O_4), and **hibonite** ((Ca,Ce)$(Al,Ti,Mg)_{12}O_{19}$) were detected in an igneous breccia in core DLP-3 at a depth of 300–340 ft. **Wollastonite,** $CaSiO_3$, was detected in several xenoliths in core DLP-3. **Pyrite, arsenopyrite, chalcopyrite, bornite,** and **molybdenite** were also detected in the Old Jim Mine, determined by scanning electron microscope backscatter imaging.

There are several unusual minerals in xenoliths in cores from within or near the Coefield Intrusive Complex, including cores DLP-2 and DLP-3, and Davidson North and Minner cores. Some of these xenoliths contain both sodium- and potassium-rich minerals, including the sodium and some unnamed garnets, which could suggest a syenite facies. Calcium carbonate and calcium silicates could suggest an igneous calcite. A high-temperature silicate, tridymite, was detected in several xenoliths. Additional spodumene, zircon, metal sulfides, and oxides, including uraninite, were also identified, but more analysis is needed to determine any xenolith source rocks. The presence of these minerals is significant because many of them have never before been noted in or described for the Western Kentucky Fluorspar District, and the variability of their occurrence indicates that the dikes represent a wide spectrum of lithofacies of an alkaline igneous complex. Many of these rare minerals imply deep mantle sources for the mantle-derived igneous rocks of the district, including depths near the wüstite-iron boundary in sublithospheric mantle rocks.

REE in Dikes

Background. REE are enriched in magma melts, depending on the degree of melting, fractionation, and metasomatic influence and the final petrologic lithofacies. Normally during fractionation, low degrees of partial melting of mantle peridotite will enrich the LREE and in the presence of garnet, buffer the HREE (Figs. 12–19). The La/Yb ratio is frequently used to measure the degree of fractionation, enrichment, and depletion in an igneous body; Kay and Mahlburg-Kay (1991) used La/Yb, Tb/Yb, and Sm/Yb ratios to record degrees of melting and fractionation.

Carbonatites contain the most enrichment of REE in the world, and their La/Yb ratios generally range between 100 and 1,000. According to Mitchell (1986), some kimberlites have a La/Yb ratio of 80 to 200, and Tappe and others (2005, 2006) stated that the La/Yb ratio should range between 70 and 130 for extremely fractionated magmas. High-titanium kimberlites have La/Yb ratios greater than 70 (Kononova, 1984) and an extremely fractionated kimberlite body would have higher La/Yb ratios, greater than 100 (Mitchell, 1986). Extremely high La/Yb ratios (greater than 100) have not been observed in the Western Kentucky Fluorspar District, which implies the lower La/Yb ratio and Ti/Eu ratio represent a moderately fractionated, nonkimberlitic source rock (Figs. 12–19). According to Liu and others (2011), La/Yb ratios for Chinese fractionated nepheline syenites range from 29.1 to 36.1, much lower values and a much smaller range than for kimberlites. Similar studies in the East African Rift (Eby and others, 2003) suggest that high-titanium garnets increase Tb and Yb concentrations in the source rocks because of garnet-present versus spinel-present melting and fractionation (Rogers, 2006). The presence of clinopyroxene and garnet in a melt causes enrichment of LREE and depletion of HREE (Hanson, 1980). Analysis of clinopyroxene has been used to examine the La/Yb versus Ti/Eu ratios to discriminate between carbonatite and silicate metasomatism (Rudnick and others, 1993; Coltorti and others, 1999). The presence of plagioclase in a melt can produce a negative europium anomaly. Titanium and silicon have been used to analyze kimberlite and lamproite facies, in which lamproite contains higher silicon and kimberlite contains higher titanium (Kononova, 1984). High-titanium magmas, similar to those that formed the Coefield Intrusive Complex, have a high La/Yb and Tb/Yb ratio (Fig. 13). Compared to other lamproites (Rock, 1991), low values of barium, strontium, zirconium, and lanthanum suggest that there is unlikely to be a lamproite facies in this dataset.

Niobium-bearing rutile occurred in several dikes and is a pathfinder mineral for carbonatite petrology (Mariano, 1989; Beattie, 1993; Green, 1995); it assists in melt partitioning of the incompatible elements niobium, tantalum, zirconium, hafnium, and yttrium. During fractional crystallization, REE are enriched, but each of the incompatible elements are not easily fractionated and instead change during metasomatism, during which zirconium increases compared to hafnium and yttrium (Rudnick and others, 1993). Enrichment of these elements suggests carbonatite metasomatism has enriched niobium (Fig. 18). Post-crystallization perovskite alteration to rutile/anatase is a measure of late-stage CO_2-rich alteration events (Haggerty and Baker, 1967; Haggerty, 1976) and indicates carbonatite formation. Niobium is of special importance because it seems to increase in more evolved rocks, as in the carbonatite at Magnet Cove, Ark. (Erickson and Blade, 1963), which contains higher niobium concentrations (4–9 percent) than the associated syenite-type rocks.

Experimental data from partitioning studies related to ratios of U/Th and La/Yb (Beattie, 1993) also suggest that melt excesses in the garnet stability field allow fractionation of thorium from uranium, and confirm some data shown in Figure 16 that indicate increased thorium fractionation in the Coefield Intrusive Complex.

Discussion of Elemental Data From Dikes. Chondrite-normalized REE patterns of the dikes analyzed in this study (Figs. 12–19) show a family of alkaline dikes with variable enrichment of LREE. Ratios of La/Yb are an estimate of the enrichment of LREE (lanthanum) and HREE (ytterbium). La/Yb ratios (Figs. 12–15) illustrate the set of ultramafic dikes at the Coefield Intrusive Complex with values between 55 and 75, significantly higher than for the other analyzed samples. This same family of dikes has LREE enrichment (Figs. 12–13) and a trend toward carbonated peridotite (Figs. 13–14).

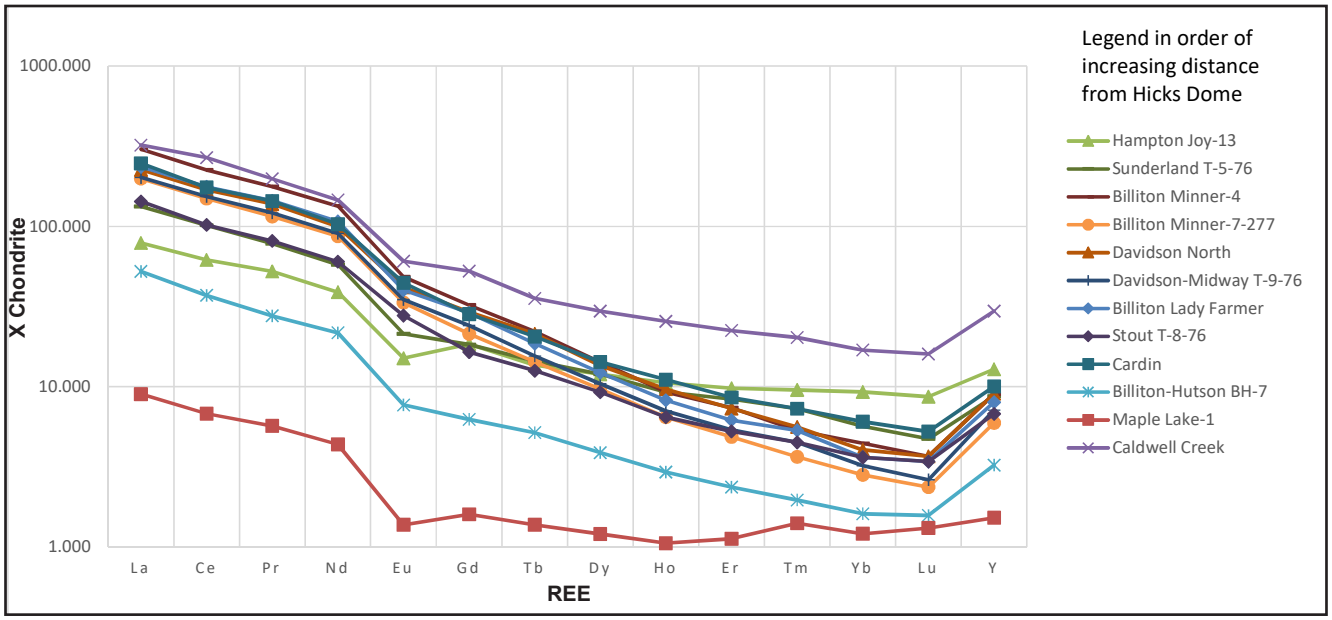

Figure 12. Normalized REE concentrations of selected dikes in the Western Kentucky Fluorspar District. The moderate slope suggests a low percentage of the magma melt and fractionated enrichment of LREE in all dikes. Higher values of LREE in the Coefield Intrusive Complex indicate an enrichment event trending toward carbonatite values, whereas the Maple Lake values reflect a depleted mantle composition of total REE. A complex metasomatism, less garnet influence, or higher degree of melting and less fractionated enrichment may be explained by crossover values from the Hampton Joy and Sunderland dikes. Caldwell Creek and Maple Lake dikes, both of which are located farthest from Hicks Dome but geospatially within a mile of each other, have contrasting concentrations of REE. High REE concentrations at Caldwell Creek and low REE concentrations at Maple Lake suggest a reactivated plumbing system, one containing a primitive dike (Maple Lake) and the other a metasomatically enriched dike (Caldwell Creek).

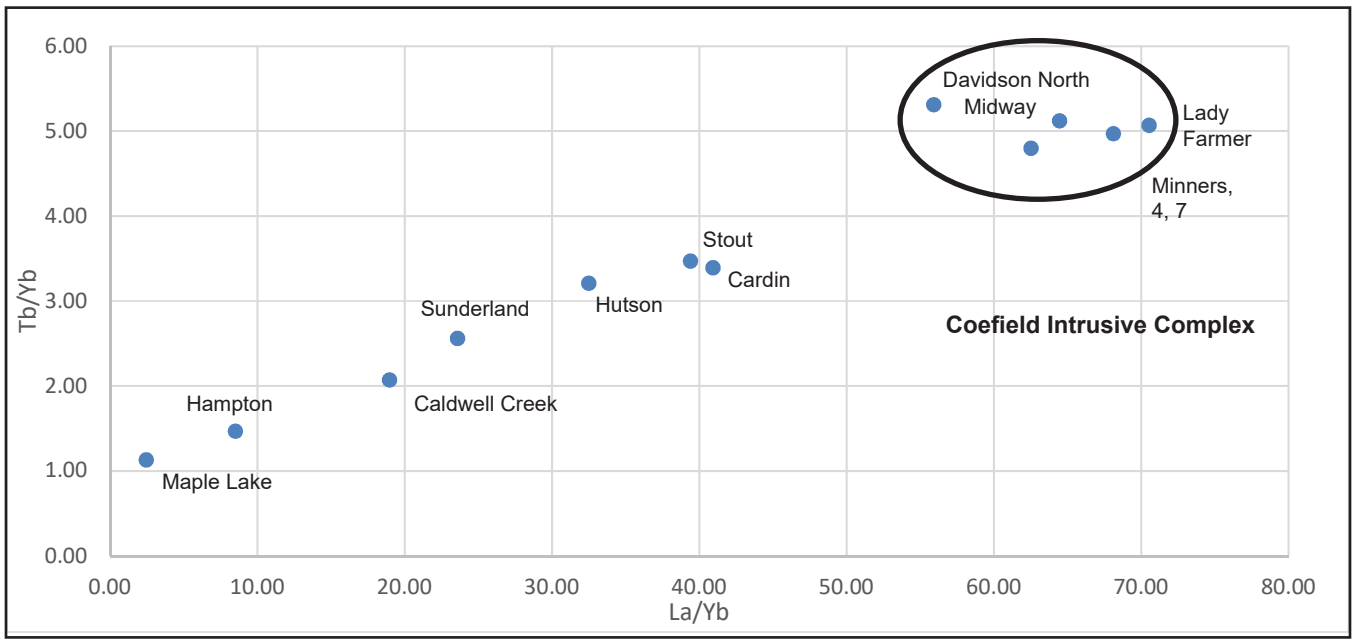

Figure 13. La/Yb ratios versus Tb/Yb ratios (light to heavy rare earth elements) are indicative of fractionated melt crystallization and metasomatism of high-titanium alkaline ultramafic magmas in the Western Kentucky Fluorspar District. The linear trend from lower to higher La/Yb and Tb/Yb ratios at Coefield and Midway indicates carbonatite metasomatism and the enrichment of REE-bearing dikes in the Coefield Intrusive Complex.

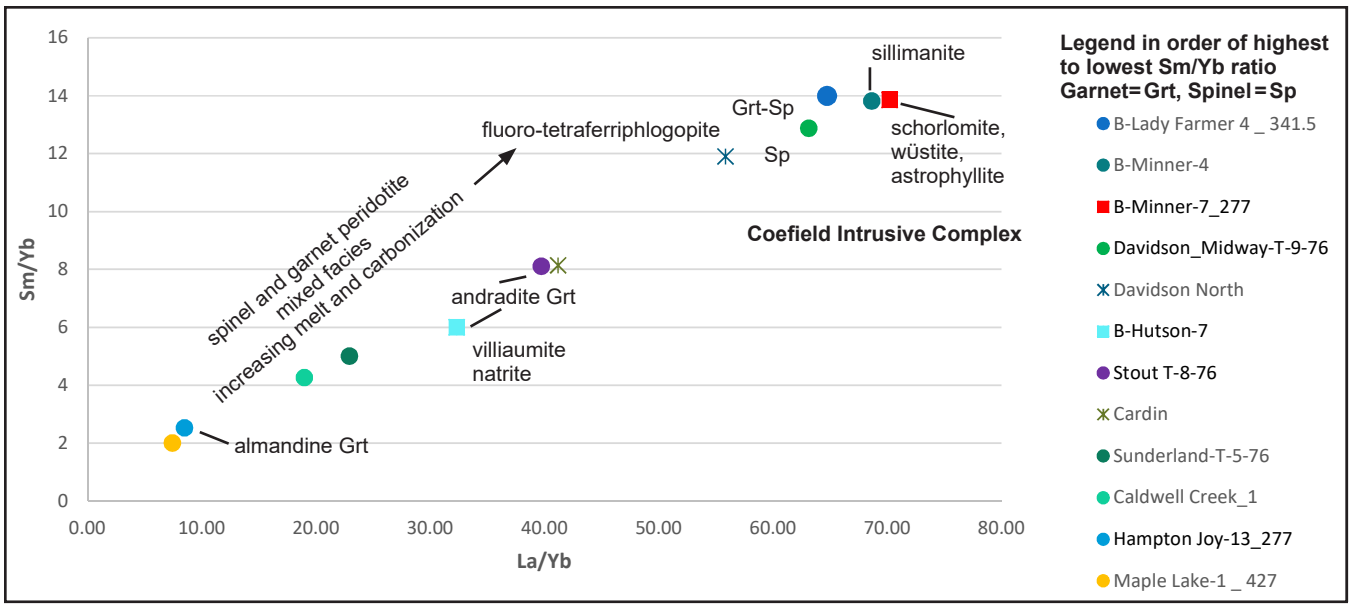

Figure 14. Bivariate linear plot of La/Yb ratio versus Sm/Yb ratio shows significant changes in dike mineralogy for an evolving peridotite melt. Titanium increases in the melt during calcium-titanium garnet crystallization, and the metasomatism or carbonization of peridotite increases REE ratios toward the Coefield Intrusive Complex field. In the model hypothesized in this study, a dynamic melt with xenocrysts of deep-seated mantle material evolved to a high-titanium garnet peridotite lithofacies containing enriched concentrations of La/Yb and Sm/Yb caused by melting in the garnet stability field and mantle metasomatism.

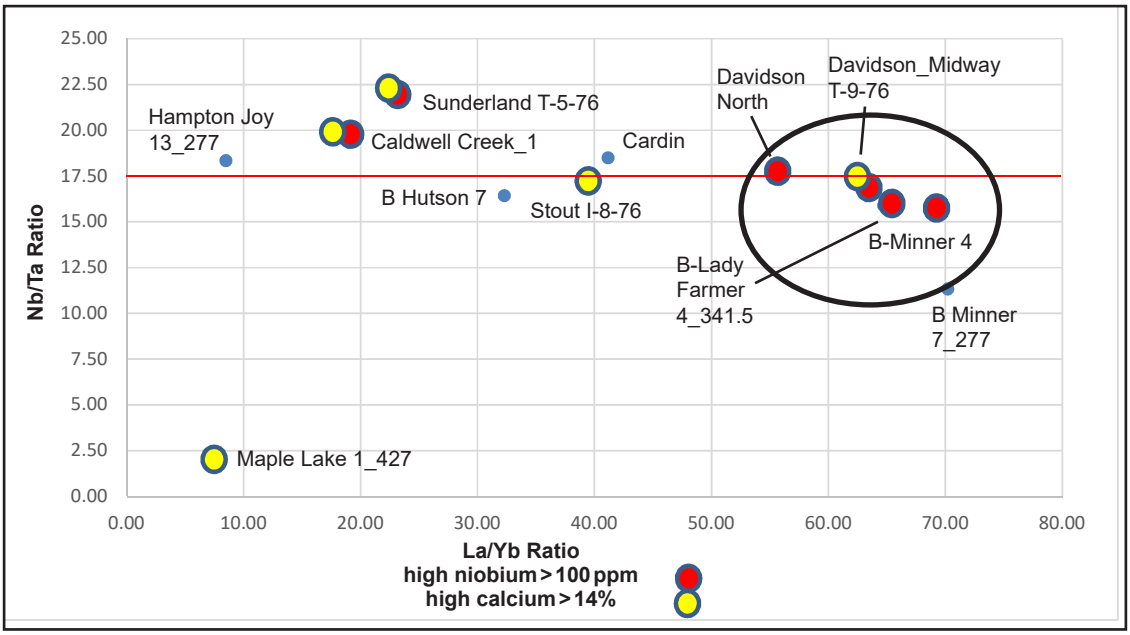

Figure 15. Plot of whole-rock La/Yb and Nb/Ta ratios shows elevated concentrations in both superchondritic (greater than 17.5 Nb/Ta ratio) and subchondritic (less than 17.5 Nb/Ta ratio) niobium-rich ilmenite and rutile fields. Titanium-niobium-rich phases partially control fractionation in magma melts (Beattie, 1993; Green, 1995), and these two clusters of data give some insight into the mantle-sourced magmas in the Western Kentucky Fluorspar District. Fractionation of ilmenite and rutile suggests that magma was generated in the superchondritic melt and fractionated niobium to create higher Nb/Ta ratios in a superchondritic peridotite (Sunderland and Caldwell Creek dikes). The near-chondritic and subchondritic data with La/Yb ratios greater than 50 may record a high degree of partial melting (or remelting) and metasomatism of a garnet peridotite facies containing dikes with high La/Yb ratios (50–70) in the Coefield Intrusive Complex. These subchondritic compositions may also represent mixing with a crustal component or depleted metasomatic fluids, which produced slightly enriched REE in peridotite in dikes of the Coefield Intrusive Complex.

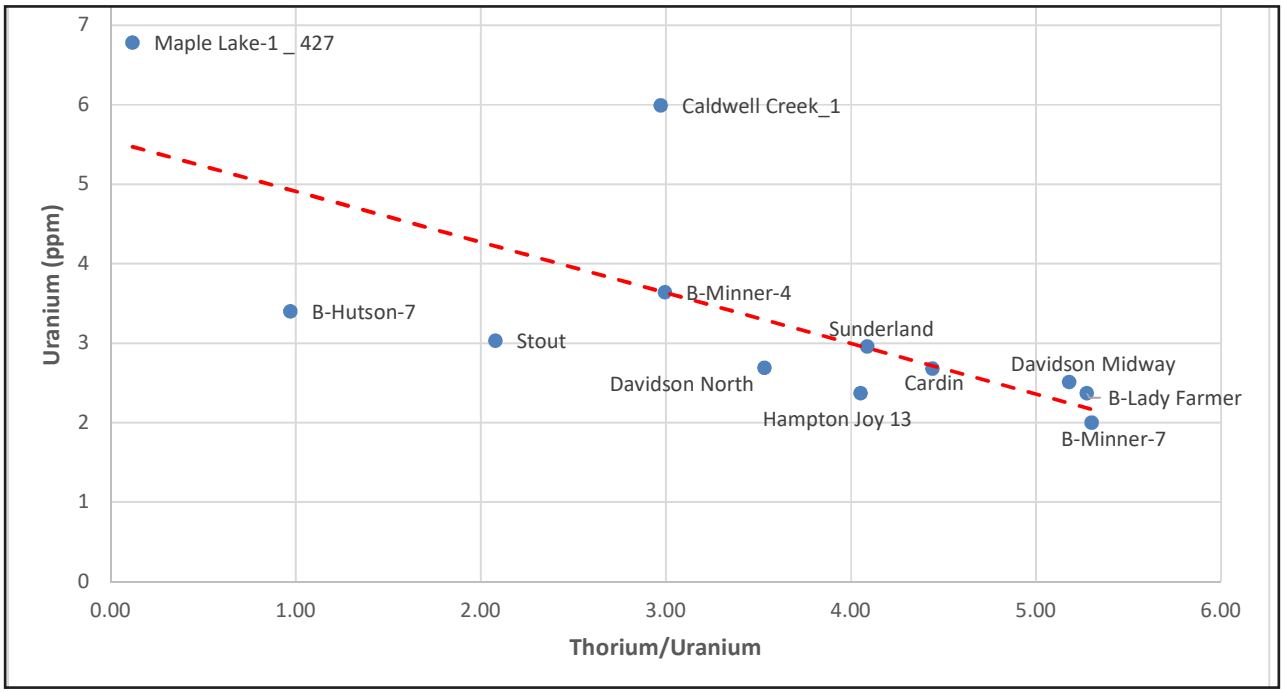

Figure 16. Bivariate diagram of whole-rock uranium/thorium element fractionation, which is thermal-inducing in magma melts; their partitioning is indicative of the degree of partial melting and fractionation. The trend line demonstrates thorium enrichment and uranium depletion during these events, and increasing Th/U ratios toward the Coefield Intrusive Complex, which is the site of high-titanium garnets. Thorium fractionation from uranium generates a thermal engine for further metasomatism. Fluoro-phosphate mineralogy is abundant in these dikes and probably accounts for most of the radionuclides, since X-ray diffraction found only two zircons and one monazite in core DLP-2.

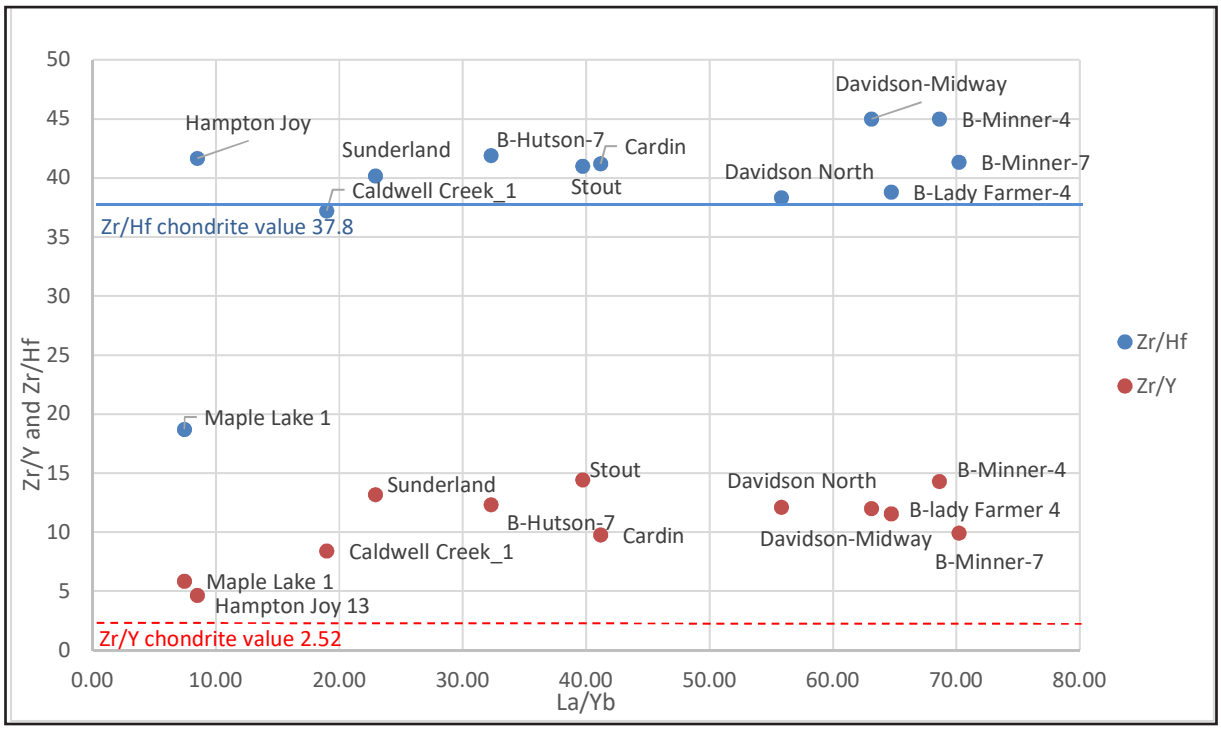

Figure 17. Zr/Y and Zr/Hf ratios versus La/Yb ratios, showing superchondritic dikes in both sample sets, which indicates mantle and metasomatic geochemical enrichment in the Western Kentucky Fluorspar District.

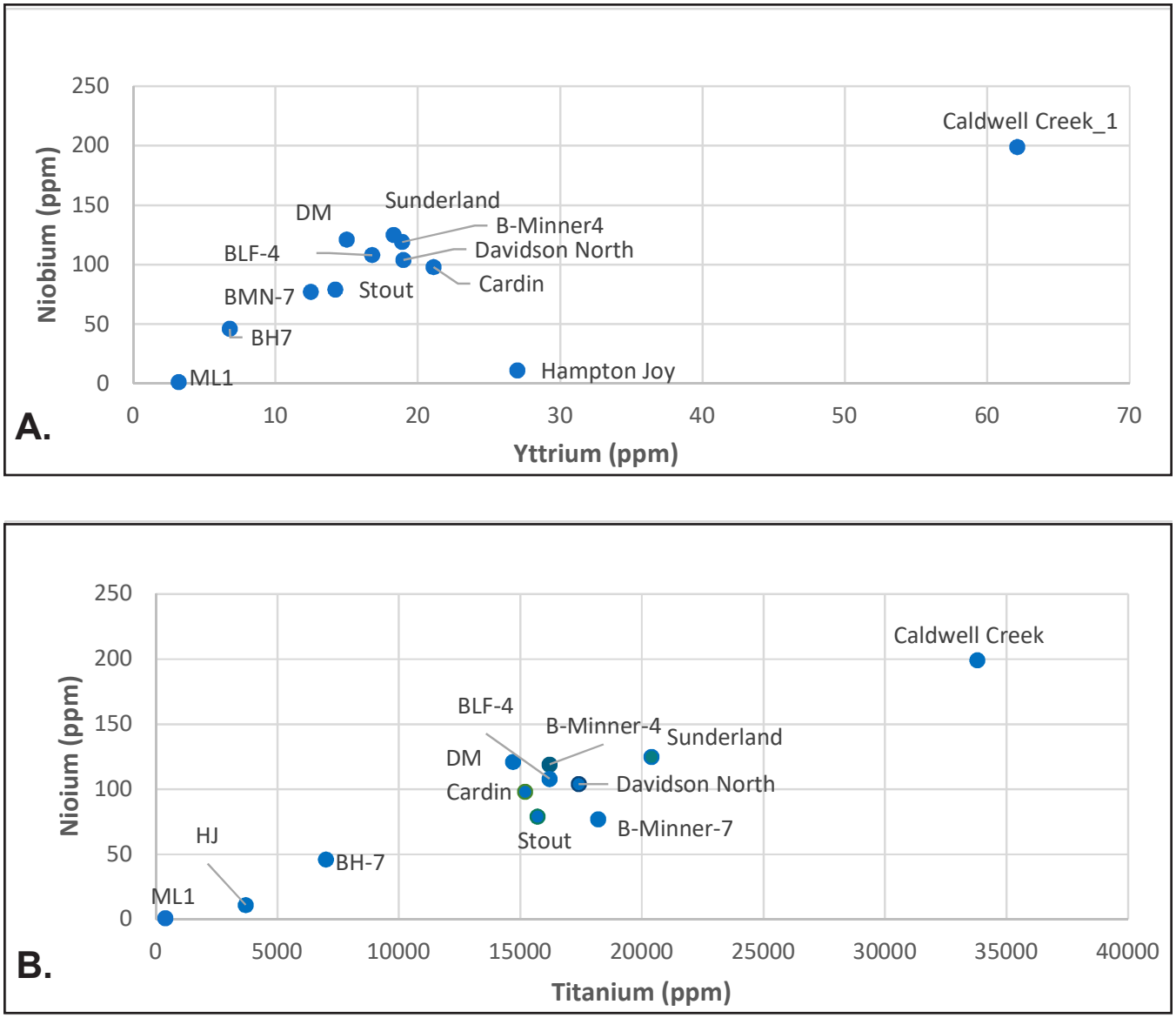

Figure 18. A. Increasing niobium and yttrium concentrations suggest some variable degrees of partial melting and enrichment in a fractionated titanium-niobium-rich carbonatite near the Coefield anomaly. The high-niobium cluster around the dikes of the Coefield Intrusive Complex became enriched in a melt and the high yttrium, niobium, and titanium concentrations suggest further alkaline mantle metasomatism in these incompatible elements at Caldwell Creek. Imenite was detected at Minner and in the Coefield Intrusive Complex, and abundant niobium-rich rutile (anatase, brookite) was detected at the Davidson North, Sunderland, Lady Farmer, and Minner dikes; yttrium-fluorite was detected at the Cardin dike. These enrichments are commonly associated with enriched alkaline deposits in carbonatites or nepheline syenite source rocks. B. Ti/Nb ratio shows increasing niobium in response to increased differentiation of high-titanium magma. The most important data points in these plots are the Caldwell Creek concentrations of niobium, titanium, and yttrium, which, when combined with the high La/Yb ratio (Fig. 12) are highest in the district. This suggests another source of high-REE enrichment in the district and implies that another carbonatite or metasomatic alteration event was centered in the southern part of the district near the Tabb Fault System.

Numerous dikes are enriched in LREE (Fig. 12); normalized values are shown for Caldwell Creek, BLF-4 Lady Farmer, BMN-4 Minner, and BMN-7 Minner dikes (Figs. 12–13). Depletion of LREE occurs at Maple Lake and Hutson dikes. Maple Lake and Hampton Joy dikes have minor europium depletion, whereas Stout, Minner, and Cardin dikes have slightly positive europium anomalies, although not significant enough to be used as a petrogenetic indicator. The range of raw

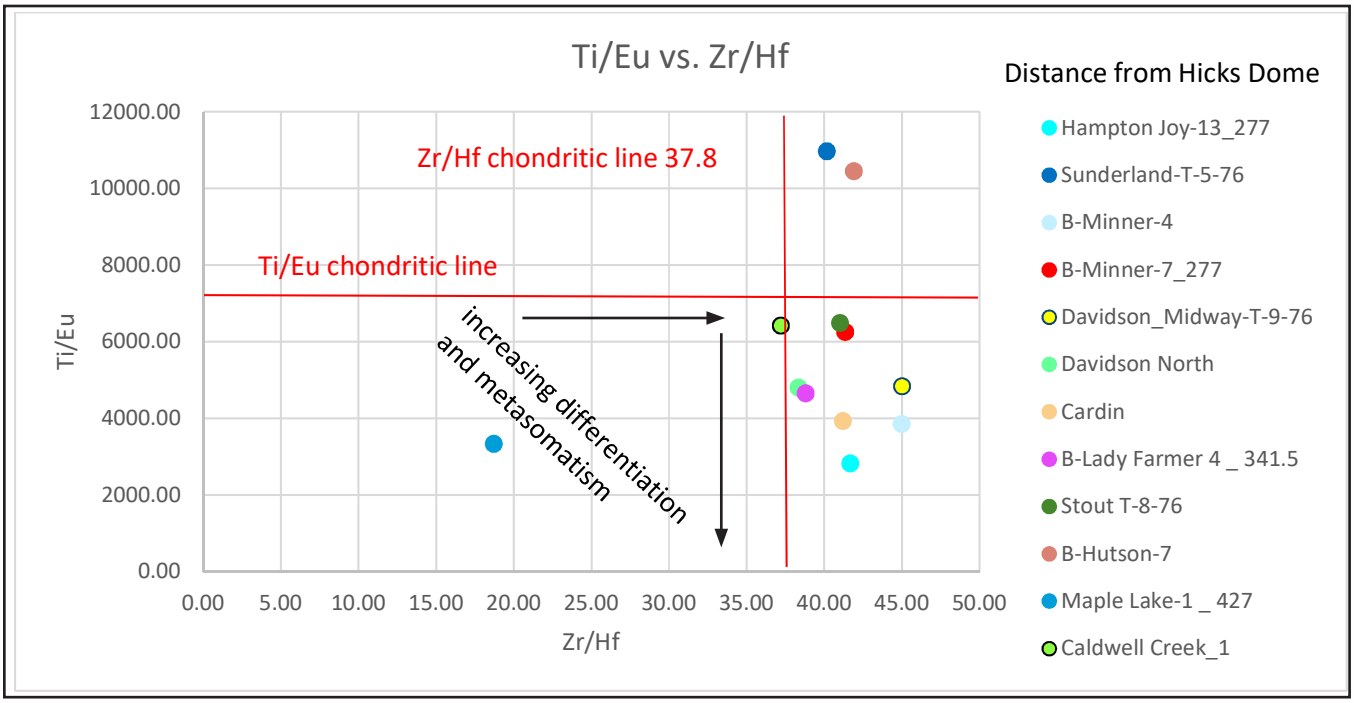

Figure 19. Ti/Eu and Zr/Hf ratios show increasing differentiation in the magma. The Zr/Hf ratio indicates increasing zirconium in the magma caused by superchondritic metasomatism. Titanium is elevated, and the titanium garnets crystallize in the Coefield Intrusive Complex dikes, decreasing the titanium content while the europium content increases. As the melt evolves, increasing enrichment of europium and REE occurs in some of the dikes during late-stage crystallization in the Western Kentucky Fluorspar District. Several core analyses, including for the Minner-4, Davidson-Midway, Cardin, and Davidson North dikes, indicate that these were the most differentiated rocks and the most enriched in REE that were analyzed in the district. The high-titanium, low-REE dikes are the Hutson and Sunderland in Livingston County. Hampton Joy and Maple Lake dikes are unusual because they have low La/Yb and Ti/Eu ratios. The Hampton Joy dike is closest to Hicks Dome and Maple Lake is the farthest from Hicks Dome, occurring in the southern part of Crittenden County, but Maple Lake is less differentiated than Hampton Joy.

REE data (Fig. 4), such as concentrations of lanthanum (3.3–118 ppm), cesium (6.6–257 ppm), europium (0.12–5.27 ppm), and ytterbium (0.3–4.2 ppm) also indicates extensive fractionation and metasomatism, which occurred prior to intrusion of the dikes. Total REE concentrations for these dikes range from 41 at Maple Lake to 1,320 at Caldwell Creek.

The Caldwell Creek dike is somewhat unusual in that it has the highest REE values (Fig. 12), but is not located in the Coefield Intrusive Complex, and it has the highest niobium, yttrium, and titanium values of the samples analyzed (Fig. 18). The Caldwell Creek dike is altered, containing clays and carbonates, and is located near the Maple Lake dikes, which contain yttrium fluorite and calcite.

The enrichment of REE is primarily a fractionation event, whereas high values of titanium, niobium, phosphorus, thorium, and zirconium (Fig. 12) also suggest a metasomatic enrichment. These data, along with the abundance of titanium alteration and magnesium enrichment in many dikes, might be an avenue to examine the alteration mineralogy as a pathfinder to REE anomalies (Fig. 19). For example, and based on the limited sample set, the higher magnesium values near the Coefield Intrusive Complex and the ilmeno-magnetite/leucoxene alteration in the Clay Lick (T-798a) dike area indicate that some areas are more altered than other dikes in the district, but more research is needed to determine any correlation between regional zonation and REE in dike alteration patterns.

Only moderate elemental zinc (10–353 ppm) was detected in the dikes. The most zinc-enriched dike was Sunderland, which contained 353 ppm, whereas the dike at Hutson Mine, which was primarily a zinc mine, only contained 10 ppm zinc.

Some molybdenum was noted in the Old Jim dike, and iridium was noted in core DLP-2 at

112 ft, in a monazite phosphate; this was confirmed by scanning electron microscope analysis (Fig. 11). Iridium, osmium, and ruthenium were noted in core BH-7 at 74 ft, according to X-ray diffraction. The presence of iridium and other metals could imply that there could be phases of platinum group elements in the Western Kentucky Fluorspar District.

U/Th ratios (Fig. 16) show a decrease in uranium and enrichment of thorium toward the Coefield Intrusive Complex, another indication of thorium fractionation from uranium during metasomatism of the magma.

During fractionation in an alkaline melt, the incompatible elements, including zirconium and hafnium, will increase only slightly in the remaining melt, because of their similar ionic properties, so the higher, above-chondrite values of zirconium and hafnium and zirconium and yttrium indicate a carbonatite metasomatic influence (Figs. 15–19), as previously discussed in Eby and others (2003) and Pearson and others (2004). Some of the dikes in this study have higher Zr/Y and Zr/Hf ratios (Figs. 17, 19) compared to chondrite values, and the zirconium and hafnium values are compatible with the values related to carbonatite sourcing described by Chakhmouradian (2006). Carbonatites can be a metasomatic influence on a mantle magma, and the enrichment of some of the incompatible elements (titanium, zirconium, hafnium, niobium, tantalum, uranium, and thorium) (Beattie, 1993) confirms this (Figs. 15–19). Many of the incompatible elements were concentrated above chondrite values and may have helped concentration of titanium and fractionation of thorium and uranium.

The wide range in concentration of elements in the analyzed dikes suggests a heterogeneous mix of ultramafic rocks resulting from complex metasomatic reactions, perhaps both silicate and carbonatite, which directly affects the rocks' REE content (Figs. 16–20). These metasomatic processes are somewhat gradational, and significant overlap creates high variability in REE; iron, niobium, titanium, carbon, and calcium values allow for REE enrichment in some of the dikes.

REE in Ore-Stage Fluorite

Rare earth elements in fluorite were analyzed, and normalized REE patterns are displayed in Figures 20 through 23. These patterns suggest two distinct low-value REE signatures in fluorite, assuming the REE values were within the fluorite crystal structure and not in the fluorite inclusions. One pattern shows enrichment of MREE (Figs. 20–22) and matches Trinkler and others' (2005) data on MREE enrichment in several of the fluorite samples. The second pattern, seen in dark purple fluorite from the Davenport Mine, shows some enrichment of LREE; a duplicate analysis was performed to confirm the analysis.

Fluorite in dikes was detected by X-ray diffraction as sodium fluoride, yttrium fluoride, cadmium fluoride, and an unnamed REE-bearing fluoride, in addition to calcium fluoride. Many of the Kentucky ore-stage fluorites contain REE, but the values are low compared to those from the purple fluorite at the Rose Mine (Burruss and others, 1992b) and the Hicks Dome fluorite (Hall and Heyl, 1968). Dark purple fluorite from the Davenport Mine has high LREE values and other purple fluorite from the Western Kentucky Fluorspar District shows a slight increase in La/Yb ratio at comparable Tb/Yb ratios, suggesting that purple fluorite is slightly more enriched in REE than yellow fluorite (Figs. 20–21).

Uranium and thorium concentrations in the fluorite were also determined because these radionuclides are associated with igneous processes and they have a potential contribution to fluorite coloration. The uranium and thorium concentrations were very low, many samples below the detection limit, but some values were of interest. The Davenport deep purple fluorite contained the highest thorium concentrations: 10.7 and 13.1 ppm (Fig. 22). In contrast, dark purple fluorite from the Joy Mine had a high uranium concentration (3 ppm) but low thorium concentration (Fig. 23) and high barium-strontium concentration.

Discussion of REE in Fluorite

Analysis of REE in ore-stage fluorite indicates two REE phases (Fig. 20). Five fluorites showed MREE enrichment: the Joy purple, Hastie-Victory dark and light yellow, Big Four, and Eagle Babb purple. The Davenport purple fluorite was one sample, split and analyzed at two different times, to show enrichment in LREE. The REE patterns at Joy and Davenport indicate two mineral-forming

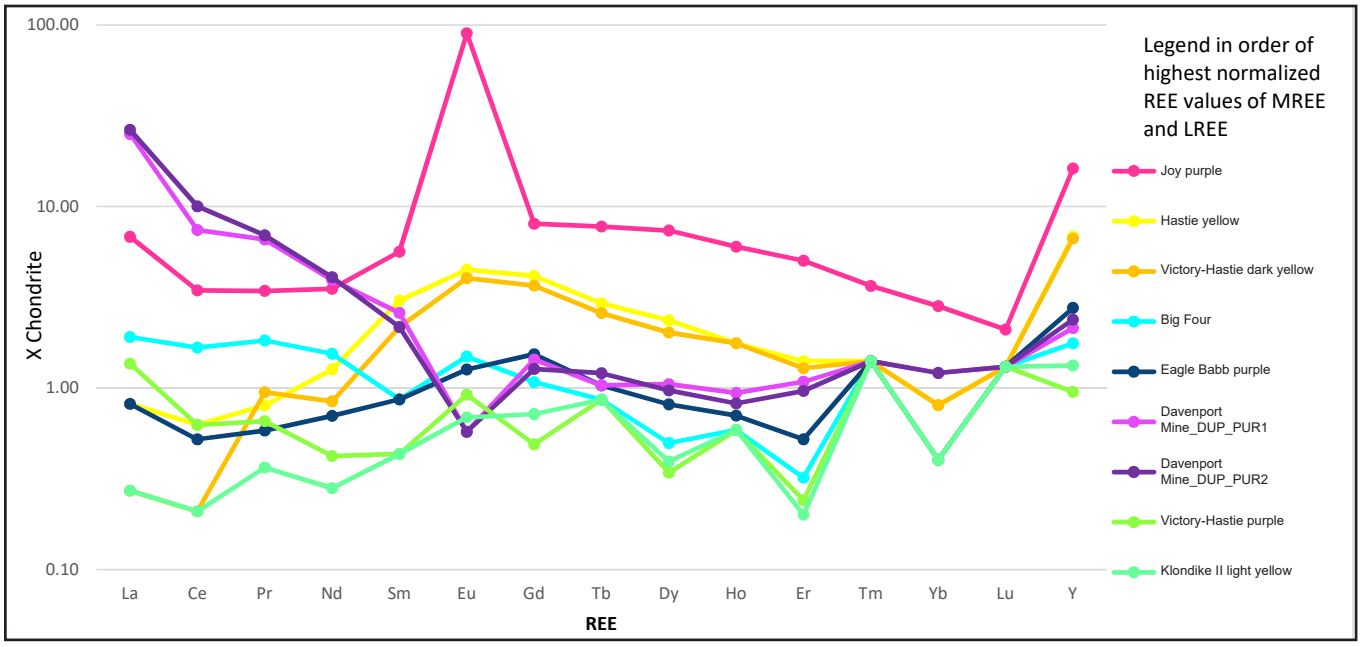

Figure 20. Patterns of REE in fluorite from the Western Kentucky Fluorspar District. One group is enriched in MREE, irrespective of color; in decreasing order of MREE abundance, these are Joy purple, Hastie yellow, Victory-Hastie dark yellow, Eagle Babb purple, and Big Four. A second group composed of two Davenport Mine samples is enriched in LREE. A third group is depleted in REE: the Hastie purple and Klondike II light yellow. The variation between the two enriched-fluorite sample sets suggests a high-temperature-differentiated fluorine-rich fluid, one fraction enriched in LREE and another low-temperature fraction enriched in MREE. Both carbonatite and MVT fluids may have mixed. Some fluorites with elemental values near the lower limit of detection may represent fluids depleted in REE.

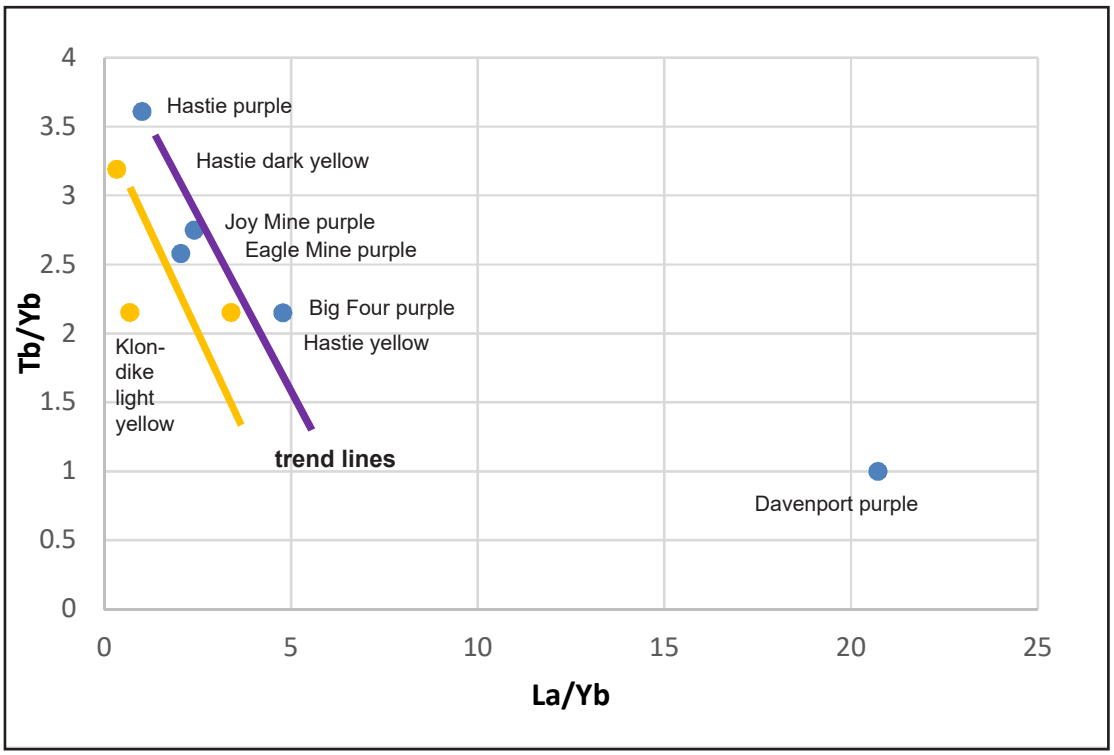

Figure 21. Ratios of REE in fluorite. La/Yb and Tb/Yb ratios were plotted to characterize REE distribution in colored fluorite from the Western Kentucky Fluorspar District. These limited data suggest that purple fluorite is slightly more REE-enriched compared to yellow. The Davenport purple may have formed from a separate fluid phase strongly enriched in LREE.

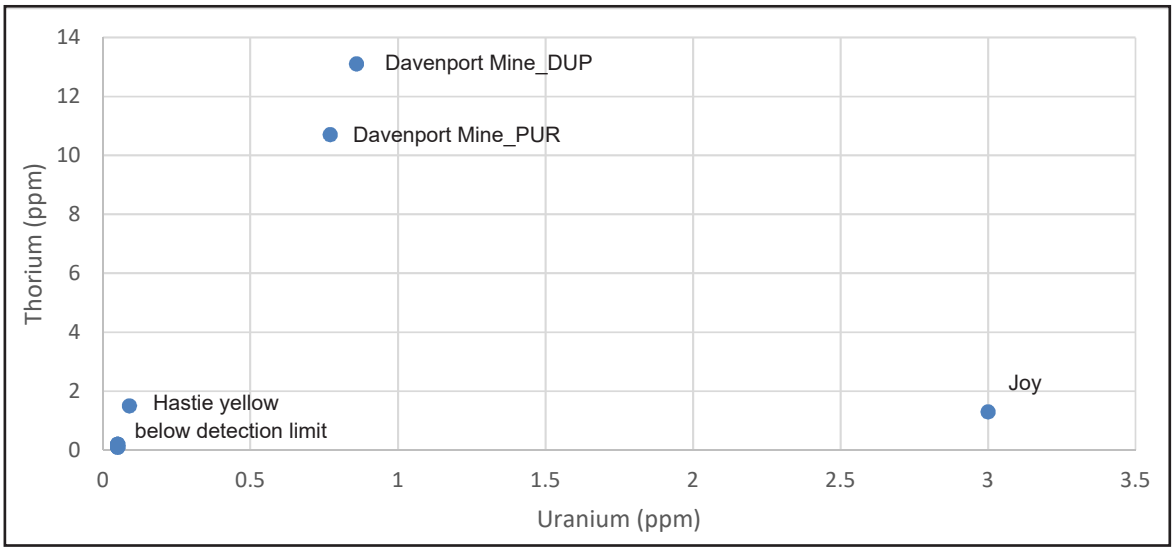

Figure 22. Uranium-thorium concentrations in fluorite show high uranium in fluorite from the Joy Mine and high thorium in fluorite from the Davenport Mine. The wide variance in uranium and thorium concentrations in fluorite from the Davenport and Joy Mines might suggest more fractionation with higher LREE values at Davenport. A previous study by Beattie (1993) suggest that high-garnet facies may influence thorium-uranium fractionation.

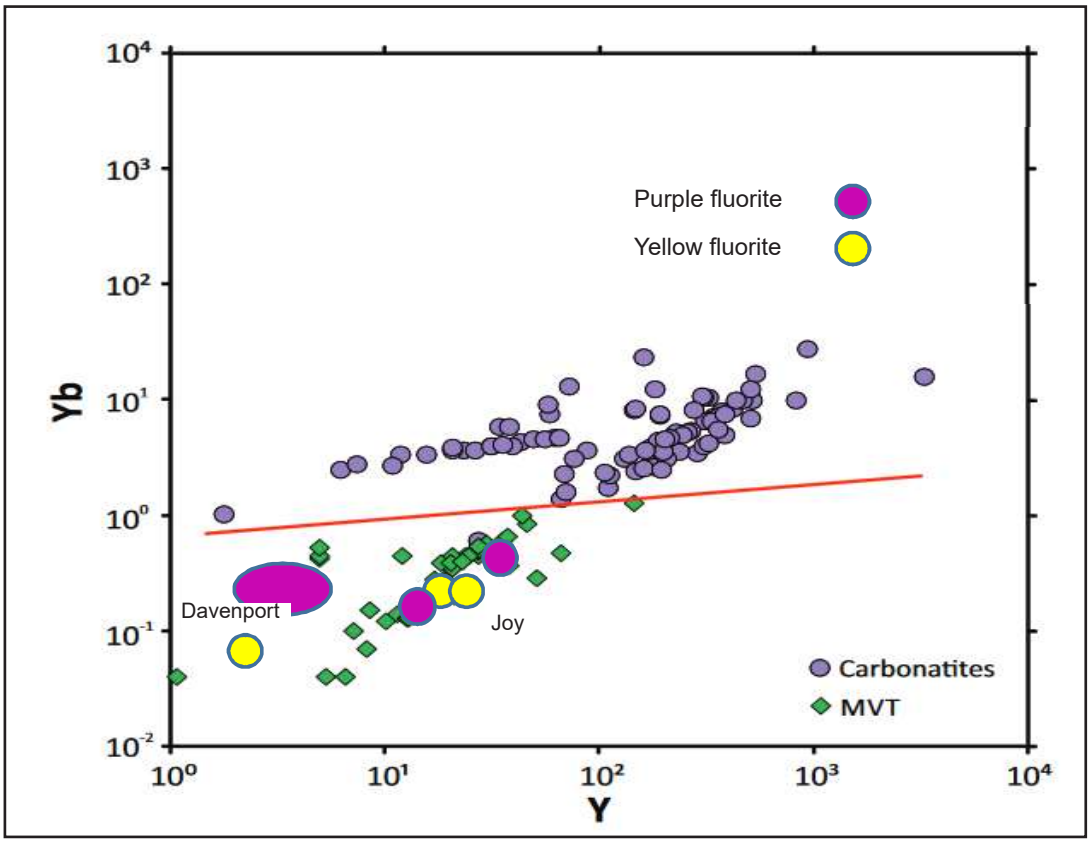

Figure 23. Y/Yb ratios place the Western Kentucky Fluorspar District fluorites in the MVT hydrothermal category and conflict somewhat with the REE signature previously discussed. Several fluorites analyzed in this study had concentrations below detection limits, so these data might be skewed; more analyses should be completed to determine genetic sourcing of the fluorite. The dark purple fluorite from the Davenport Mine and other purple and yellow fluorites fit mostly into the MVT and hydrothermal categories, based on available data and analytical techniques. Baseline compositional data for MVT and carbonatite data from Makin and others (2014) and Möller and others (1998).

episodes or variously timed and differently enriched fluids in the district: one enriched in MREE and one enriched in LREE. The light yellow fluorite from the Klondike II Mine had the lowest concentration of REE (less than 1 ppm) and could have formed from a very late-stage depleted-REE fluid or was lower temperature or was sourced differently. The high uranium content in the Joy Mine purple fluorite suggests a fluorite source that was less metasomatized and fractionated than the Davenport Mine purple fluorite, which was higher in thorium, lower in uranium, and had a higher La/Yb ratio, indicating LREE enrichment (Figs. 21–22). The Joy Mine fluorite had a higher Tb/Yb ratio (HREE) (Fig. 21), as did Hastie Mine purple and yellow, Eagle, and Big Four purple fluorites, compared to Davenport purple fluorite. No fluorites from the Coefield Intrusive Complex were sampled during this study, because sampling and elemental analysis had already been conducted. Higher REE values in fluorite might be expected near or within the complex area.

The genetic origin of fluorite is the subject of much debate (Möller and others, 1998; Xu and others, 2012; Makin and others, 2014). High-temperature fluids generally are more enriched in LREE than lower-temperature fluids and will show a negative europium anomaly; lower-temperature fluids are depleted in LREE and show a positive europium anomaly, according to Möller and others (1998). Möller and others (1998) used Tb/Ca ratios to determine genetic origins, but the analytical limits of detection in this study required Y/Yb ratios to be used, as a better estimate of genetic origin. An origin from either carbonatite fluids or MVT fluids can be estimated from Y/Yb ratios (Fig. 23) and using the techniques of Makin and others (2014). The raw-data ratios of Y/Yb for several samples—the Davenport, Joy, and Hastie fluorites (Fig. 23)—indicated that most values were fully in the MVT range. Variations in trace elements may be the result of disparate origins of fluorine, or variously timed enrichments, depending on the original supply of fluorine in this complex system. For example, during the ascent of upwelling carbonatite-type magma, a gaseous CO_2-fluid phase would exsolve from a parent magma (Plumlee and others, 1995). This fluid phase would have to be from a dense, high-pressure, supercritical CO_2 fluid, which would occur at these subcontinental lithospheric mantle depths. During the ascent, the gaseous phase would expand and be enriched with REE and fluorine from the fractionated melts or metasomatized magmas. This gaseous phase would mix with MVT basinal brine fluorite to form the hydrothermal mineralization. There may have been various short-term pulses or phases of gas migration and mineralization that would not be measurable by dating techniques.

The sampled Kentucky fluorites had low values of REE (Fig. 20) compared to other carbonatite fluorite values from other parts of the world (Yang and others, 2003; Xu and others, 2012); however, as previously mentioned, no samples from the Coefield Intrusive Complex were analyzed. Confirming the lack of a carbonatite influence are the yttrium and ytterbium concentrations in fluorite (Fig. 23); however, crustal sourcing from delamination might influence some of the yttrium concentrations. The Joy Mine fluorite had the most enriched REE (with a europium anomaly) and also were high in barium and strontium; these values plot in the MVT field, suggesting mantle mixing with crustal material. The Davenport fluorite has an LREE carbonatite signature but also plots in the MVT field; duplicate samples are needed before any definitive conclusions can be drawn. The Davenport and Joy Mines have higher ytterbium concentrations than other fluorites in the district, but concentrations are still low compared with other carbonatite fluorite (Möller and others, 1998), such as at Mato Preto, Brazil (Santos and others, 1996). Further analysis and paragenetic studies could delineate which fluid types were the primary genetic carriers of REE.

Assuming a carbonatite origin, a carbonatite dike and carbonatite fluorite should have similar REE signatures because of their similar genetic origins. Fluorite from the Davenport Mine is LREE enriched and is comparable to concentrations from the Davidson Midway and Cardin dikes, which are near the Davenport Mine fluorite. The enrichment, indicated by steep negative slope in plots of LREE concentration from the dikes near the Davenport fluorite mine (Figs. 12, 20–21), show that both dike and fluorite compositions are enriched in LREE. The Joy fluorite has high MREE values, however, and the Hampton Joy dike contains somewhat of

a moderate carbonatite-type enrichment in LREE. These data indicate that the partitioning and fractionation of REE in the Davenport fluorite had to have occurred prior to mineralization and that the Davenport fluorite might be closely associated with carbonatite.

Based on fluorite paragenesis of ore-stage fluorite from the Western Kentucky Fluorspar District, Hayes and Anderson (1992) suggested that there may be several stages of fluorite mineralization. Variant fluorine fluids, thermal influences, or remobilization of fluorite may cause these stages. Based on the REE analysis in this study, thermal influences may have created an early-stage, high-temperature, LREE-enriched, dark-colored fluorite with a negative europium anomaly (Davenport Mine fluorite) and a later stage, MVT ore-stage, paragenetically correlatable phase, slightly enriched in MREE, with a positive europium anomaly, with both yellow and purple coloration, which would include fluorites from the Joy and Hastie Mines. Based on the rare-element fluorite mineralogy in dikes, other elements besides calcium were abundant in the melt, which allowed other types of unusual fluorites to precipitate, such as sodium, cadmium, yttrium, and REE fluorides. These elements were available and sourced from MVT fluids and fractionated melts, either during fractionation or metasomatism or during hydrothermal reactions. As these fluids began to ascend with the CO_2 fluid degassing, there was mixing with the various fluids, which lowered the temperature of later intrusive fluids. The fact that only some dikes were altered and mineralized with MVT minerals (mid-stage sphalerite) suggests two phases of igneous intrusion fluids—an initial intrusion of the dark-colored dikes, prior to or coincident with the initial MVT mineralization, and a second phase of CO_2-rich alteration fluids that mixed with MVT fluids to create the lighter-colored dikes associated with reddish sphalerite mineralization. Based on the paragenesis, the mid- to late-stage purple fluorites would be expected to have been deposited or altered with the second-phase fluids. Additional microchemical work on these fluorites would help explain the REE concentrations.

Conclusions

During initial Precambrian continental rifting, mantle upwelling, carbonatite metasomatism, and magmatic intrusions occurred along basement faults near the subcontinental lithospheric mantle of the New Madrid Rift Zone. This mantle upwelling introduced mafic and ultramafic plutons into the rift complex, but upward mobility of the magma melts stalled because of crustal lithostatic pressures above the subcontinental lithospheric mantle. Sublithospheric delamination of the crustal materials may have contaminated the mantle melts during structural uplift. The enriched REE and variant elemental chemistry of the dikes in this study suggest the petrology of the melts was differentiated and metasomatized by the stalled mantle melts in the early Paleozoic. These partially differentiated alkaline mantle fluids are carbonate-rich and fractionated into at least two different melts during the Paleozoic: one high-titanium, carbonatite-type, CO_2- and magnesium-rich, and another siliceous melt that is considered minor and poorly defined. These mantle fluids were intruded as dikes along initial fractures and faults during the structural extension phase in the late Paleozoic (Permian Period, 272 Ma). The CO_2-rich fluids were a volatile, late-stage carbon dioxide differentiate that mixed with and were enriched with fractionated REE fluids, and then mixed with MVT basinal brine fluids to form the concentric zonation pattern of the altered dike-mineral sequence. Most of the fractionation of the REE component occurred in the mantle during mantle upwelling, and was brought to the surface via the volatile event along preferential existing pathways in the Coefield Intrusive Complex and surrounding areas. Most of the alteration of the dikes and mineralogy occurred during the mixing and ascent with CO_2-rich volatile fluids during a second event, which explains why there are two parallel dikes in many areas: one only slightly altered and the other more severely altered. The timeframe for two events is unclear—whether it was one long event or two events—but isotopic dating should help answer this question. After the intrusion of massive amounts of igneous dike and fluorite material, the fault system collapsed, which

formed many of the grabens in the district. The complexity of the district illustrates that the thermal and mineral zonation is more complex than earlier workers described.

In addition to the Coefield Intrusive Complex, another area of interest is the Caldwell Creek dike in southern Crittenden County. The Caldwell Creek dike has the highest REE concentration analyzed in the district, and its high iron, titanium, niobium, and yttrium contents suggest extensive metasomatic alteration of the dikes in this area, and are indicative of another area of potential REE concentrations in the district. This study's dataset suggests that there are other thermal influences on the igneous and mineralization system besides Hicks Dome. More work is needed on the entire district to find other thermal centers besides the Coefield Intrusive Complex and the Maple Lake–Caldwell Creek dikes. These other centers disturb the regional patterns in both mineralogy and elemental chemistry, including the REE content.

Overall, the petrology, mineralogy, and elemental chemistry seem to confirm the evolutionary model discussed at the beginning of this report. Although a traditional carbonatite has not been observed on the surface, mineralogical and elemental analysis (Fig. 5) suggests that there are carbonatites in the subsurface and that they had a profound effect on the igneous dike chemistry and mineralogy on the enriched REE in the Coefield Intrusive Complex and upon the variant REE enrichment of fluorite in the Western Kentucky Fluorspar District. The volatile component (carbon dioxide degassing) altered both the igneous dikes and some of the MVT mineralization in the district. The presence of high magnesium in the Coefield Intrusive Complex confirms the alteration of the ferro-magnesium source melts in basement rocks and is an indicator of alteration pathways for REE enrichment.

Rare minerals associated with carbonatite occur in dikes in the district, and are similar to the Magnet Cove, Ark., and Aillik Bay, Labrador, Canada, suite of minerals; enrichment in the incompatible elements also suggests a carbonatite metasomatic influence on the dikes. The higher titanium concentrations in some dikes suggest higher titanium mineral concentrations or that titanium has been fractionated from europium to form the anomalies (Fig. 19). Zonation patterns (Plate 1), mineral differences, and LREE enrichment suggest that the fractionation occurred. Future work should be conducted to confirm the zoning of clinopyroxenes for further clarification.

Dike Petrology and Mineralogy

The mineral composition and geochemical data indicate that there are both alnöite and aillikite lamprophyres in the Western Kentucky Fluorspar District, that some dikes are more evolved than others, and that some dikes in the Coefield Intrusive Complex trend toward carbonatite and kimberlite (Figs. 5, 13–14). Alkaline ultramafic intrusive rocks in the district consist of a multi-mineral suite of titanium garnets, fluorites, base metals, and rare mantle xenoliths. Titanium garnet, altered ilmenite-magnetite oxides, niobium rutile, anatase, and REE-bearing perovskite have been identified. Rare ultra-high temperature and pressure minerals such as schorlomite, astrophyllite, wüstite, and moissanite have been detected in xenoliths that occur in breccias, suggesting deep-mantle carbonatite metasomatism in a subcontinental lithospheric mantle. Several carbonatite-type REE minerals have been detected in this study's small sample set, and other indicator minerals such as fluoro-tetraferriphlogopite, fluoro-phosphates, and sodium- and REE-bearing fluorides occur in the dikes, as do titanium- and barium-rich micas.

Many of the xenoliths contain calcite, dolomite, and magnesite, which could be igneous carbonates; further research and isotopic dating are needed for confirmation. The presence of the high-temperature silicate tridymite, unusual uranium minerals, various metals and sulfides, chromium garnet, nickel phlogopite, barium biotite, and unusual carbon minerals such as moissanite is worthy of future research.

Many of the igneous dikes in the Western Kentucky Fluorspar District are carbonate- and oxide-rich, and include phosphates, magnetite, fluorite, niobium rutile, perovskite, various titanium oxides, uranium-thorium oxides, fluoro-REE-bearing phosphates, and the base-metal-bearing minerals sphalerite, galena, native iron, and barite. The alteration minerals calcite, dolomite, biotite, phlogopite, ankerite, garnet, chrysotile, lizardite, chlorite, and clay minerals including kaolinite, vermiculite, and brucite also occur in the dikes and are common

accessory minerals in carbonatites. The presence of fluorite and sphalerite in the altered dikes suggests that base-metal-rich MVT fluids and CO_2-rich alteration fluids mixed during the Permian mineralization event.

Rare minerals indicative of fractionation and metasomatism of REE are niobium rutile and its polymorphs, anatase and brookite. The high niobium in rutile and high La/Yb ratio in the Coefield Intrusive Complex also suggest an overprint of a high level of carbonatite metasomatism on the fractionation event. The rare fluorides suggest that abundant sodium, cadmium, REE, and yttrium were available in the melt to replace calcium in the fluorine structure in an alkaline fluid. Fluoro-tetraferriphlogopite is a rare mica, and its presence suggests an evolving magma melt. The abundance of unusual garnets suggests a complex fractionation environment; some parts of the district are rich in calcium and titanium garnets, which may have facilitated the enrichment of the LREE. Sphalerite is used as a correlation mineral to determine the timing of CO_2 alteration fluid mixing with MVT mineral fluids during a mid-stage paragenetic sequence. The abundant REE-rich perovskites/loparites suggest enriched fractionation and emplacement in REE in a carbonatite environment. The presence of potassium feldspar and barium-rich mica suggests that there also are other lithofacies, because of the gradational changes of these rocks and alteration and MVT mineralization overprint on the dikes.

REE Analysis in Dikes

Plots of chondrite-normalized REE concentrations for alkaline ultramafics and fluorite in the Western Kentucky Fluorspar District (Figs. 12–19) show a family of dikes that have negative slopes; LREE enrichment in whole rocks is 100 times higher than for chondrite, which is indicative of partial melting of the sublithospheric mantle sources. The linear, increasingly higher-temperature positive trends of La/Yb versus Tb/Yb ratios and La/Yb versus Sm/Yb ratios in dikes in the district (Figs. 13–14), reaching maximum values at the Coefield Intrusive Complex, Midway, and Caldwell Creek area, indicate classic fractionation of the alkaline ultramafic body, undersaturated with silica, trending toward carbonatite and enrichment of REE in the Coefield Intrusive Complex. Garnet lithofacies in the magma melts is responsible for the enriched LREE in the complex, and the variable garnet chemistries might affect fractionation by allowing the more incompatible elements to incorporate into the garnet, and would raise the Th/U and Zr/Hf ratios to those found in the complex area (Figs. 16–17, 19).

Certain areas of the district, such as the Coefield Intrusive Complex and the Lady Farmer, Caldwell Creek, Sunderland, and Midway areas, have slightly elevated LREE concentrations. The raw data for any REE showed concentrations between 16 and 570 ppm, and the total REE concentration did not exceed 3,700 ppm for all 12 of the dikes analyzed. The La/Yb ratio for the Western Kentucky Fluorspar District varies from 10 to 70, and the carbonated high-titanium, garnet-peridotite portion of the district (in the Coefield Intrusive Complex) has La/Yb ratios between 50 and 70, which is within the range of alkaline lamprophyres, carbonatites, and nepheline syenites and trends toward carbonatite and kimberlite in some areas.

High Ca/Al, La/Yb, Zr/Hf, and Nb/Ta ratios of some dikes clearly show an enrichment above primitive mantle values and indicate a fractionation and metasomatic enrichment in the Coefield Intrusive Complex and surrounding areas (Figs. 15, 17). High magnesium values around the complex confirm earlier work on magnesium enrichment in the Minner area (Heck and others, 2006). Scatter diagrams (Figs. 12, 14, 19) depict some late-stage carbonatite-type enrichment, but none of the analyses in this study demonstrated any economic deposits of REE; more work on remaining dikes that were not analyzed in this study is warranted.

The highest REE concentrations in the Western Kentucky Fluorspar District were at Caldwell Creek; samples from this location were very altered and weathered. Although the clay dike sample from Caldwell Creek looks solid and intact, there may have been some enrichment by mechanical weathering. REE content at Caldwell Creek is the most enriched in the district, whereas REE values at the nearby Maple Lake Dike are the lowest in the district (Fig. 12). Caldwell Creek dikes may represent another area similar to the Coefield Intrusive Complex, which underwent carbonatite metaso-

matism; Caldwell Creek could be more enriched than the Coefield Intrusive Complex.

The Caldwell Creek and Maple Lake dikes are the farthest from Hicks Dome and are located within a mile of each other south of the Tabb Fault System. Their close proximity to each other illustrates a problem of two extreme REE compositional variations in a small geographic area and suggests that there may be more than one center of thermal influence or mineralization (besides Hicks Dome) in the Western Kentucky Fluorspar District, or that Hicks Dome fluids were established in multiple pulses: one enriched and one depleted in elements and CO_2 volatiles. The use or reuse of an established plumbing system may still be required by variant or episodic fluid movement and may help explain the variable dike chemistry in a small area.

High LREE concentrations in the Coefield Intrusive Complex suggest a carbonatite phase of metasomatism, and high concentrations of HREE at Caldwell Creek, Hampton Joy, Sunderland, and Cardin dikes may represent overall variability and chemistry of garnets in the magma melt. The higher LREE and rare minerals at Billiton Minner, Lady Farmer, and Davidson Midway dikes are the result of titanium garnets in the melt, a high temperature, fractionation, volatile carbonatite metasomatism. At the lower end of the LREE spectrum is the Hampton Joy dike, which has high calcium and aluminum, and is the closest of the dikes to Hicks Dome in this study; in contrast, the Hutson dike is farther from Hicks Dome and has high calcium and low aluminum. The Hutson dike has higher titanium and niobium, but slightly lower REE than the Hampton Joy dike. The variance in these elements suggests complex fractionation and metasomatism, thermal effects on fluid chemistry, and late-stage alteration events.

These fluoride and carbonate melt fluids also increased Tb/Yb ratios (Fig. 13), increased uranium-thorium mobility and thermal influence, extracted and mobilized REE, and support the chondrite-normalized dike signatures shown in Figure 12. Fluoro-phosphates are abundant in these dikes and probably account for most of the uranium-thorium radionuclides, because only two zircons and one monazite were noted in core DLP-2, and only small amounts of monazite have been noted in other investigations.

Carbonatite Metasomatism and Incompatible Element Ratios

High concentrations of the incompatible elements titanium, niobium, zirconium, hafnium, yttrium, vanadium, rubidium, uranium, thorium, potassium, and beryllium indicate magma melt metasomatism in the mantle. These elements are incompatible during partial melting and fractionation of the mantle and are usually the last to enter late-crystallizing phases during the evolution of a magma melt.

Combined results using La/Yb, Nb/Ta, Tb/Yb, Sm/Yb, Zr/Y, Zr/Hf, Nb/Y, and Ti/Eu ratios indicate fractionation and REE enrichment in the district and suggest niobium enrichment of a high-titanium garnet-present melt sourcing of differentiated magmas or variously timed metasomatized fluid movements. These processes influence the distribution of REE and imply that there may be higher concentrations of LREE in the district, possibly related to fractionation of garnet-present melt dikes in the central part of the district near the Coefield Intrusive Complex and Midway and Caldwell Creek areas.

Raw niobium concentrations range from 1 to 199 ppm, which suggests high-titanium, deep-seated alkaline mantle-melt influence. Magma generation in the superchondritic melt fractionated the niobium to create a higher Nb/Ta ratio but lower La/Yb ratio in a superchondritic silicate and carbonatite-enriched peridotite (Fig. 15) at the Sunderland, Hutson, and Caldwell Creek areas. The subchondritic Nb/Ta and high La/Yb ratios in the Coefield Intrusive Complex may reflect higher-temperature (or remelted) carbonatite fluids mixing with crustal contaminated or depleted metasomatic fluids. The high-titanium dikes reflect some degree of partial melting, with high La/Yb ratios (50–70) in the Coefield Intrusive Complex, which represents carbonatite mantle metasomatism, and produced slightly enriched LREE and depleted HREE in basement peridotite (Figs. 12–13). Increasing niobium (Figs. 15, 18), yttrium, and ytterbium concentrations, and increasing Nb/Ta ratios (Fig. 17) indicate increasing differentiation of magma melts, whereas decreasing titanium and increasing europium concentrations (Fig. 19) indicate a late-stage differentiate enrichment in REE as the titanium elements crystallized in minerals

(schorlomite and rutile) and that a carbonate volatile phase mixed with peridotite dikes at the Coefield Intrusive Complex.

Because zircon crystals are more soluble in alkaline melts (Wilke and others, 2012), they would not be expected to be identified by X-ray diffraction; in fact, only two zircon crystals were noted in our extensive X-ray diffraction analysis. High zirconium concentrations were recorded in many dikes, however, Zr/Y ratios (Fig. 17) are fairly constant during fractional crystallization because of their similar atomic features, but this ratio varies during magma melting and can be used to measure the degree of melting (Nicholson and Latin, 1992). The Zr/Y ratios for the Western Kentucky Fluorspar District range from 4 to 15 (Fig. 17), compared to a Zr/Y chondrite ratio of 2.52; most of the Zr/Y ratios are greater than 10. Likewise, Zr/Hf ratios (Fig. 17) for the district range between 37 and 45 and are superchondritic (greater than 37.8), indicating enriched zirconium and a metasomatic enrichment event in the higher-temperature garnet facies. Higher zirconium concentrations imply a high degree of melting and metasomatism; the fractionated melt trends toward a more alkaline and carbonated peridotite melt, with higher REE values in the Coefield Intrusive Complex and lower values in the peripheral zones (Fig. 17). The high yttrium concentrations (3.2–62) are evidence for differentiated REE in alkaline ultramafic rocks, possibly indicating low-yttrium parent material and high-yttrium alkaline fractionated material.

Dikes in the Coefield Intrusive Complex contain REE in perovskite, and, as shown in Figures 18 and 19, raw titanium values are high in some of the dikes, ranging from 0.04 to 3.3 percent (Figs. 4, 18), and many dikes contain visible rutile. The normalized Ti/Eu ratios range from 2,824 to 10,967, and the enrichment of europium during differentiation is indicated by the data shown in Figure 19. The Ti/Eu diagram (Fig. 19) shows the variable influence of garnet content in the melt or increased fractionation-differentiation of carbonate and silicate magmas, where the carbonate magma trends toward carbonatite and has lower Ti/Eu ratios (higher REE). The higher-REE perovskites in the Coefield Intrusive Complex are examples of a carbonatite mineral phase that fractionates REE. Results from this study confirm experimental work by Beyer and others (2013), demonstrating that the perovskite partition coefficients are higher in carbonate melts and that they fractionate trace elements such as zirconium, hafnium, and REE in the carbonate melts more efficiently than in silicate melts.

The uranium decline curve and increasing Th/U ratio (Fig. 16) support metasomatism trending toward a carbonatite in the Coefield Intrusive Complex dikes. The fractionated dikes signify a deeper-asthenosphere fractionated and metasomatized magma melt that also demonstrates an increasing uranium/thorium thermal influence on fluids and REE in the Coefield Intrusive Complex. The thorium concentration at Caldwell Creek is 17.5 ppm, whereas at Maple Lake it is 0.8 ppm; uranium values are nearly identical at Maple Lake (6.78 ppm) and Caldwell Creek (5.99 ppm), also suggesting a weakly defined trend toward carbonatite.

Several of the Ti/Eu versus Zr/Hf ratios shown in Figure 19, including for the Minner-4, Davidson-Midway, Cardin, and Davidson North dikes, indicate that these were the most differentiated and metasomatized rocks in the samples examined and the most enriched in REE that were analyzed. Carbonization of peridotite and REE concentration in perovskite indicate that various mineral carriers could concentrate the REE. Hampton Joy, Hutson, and Sunderland dikes do not have a significant carbonatite LREE signature, but have a more uniform distribution of REE.

The lone dike that is most primitive and not highly differentiated is the one at Maple Lake in the southern part of Crittenden County; it confirms a primitive, porphyritic, un- or very weakly metasomatized lamprophyre mantle dike with low Zr/Hf, Nb/Ta, and La/Yb ratios (Figs. 17–19). The Caldwell Creek dike is almost the opposite of the Maple Lake dike, in that it has the highest REE, titanium, niobium, zirconium, and yttrium concentrations in the sample set and the highest La/Yb ratio (Figs. 12, 18). These two dikes, located within a short distance of each other, could provide a snapshot and explain the complex relationship between fractionation, metasomatism, and evolution of CO_2 fluids that have intruded the district. Caldwell Creek is also a potential data point for another REE anomaly in the southern part of the district, with increased lanthanum, ytterbium, ti-

tanium, niobium, and thorium concentrations. In contrast, the Maple Lake dike is a depleted primitive mantle, perhaps suggesting two generations of intrusions that are using the same plumbing systems. The Caldwell Creek dike is near the Tabb Fault System, which has produced about 70 percent of the fluorite mined in the Western Kentucky Fluorspar District; much more work is needed to further understand the type of magma melts and metasomatism in this area.

The trace and incompatible-element ratios suggest that a primary district-wide fractionation-metasomatic event focused CO_2 and high-temperature fluids toward the Coefield Intrusive Complex and possibly other areas such as Caldwell Creek. The fractionated alkali-rich melt would have crystallized slowly, causing enrichment of the La/Yb portion of the REE, whereas the higher-temperature, more volatile metasomatic event would have caused enriched La/Yb, Zr/Hf, Ti/Eu, and Nb/Ti ratios (Figs. 17, 19).

REE in MVT-Stage Fluorite

REE in the MVT-stage fluorite are only slightly enriched with LREE and MREE (Fig. 20). Based on the uniform distribution of REE in fluorite, the REE is assumed to be within the crystal structure of the fluorite and not as microscopic inclusions within the fluorite. One fluorite sample from the Davenport Mine is enriched in LREE (Fig. 20); the other, a Joy Mine fluorite sample, is enriched in MREE. These two values suggest a differentiated REE source of fluorite deposition, where early fluorite fluids were enriched in LREE and later fluorite fluids were enriched in MREE. The Joy and Davenport Mine dark purple fluorites have the highest REE concentrations in the fluorite samples analyzed for this study (Fig. 21). Based on thermal influence on fluorite deposition (Möller and others, 1998), the Davenport fluorite would be high-temperature and have a carbonatite LREE signature whereas the Joy would be a later-stage, cooler-temperature fluorite depleted in LREE and enriched in MREE. The oxidizing effect of CO_2-rich fluids may have lowered the fluid temperature and influenced the later Joy fluorite composition.

Several of the purple and yellow fluorites fall into the MVT or hydrothermal category (Fig. 23). Use of the Y/Yb ratio results in most of the data falling within the MVT category. Ratios of Y/Yb are used to measure the origin of fluorite (Makin and others, 2014) and suggest a genetic MVT and hydrothermal origin for most of the fluorite in this study. A low Y/Yb ratio falls into the MVT genetic category (Fig. 23), which conflicts with some of the REE carbonatite signature data. The MREE enrichment (Fig. 21) in the Joy purple fluorite suggests hydrothermal sourcing; it is not a typical carbonatite fluorite LREE signature—most carbonatite fluorite contains significant enrichment of the LREE fraction. The Y/Yb ratio indicating genetic origin (Fig. 23) shows that the Joy fluorite plots closest to the carbonatite category, however. Because of barium, strontium, and REE's similar ionic values, high concentrations of barium and strontium (greater than 5,000 ppm) in the Joy Mine fluorite may have influenced this fluorite's REE signature by displacing some of the REE elements.

The plot of U/Th ratio in fluorite (Fig. 22) suggests a diverse enrichment in two distinct uranium and thorium sources in fluorite at the Joy and Davenport Mines and may suggest silicate-carbonatite fractionation in the presence of garnet. These different fluorites suggest that the Davenport fluorite, with its high thorium concentration and La/Yb ratio, was sourced from a carbonatite melt whereas the Joy fluorite, with its high uranium concentration, might be sourced from more of a silicate fluid.

Conflicts in fluorite genetic sourcing may be the result of different fluorite inclusions being analyzed or cross-contamination of various fluorites during mixing of two or three fluorine fluids, MVT fluids, carbonatite, and silicate fluids during transit and final deposition. A larger sample set and better analytical capabilities would be of great value for future research.

All raw-data concentrations for REE in fluorite were under 15 ppm and total REE did not exceed 31 ppm. Purple fluorite has higher REE values than yellow fluorite (Fig. 21). Trace-mineral concentrations, including REE, seem to decrease in abundance away from Hicks Dome, except around the Coefield Intrusive Complex, which has a heterogeneous melt of enriched REE. Generally, across the district, large-scale vertical and horizontal patterns of MVT-stage hydrothermal fluid movement that mixed with igneous-dike alteration fluids is evidenced by the variation in content of sphalerite

and REE in fluorite. Limited fluorite samples were analyzed during this preliminary study, and no fluorite samples from near the Coefield Intrusive Complex, but current data suggest that the hydrothermal origin of the fluorite is responsible for the low REE concentrations compared to typical carbonatite REE concentrations.

Acknowledgments

I would like to thank the many people who assisted in this investigation by providing mine access, samples, analysis, or thoughtful discussion and reviews of this manuscript. Special appreciation is extended to Robert Trace, whose field and mine notes and guardianship of cores and igneous dike samples have provided a wealth of information.

Special thanks go to Tim Hayes, research geologist and fluorite expert with the U.S. Geological Survey, and Craig Dietsch, igneous petrologist and associate professor of geology at the University of Cincinnati, for their thorough reviews of the manuscript and insightful discussion. I thank Brett Denny, research geologist with the Illinois State Geological Survey, and Kentucky Geological Survey colleagues Matt Massey, research geologist and igneous petrologist; Meg Smath, editor; David Harris, head of the Energy and Minerals Section; and Jerry Weisenfluh, interim director, for their kind and thoughtful reviews and considerable patience in helping develop this manuscript.

Appreciation is also extended to Jason Backus, KGS laboratory manager, for his assistance in sample preparation, thoughtful discussion on preparation and analytical techniques, and supervision of much of the analysis; to SGS Laboratories of Canada for final analytical work; and to Thomas Brackman, director of the geophysical laboratory at Northern Kentucky University, for use of their scanning electron microscope.

Thanks also go to other KGS colleagues: Brandon Nuttall, for help with ternary diagrams; Terry Hounshell, for cartographic work on maps and diagrams; Scott Waninger and Richard Smath for field work, sample collection, scanning, and database work; and Tom Sparks, for assistance with creating the minerals and dike databases.

Thank you to mining industry professionals Don Hastie and Jim Watson of Hastie Brothers Mining; Ryan Prosser of Rogers Group Inc.; and William Frazier, Boyce Moody, and Buddy Davidson for access to mines, data, and cores.

Finally, students Jason Heck, using the UK scanning electron microscope microprobe; Hannah Utterback, using the Northern Kentucky University scanning electron microscope; and Jerrad Grider at UK also contributed to this project, as did David Moecher, chair of the Department of Earth and Environmental Sciences at UK, who discussed the manuscript with me and allowed the use of the department's scanning electron microscope microprobe.

References Cited

Anderson, W.H., and Sparks, T.N., 2012, Mines and minerals map of the Western Kentucky Fluorspar District: Kentucky Geological Survey, ser. 12, Map and Chart 201, scale 1:50,000.

Anderson, W.H., Trace, R.D., and McGrain, P., 1982, Barite deposits of Kentucky: Kentucky Geological Survey, ser. 11, Bulletin 1, 56 p.

Arculus, R.J., and Delano, J.W., 1987, Oxidation state of the upper mantle: Present conditions, evolution, and controls, *in* Nixon, P.H., Mantle xenoliths: New York, Wiley, p. 589–598.

Barnett, R.L., 1995, Geochemistry of the Lollipop anomaly: Private consulting report, 48 p.

Beattie, P., 1993, The generation of uranium series disequilibria by partial melting of spinel peridotite: Constraints from partitioning studies: Earth and Planetary Science Letters, v. 117, p. 379–391.

Bell, K., Kjarsgaard, B.A., and Simonetti, A., 1998, Carbonatites—Into the twenty-first century: Journal of Petrology, v. 39, nos. 11–12, p. 1839–1845.

Beyer, C., Tappe, S., Berndt, J., and Klemme, S., 2013, Trace element partitioning between perovskite and kimberlite to carbonatite melt: New experimental constraints: Chemical Geology, v. 353, p. 132–139, doi:10.1016/j.chemgeo.2012.03.025.

Bradbury, J.C., 1962, Trace elements, rare earths and chemical composition of southern Illinois igneous rocks: Illinois State Geological Survey Circular 330, 12 p.

Bradbury, J.C., and Baxter, J.W., 1992, Intrusive breccias at Hicks Dome, Hardin County, Illinois: Illinois State Geological Survey Circular 550, 23 p.

Braile, L.W., Hinze, W.J., Keller, G.R., Lidiak, E.G., and Sexton, J.l., 1986, Tectonic development of the New Madrid Rift Complex, Mississippi Embayment, North America: Tectonophysics, v. 131, p. 1–21.

Burruss, R.C., Ging, T.G., Eppinger, R.G., and Samson, A.M., 1992a, Laser-excited fluorescence of rare earth elements in fluorite: Initial observations with a laser Raman microprobe: Geochimica et Cosmochimica Acta, v. 56, issue 7, p. 2713–2723.

Burruss, R.C., Richardson, C.K., Grossman, J.N., Lichte, F.E., and Goldhaber, M.B., 1992b, Regional and microscale zonation of rare earth elements in fluorite of the Illinois-Kentucky Fluorspar District [abs.], *in* Goldhaber, M.B., and Eidel, J.J., eds., Mineral resources of the Illinois Basin in the context of basin evolution: Program and abstracts: U.S. Geological Survey Open-File Report 92-1, p. 6.

Castor, S.B., 2008, The Mountain Pass rare-earth carbonatite and associated ultrapotassic rocks, California: The Canadian Mineralogist, v. 46, p. 779–806, doi:10.3749/canmin.46.4.779.

Chakhmouradian, A.R., 2006, High-field strength elements in carbonatitic rocks: Geochemistry, crystal chemistry, and significance for constraining the sources of carbonatites: Chemical Geology, v. 235, p. 138–160, doi:10.1016/j.chemgeo.2006.06.008.

Chesley, J.T., Halliday, A.N., Kyser, K.T., and Spry, P.G., 1994, Direct dating of the Mississippi Valley-type mineralization; use of Sm-Nd in fluorite: Economic Geology, v. 89, p. 1192–1199, doi.org/10.2113/gsecongeo.89.5.1192.

Coltorti, M., Bonadiman, C., Hinton, R., Siena, F., and Upton, B., 1999, Carbonatite metasomatism of the oceanic upper mantle: Evidence from clinopyroxenes and glasses in ultramafic xenoliths of Grande Comore, Indian Ocean: Journal of Petrology, v. 40, p. 133–165, doi:10.1093/petrology/40.1.133.

Condie, K.C., 1997, Plate tectonics and crustal evolution [4th ed.]: Oxford, Butterworth Heinemann, 282 p.

Denny, F.B., 2010, Igneous activity and Hicks Dome, *in* Smath, R.A., Nelson, J.W., Denny, B.F., Goldstein, A., and Anderson, W.A., comps., Selected areas within the Western Kentucky Fluorspar District and the Illinois

Fluorspar District and a tour of the Ben Clement Mineral Museum: Kentucky Society of Professional Geologists guidebook, 24 p.

Denny, F.B., Maria, A.H., Mulvaney-Norris, J.L., Guillemette, R.N., Cahill, R.A., Fifarek, R.H., Freiburg, J.T., and Anderson, W.H., 2017, Geochemical and petrographic analysis of the Sparks Hill diatreme and its relationship to the Illinois-Kentucky Fluorspar District: Illinois State Geological Survey Circular 588, 51 p.

Dynamex Resources Corp., 2008, Total intensity magnetic map of Livingston and Crittenden County, KY: North American Exploration LLC, scale 1:100,000.

Eby, G.N., Lloyd, F.E., Woolley, A.R., Stoppa, F., and Weaver, S.D., 2003, Geochemistry and mantle source(s) for carbonatitic and potassic lavas, western branch of the East-African Rift System, SW Uganda: Geolines, v. 15, p. 23–27.

Erickson, R.L., and Blade, L.V., 1963, Geochemistry and petrology of the alkali igneous complex at Magnet Cove, Arkansas: U.S. Geological Survey Professional Paper 425, 95 p.

Fohs, F.J., 1907, The fluorspar deposits of Kentucky: Kentucky Geological Survey, ser. 3, Bulletin 9, 296 p.

Gaylord, W., Frazer, W., and Gabbard, T., 1998, Aeromagnetic map of Western Kentucky Fluorspar District: Savage Zinc Corp., scale 1:50,000.

Green, T.H., 1995, Significance of Nb/Ta as an indicator of geochemical processes in the crust-mantle system: Chemical Geology, v. 120, issues 3–4, p. 347–359, doi.org/10.1016/0009-2541(94)00145-X.

Grogan, R.M., and Bradbury, J.C., 1968, Fluorite zinc-lead deposits of the Illinois-Kentucky mining district, *in* Ridge, J.D., ed., Ore deposits of the United States: American Institute of Mining, Metallurgical, and Petroleum Engineers, p. 370–399.

Goldhaber, M.B., and Eidel, J.J., eds., 1992, Mineral resources of the Illinois Basin in the context of basin evolution: Program and abstracts: U.S. Geological Survey Open-File Report 92-1, 68 p.

Haggerty, S.E., 1976, Opaque mineral oxides in terrestrial igneous rocks, *in* Rumble, D., III, ed., Oxide minerals: Mineralogical Society of America Short Course Notes, v. 3, p. Hg1–Hg100.

Haggerty, S.E., and Baker, I., 1967, The alteration of olivine in basaltic and associated lavas—Part 1: High temperature alteration: Contributions to Mineralogy and Petrology, v. 16, issue 3, p. 233–257.

Hall, W.E., and Heyl, A.V., 1968, Distribution of minor elements in ore and host rock, Illinois-Kentucky Fluorite District and Upper Mississippi Valley Zinc-Lead District: Economic Geology, v. 63, no. 6, p. 655–670, doi:10.2113/gsecongeo.63.6.655.

Hanley, E., and Vorhees, D., 1984, Residual magnetic map of Livingston and Crittenden County, Kentucky: Billiton Exploration USA Inc., scale 1:24,000.

Hanson, G., 1980, Rare earth elements in petrogenetic studies of igneous systems: Annual Review of Earth and Planetary Sciences, v. 8, p. 371–406, doi.org/10.1146/annurev.ea.08.050180.002103.

Hayes, T.S., and Anderson, W.H., 1992, Region wide correlation of the hydrothermal paragenesis of the Illinois-Kentucky Fluorspar District [abs.], *in* Goldhaber, M.B., and Eidel, J.J., eds., Mineral resources of the Illinois Basin in the context of basin evolution: Program and abstracts: U.S. Geological Survey Open-File Report 92-1, p. 19–22.

Heck, J.N., Sr., Moecher, D.P., and Anderson, W.H., 2006, The petrology and mineral chemistry of select lamprophyre dike intrusions in western Kentucky [abs.]: Geological Society of America Abstracts with Programs, v. 38, no. 3, p. 34.

Henmi, C., Kusachi, I., and Henmi, K., 1995, Morimotoite, $Ca_3TiFe^{2+}Si_3O_{12}$, a new titanium garnet from Fuka, Okayama Prefecture, Japan: Mineralogical Magazine, v. 59, no. 394, p. 115–120.

Heyl, A.V., 1983, Geologic characteristics of three major Mississippi Valley districts, *in* Kisvarsanyi, G., Grant, S.K., Pratt, W.P., and Koenig, J.W., eds., International Conference on Mississippi Valley-Type Zinc-Lead Deposits: Rolla, University of Missouri–Rolla, p. 27–42.

Hildenbrand, T.G., and Hendricks, J.D., 1995, Geophysical setting of the Reelfoot Rift and relations between rift structures and the New Madrid Seismic Zone: U.S. Geological Survey Professional Paper 1538-E, 30 p.

Howard, J.M., and Chandler, A., 2007, Magnet Cove: Arkansas Geological Survey Brochure Series 004, 11 p.

Jones, A.P., Genge, M., and Carmody, L., 2013, Carbonate melts and carbonatites: Reviews in Mineralogy and Geochemistry, v. 75, no. 1, p. 289–322, doi.org/10.2138/rmg.2013.75.10.

Kay, R.W., and Mahlburg Kay, S., 1991, Creation and destruction of lower continental crust: Geologische Rundschau, v. 80, no. 2, p. 259–277, doi:10.1007/BF01829365.

Koenig, J.B., 1956, The petrology of certain igneous dikes in Kentucky: Kentucky Geological Survey, ser. 9, Bulletin 21, 57 p.

Kogut, A.I., Hagni, R.D., and Schneider, G.I.C., 1996, The Okorusu, Namibia carbonatite-related fluorite deposit and a comparison with the Illinois-Kentucky Fluorite District/Hicks Dome, *in* Sangster, D.F., Carbonate-hosted lead-zinc deposits: 75th anniversary volume: Society of Economic Geologists Special Publication 4, p. 290–297.

Kolata, D.R., and Nelson, W.J., 2010, Tectonic history, *in* Kolata, D.R., and Nimz, C.K., eds., The geology of Illinois: Illinois State Geological Survey, chapter 3, p. 105–119.

Kononova, V.A., ed., 1984, Magmatic rocks: Vol. 2. Alcaline rocks: Moscow, Nauka, 415 p.

Lapin, A.V., 1982, Carbonatite differentiation processes: International Geology Review, v. 24, issue 9, p. 1079–1089, doi:10.1080/00206818209451046.

Lee, W.-J., and Wyllie, P.J., 1998, Petrogenesis of carbonatite magmas from mantle to crust, constrained by the system CaO–(MgO + FeO*)–(Na_2O + K_2O)–(SiO_2 + Al_2O_3 + TiO_2)–CO_2: Journal of Petrology, v. 39, no. 3, p. 495–517, doi.org/10.1093/petroj/39.3.495.

Le Maitre, R.W., ed., 2002, Igneous rocks: A classification and glossary of terms: Recommendations of the International Union of Geological Sciences Subcommission on the Systematics of Igneous Rocks [2nd ed.]: New York, Cambridge, 236 p.

Lewis, R.D., and Mitchell, R.H., 1987, Alnöite intrusions associated with rifting in the New Madrid Seismic Zone [abs.]: Geological Society of America Abstracts with Programs, v. 19, no. 7, p. 745.

Liu, S., Hu, R., Gao, S., Fend, C., Coulson, I., Feng, G., Yang, Y., Qi, Y., and Tang, L., 2011, Age and origin of a Paleozoic nepheline syenite from northern Shanxi Province, China: U-Pb zircon age and whole-rock geochemical and Sr-Nd isotopic constraints: International Geology Review, v. 54, issue 11, p. 1296–1308, doi.org/10.1080/00206814.2011.638436.

Long, K.R., Van Gosen, B.S., Foley, N.K., and Cordier, D., 2010, The principal rare earth elements deposits in the United States—A summary of domestic deposits and a global perspective: U.S. Geological Survey Scientific Investigations Report 2010-5220, 95 p.

Makin, S.A., Simandl, G.J., and Marshall, D., 2014, Fluorite and its potential as an indicator mineral for carbonatite related rare earth element deposits, *in* Geological fieldwork 2013: British Columbia Ministry of Energy and Mines, British Columbia Geological Survey Paper 2014-1, p. 207–212.

Maria, A.H., and King, M.D., 2012, Petrography and geochemistry of an ultramafic dike in southern Illinois [abs.]: Geological Society of America Abstracts With Programs, v. 44, no. 7, p. 541.

Mariano, A.N., 1989, Nature of economic mineralization in carbonatites and related rocks, *in*

Bell, K., ed., Carbonatites: Genesis and evolution: London, Unwin Hyman, p. 140–176.

Mathez, E.A., Fogel, R.A., Hutchson, I.D., and Marshintsev, V.K., 1995, Carbon isotopic composition and origin of SiC from kimberlites of Yakutia, Russia: Geochimica et Cosmochimica Acta, v. 59, issue 4, p. 781–791, doi.org/10.1016/0016-7037(95)00002-H.

McDonough, W.F., and Sun, S.-S., 1995, The composition of the Earth: Chemical Geology, v. 120, issues 3–4, p. 223–253, doi.org/10.1016/0009-2541(94)00140-4.

Mitchell, R.H., 1986, Kimberlites: Mineralogy, geochemistry, and petrology: New York, Plenum Press, 442 p.

Mitchell, R.H., 1993, Kimberlites and lamproites, *in* Sheahan, P.A., and Cherry, M.E., eds., Ore deposit models: Volume II: Geoscience Canada Reprint Series 6, p. 13–28.

Mitchell, R.H., 1994, Suggestions for revisions to the terminology of kimberlites and lamprophyres from a genetic viewpoint, *in* Meyer, H.O.A., and Leonardos, O.H., eds., Proceedings of the Fifth International Kimberlite Conference, Araxá, Brazil, 1991: Kimberlites, related rocks and mantle xenoliths: Companhia de Pesquisa de Recursos Minerais, Special Publication 1/A, p. 15–26.

Mitchell, R.H., 2005, Carbonatites and carbonatites and carbonatites: The Canadian Mineralogist, v. 43, no. 6, p. 2049–2068, doi:10.2113/gscanmin.43.6.2049.

Mitchell, R.H., 2008, Petrology of hypabyssal kimberlites: Relevance to primary magma compositions: Journal of Volcanology and Geothermal Research, v. 174, issues 1–3, p. 1–8.

Mitchell, R.H., and Chakhmouradian, A.R., 1996, Compositional variation of loparite from the Lovozero alkaline complex, Russia: The Canadian Mineralogist, v. 34, no. 5, p. 977–990.

Miyawaki, R., Shimazaki, H., Shigeoka, M., Yokoyama, K., Matsubara, S., Yurimoto, H., Yang, Z., and Zhang, P., 2011, Fluorokinoshitalite and fluorotetraferriphlogopite: New species of fluoro-mica from Bayan Obo, Inner Mongolia, China: Clay Science, v. 15, p. 13–18.

Modreski, P.J., Armbrustmacher, T.J., and Hoover, D.B, 1995, Carbonatite deposits (model 10; Singer, 1986a), *in* DuBray, E.A., ed., Preliminary compilation of descriptive geoenvironmental mineral deposit models: U.S. Geological Survey Open-File Report 95-0831, p. 47–49.

Möller, P., Bau, M., Dulski, P., and Lüders, V., 1998, REE and yttrium fractionation in fluorite and their bearing on fluorite formation: Proceedings of the Ninth Quadrennial IAGOD Symposium, Stuttgart, E. Schweizerbart'sche Verlagsbuchhandlung, p. 575–592.

Moorehead, A.J., 2013, Igneous intrusions at Hicks Dome, southern Illinois, and their relationship to fluorine-base metal-rare earth element mineralization: Carbondale, Southern Illinois University, master's thesis, 452 p.

Nelson, W.J., 2010, Structural features, *in* Kolata, D.R., and Nimz, C.K., eds., The geology of Illinois: Illinois State Geological Survey, chapter 4, p. 90–104.

Nicholson, H., and Latin, D., 1992, Olivine tholeiites from Krafla, Iceland: Evidence for variations in melt fraction within a plume: Journal of Petrology, v. 33, issue 5, p. 1105–1124, doi.org/10.1093/petrology/33.5.1105.

Nixon, P.H., ed., 1987, Mantle xenoliths: New York, Wiley, 844 p.

Ohle, E.L., 1959, Some considerations in determining the origin of ore deposits of the Mississippi Valley type: Economic Geology, v. 54, no. 5, p. 769–789, doi.org/10.2113/gsecongeo.54.5.769.

Parekh, P.P., and Möller, P., 1977, Revelation of the genesis of minerals in paragenesis with fluorites, calcites, and phosphates via rare earth fractionation, *in* Nuclear techniques and mineral resources 1977: Proceedings of the International Symposium on Nuclear Techniques in Exploration, Extraction, and Processing of Mineral Resources: International Atomic Energy Agency, p. 353–368.

Pearson, D.G., Irvine, G.J., Ionov, D.A., Boyd, F.R., and Dreibus, G.E., 2004, Re-Os isotope systematics and platinum group element fractionation during mantle melt extraction: A study of massif and xenolith peridotite suites: Chemical Geology, v. 208, nos. 1–4, p. 29–59, dx.doi.org/10.1016/j.chemgeo.2004.04.005.

Pinckney, D.M., 1976, Mineral resources of the Illinois-Kentucky Mining District: U.S. Geological Survey Professional Paper 970, 15 p.

Plumlee, G.S., Goldhaber, M.B., and Rowan, E.L., 1995, The potential role of magmatic gases in the genesis of Illinois-Kentucky fluorspar deposits: Implications from chemical reaction path modeling: Economic Geology, v. 90, issue 5, p. 999–1011.

Pollitz, F.F., and Mooney, W.D., 2014, Seismic structure of the central US crust and shallow upper mantle—Uniqueness of the Reelfoot Rift: Earth and Planetary Science Letters, v. 402, p. 157–166, dx.doi.org/10.1016/j.epsl.2013.05.042.

Potter, C.J., Goldhaber, M.B., Heigold, P.C., and Drahovzal, J.A., 1995, Structure of the Reelfoot–Rough Creek Rift System, Fluorspar Area Fault Complex, and Hicks Dome, southern Illinois and western Kentucky—New constraints from regional seismic reflection data: U.S. Geological Survey Professional Paper 1538-Q, 19 p.

Richardson, C.K., and Pinckney, D.M., 1984, The chemical and thermal evolution of the fluids in the Cave-in-Rock Fluorspar District, Illinois; mineralogy, paragenesis, and fluid inclusions: Economic Geology, v. 79, no. 8, p. 1833–1856, doi.org/10.2113/gsecongeo.79.8.1833.

Rock, N.M.S., 1986, The nature and origin of ultramafic lamprophyres: Alnöites and allied rocks: Journal of Petrology, v. 27, issue 1, p. 155–196, doi.org/10.1093/petrology/27.1.155.

Rock, N.M.S., 1987, The nature and origin of lamprophyres: An overview: Geological Society, London, Special Publications, v. 30, p. 191–226, doi.org/10.1144/GSL.SP.1987.030.01.09.

Rock, N.M.S., 1991, Lamprophyres: New York, Springer US, 285 p.

Rogers, N.W., 2006, Basaltic magmatism and the geodynamics of the East African Rift System, *in* Yirgu, G., Ebinger, C.J., and Maguire, P.K.H., eds., The Afar Volcanic Province within the East African Rift System: Geological Society, London, Special Publications, v. 259, p. 77–93, doi.org/10.1144/GSL.SP.2006.259.01.08.

Rudnick, R.L., McDonough, W.F., and Chappell, B.W., 1993, Carbonatite metasomatism in the northern Tanzanian mantle: Petrographic and geochemical characteristics: Earth and Planetary Science Letters, v. 114, issue 4, p. 463–475, doi.org/10.1016/0012-821X(93)90076-L.

Santos, R.V., Augusts, M., and Oliveira, C., 1996, Rare earth elements geochemistry of fluorite from the Mato Preto carbonatite complex, southern Brazil: Revista Brasileira de Geociências, v. 26, no. 2, p. 81–86, doi:10.25249/0375-7536.199628186.

Schmidt, M.W., Changgui, G., Golubkova, A., Rohrback, A., and Connolly, J.A.D., 2014, Natural moissanite (SiC)—A low temperature mineral formed from highly fractionated ultra-reducing COH-fluids: Progress in Earth and Planetary Science, v. 1, no. 27, 14 p., doi.org/10.1186/s40645-014-0027-0.

Schwinn, G., and Markl, G., 2005, REE systematics in hydrothermal fluorite: Chemical Geology, v. 216, issues 3–4, p. 225–248, doi:10.1016/j.chemgeo.2004.11.012.

Scott Smith, B.H., and Skinner, E.M.W., 1984, A new look at Prairie Creek, Arkansas: Developments in Petrology, v. 11, pt. A, p. 255–283, doi.org/10.1016/B978-0-444-42273-6.50024-9.

Shavers, E.J., Ghulam, A., Encarnacion, J., Bridges, D.L., and Luetkemeyer, P.B., 2016, Carbonatite associated with ultramafic diatremes in the Avon Volcanic District, Missouri, USA: Field, petrographic, and geochemical constraints: Lithos, v. 248–251, p. 506–516, doi.org/10.1016/j.lithos.2016.02.005.

Simandl, G.J., 2015, Carbonatites and related exploration targets: Symposium on Critical and

Strategic Materials: British Geological Survey Paper 2015-3, p. 31–37.

Snee, L.W., and Hayes, T.S., 1992, $^{40}Ar/^{39}Ar$ geochronology of intrusive rocks and Mississippi Valley-type mineralization and alteration from the Illinois-Kentucky Fluorspar District [abs.], *in* Goldhaber, M.B., and Eidel, J.J., eds., Mineral resources of the Illinois Basin in the context of basin evolution: Program and abstracts: U.S. Geological Survey Open-File Report 92-1, p. 59–60.

Streckeisen, A.L., 1978, Classification and nomenclature of volcanic rocks, lamprophyres, carbonatites and melilite rocks: Recommendations and suggestions: Neues Jahrbuch Mineralogie, Abhandlungen, v. 141, p. 1–14.

Tappe, S., Foley, S.F., Jenner, G.A., Heaman, L.M., Kjarsgaard, B.A., Romer, R.L., Stracke, A., Joyce, N., and Hoefs, J., 2006, Genesis of ultramafic lamprophyres and carbonatites at Aillik Bay, Labrador: A consequence of incipient lithospheric thinning beneath the North Atlantic craton: Journal of Petrology, v. 47, issue 7, p. 1261–1315, doi.org/10.1093/petrology/egl008.

Tappe, S., Foley, S.F., Jenner, G.A., and Kjarsgaard, B.A., 2005, Integrating ultramafic lamprophyres into the IUGS classification of igneous rocks: Rationale and implications: Journal of Petrology, v. 46, issue 9, p. 1893–1900, doi:10.1093/petrology/egi039.

Taylor, C.D., Rowan, E.L., Goldhaber, M.B., and Hayes, T.S., 1992, A relationship between Hicks Dome and temperature zonation in fluorite in the Illinois-Kentucky Fluorspar District, a fluid inclusion study [abs.], *in* Goldhaber, M.B., and Eidel, J.J., eds., Mineral resources of the Illinois Basin in the context of basin evolution: Program and abstracts: U.S. Geological Survey Open-File Report 92-1, p. 19–22.

Taylor, S.R., and McLennan, S.M., 1985, The continental crust: Its compositions and evolution: Oxford, Blackwell Scientific, 312 p.

Trace, R.D., 1974, Illinois-Kentucky Fluorspar District, *in* Hutcheson, D.W., ed., A Symposium on the Geology of Fluorspar: Kentucky Geological Survey, ser. 10, Special Publication 22, p. 58–76.

Trace, R.D., and Amos, D.H., 1984, Stratigraphy and structure of western Kentucky: U.S. Geological Survey Professional Paper 1151-D, 41 p.

Trinkler, M., Monecke, T., and Thomas, R., 2005, Constraints on the genesis of yellow fluorite in hydrothermal barite-fluorite veins of the Erzgebirge, eastern Germany: Evidence from optical absorption spectroscopy, rare earth element data, and fluid inclusion investigations: The Canadian Mineralogist, v. 43, no. 3, p. 883–898, doi:10.2113/gscanmin.43.3.883.

Ulrich, E.O., and Smith, W.S.T., 1905, Lead, zinc, and fluorspar deposits of western Kentucky: U.S. Geological Survey Professional Paper 36, 218 p.

Verplanck, P.L., Van Gosen, B.S., Seal, R.R., II, and McCafferty, A.E., 2014, A deposit model for carbonatite and perakaline intrusion–related rare earth element deposits, *in* Mineral deposit models for resources assessment: U.S. Geological Survey Scientific Investigations Report 2010-5070, Chapter J, 58 p., doi.org/10.3133/sir20105070J.

Wall, F., and Zaitsev, A.N., eds., 2004, Phoscorites and carbonatites from mantle to mine: The key example of the Kola alkaline province: Mineralogical Society of Great Britain and Ireland, 498 p., doi.org/10.1180/MSS.10.

Wilke, M., Schmidt, C., Dubrail, J., Appel, K., Borchert, M., Kvashnina, K., and Manning, C., 2012, Zircon solubility and zirconium complexation in H2O+Na2O+SiO2+Al2O3 fluids at high pressure and temperature: Earth and Planetary Science Letters, v. 15–25, p. 349–350, doi:10.1016/j.epsl.2012.06.054.

Woolley, A.R., Bergman, S.C., Edgar, A.D, Le Bas, M.J., Mitchell, R.H., Rock, N.M.S., and Scott Smith, B.H., 1996, Classification of lamprophyres, lamproites, kimberlites, and the kal-

silitic, melilitic, and leucitic rocks: The Canadian Mineralogist, v. 34, no. 2, p. 175–186.

Woolley, A., and Kjarsgaard, B., 2008, Paragenetic types of carbonatite as indicated by the diversity and relative abundances of associated silicate rocks: Evidence from a global database: Geochimica et Cosmochimica Acta, v. 46, no. 4, p. 741–752, doi:10.3749/canmin.46.4.741.

Xu, C., Taylor, R.N., Li, W., Kynicky, J., Chakhmouradian, A.R., and Song, W., 2012, Comparison of fluorite geochemistry from REE deposits in the Panxi region and Bayan Obo, China: Journal of Asian Earth Sciences, v. 57, p. 76–89, doi:10.1016/j.jseaes.2012.06.007.

Yang, X.M., Yang, X.Y., Sheng, Y.F., and Le Bas, M.J., 2003, A rare earth element–rich carbonatite dyke at Bayan Obo, Inner Mongolia, north China: Mineralogy and Petrology, v. 78, issues 1–2, p. 93–110.

Zeng, G., Chen, L.-H., Xu, X.-S., Jiang, S.-Y., and Hofmann, A., 2010, Carbonated mantle sources for Cenozoic intra-plate alkaline basalts in Shandong, north China: Chemical Geology, v. 273, nos. 1–2, p. 35–45, doi:10.1016/j.chemgeo.2010.02.009.

Samples of altered and unaltered intrusive dikes

Top row, altered, from left to right:

- Hutson Mine mica peridotite, BH-7_74, pebble breccia
- Hutson Mine mica peridotite, BH-7_125, altered
- Midway (Davidson dike), T-9-76, porphyritic, altered
- Sunderland lamprophyre, T-5-76, altered
- Little Hurricane lamprophyre, 597-V, altered

Bottom row, unaltered, from left to right:

- Hutson Mine shaft mica peridotite, T-10-76
- Stout lamprophyre, T-8-76
- Minner alnöite, BMN-4
- Guilless Mine lamprophyre, T-1-76
- Clay Lick East mica peridotite, T-1136